高解像度シミュレーションによるプラズマバブル内部構造の発達と減衰過程

横山 竜宏 [1]; 陣 英克 [2]; 品川 裕之 [2]; Rino Charles[3]; Carrano Charles[3]
[1] 京大生存研; [2] 情報通信研究機構; [3] ISR, Boston College

Structuring and decaying of equatorial plasma bubbles simulated by High-Resolution Bubble model

Tatsuhiro Yokoyama[1]; Hidekatsu Jin[2]; Hiroyuki Shinagawa[2]; Charles Rino[3]; Charles Carrano[3]
[1] RISH, Kyoto Univ.; [2] NICT; [3] ISR, Boston College

Equatorial plasma bubble (EPB) is a well-known phenomenon in the equatorial ionospheric F region. As it causes severe scintillation in the amplitude and phase of radio signals, it is important to understand and forecast the occurrence of EPB from a space weather point of view. In order to simulate the instability in the equatorial ionosphere, a 3D High-Resolution Bubble (HIRB) model with a grid spacing of as small as 200 m has been developed. It provides a unique opportunity to characterize intermediate-scale EPB structure, which was not well resolved until very recently. It was shown that developed structure is characterized by a two-component power law spectral density which fully supports the reported EPB diagnostics from previous in situ measurements. Changing the background electric field from eastward to westward after EPBs are fully developed, the decay phase of EPBs can be simulated. The structures tend to have a single power law and the decay speed depends on the background neutral density.

赤道電離圏においては、赤道スプレッド F/プラズマバブルと呼ばれる現象の研究が古くから行われている。プラズマバブルに伴う局所的なプラズマ密度の不規則構造が発生した場合には、電波の振幅、位相の急激な変動、すなわちシンチレーションが生じるため、GPS 等による電子航法に深刻な障害を及ぼすことが知られている。現在までに開発を進めてきた High-Resultion Bubble (HIRB) モデルの空間分解能を、最大 200m にまで向上させることで、プラズマバブル内部の非線形成長過程をより詳細に理解することが可能となった。内部構造のパワースペクトルはべき乗則に従い、プラズマバブル成長過程では、2 つの傾き成分を持つことが示された。一方、成長後に背景電場を西向きに変化させると、プラズマバブルは減衰過程に入り、パワースペクトルは 1 つの傾き成分に近づく様子が示された。また、背景の大気密度によって減衰速度が変化することも確認された。これらの結果は、従来の観測結果を支持するものであり、シンチレーション発生の周波数特性、緯度特性等とも整合する結果である。

Role of pre-reversal enhancement in the generation of equatorial plasma bubble using observation and model simulation

Priyanka Ghosh[1]; Yuichi Otsuka[2]; Sivakandan Mani[1]; Takuya Tsugawa[3]; Kornyanat Hozumi[4]; Hiroyuki Shinagawa[3]
[1] ISEE, Nagoya Univ.; [2] ISEE, Nagoya Univ.; [3] NICT; [4] NICT

The equatorial plasma bubble (EPB) or equatorial spread-F (ESF) generated during post sunset hours due to the transition in the E- and F-layers of the ionosphere are well-known due to their unique nature and adverse effects on communication and navigation systems. Although the Rayleigh Taylor instability (RTI) is known to be the governing mechanism of EPB, the exact seeding mechanism is not clear yet. Pre-reversal enhancement (PRE) is believed to be one of the main controlling factor for the generation of EPB in spite of its asymmetric distribution and longitudinal variation. However, the relation between PRE and EPB generation is not explored quantitatively.

In the present study, ionosonde observations at Chumphon (10.7^{o}N, 99.4^{o}E; 0.86^{o}N magnetic latitude) in Thailand and Bac Lieu (9.3^{o}N, 105.7^{o}E; 0.62^{o}N magnetic latitude) in Vietnam are used to calculate the day to day variation of PRE during the equinoxial months of March, April, September and October of 2011-2013. The observations are compared with the whole atmosphere ionosphere coupled model Ground-to-topside model of Atmosphere-ionosphere for Aeronomy (GAIA) consisting of three models (an ionosphere model, a neutral atmosphere model, and an ionospheric electrodynamic model). The virtual height (h'F) are manually scaled from the ionograms at time intervals of 5 min between 17:00 and 24:00 LT (LT = UT + 7 h) during 01-16 March 2011 (equinoxial month) over Chumphon in Thailand. The vertical drift is derived from rate of change of h'F (dh'F/dt with h'F, above 300 km) is considered as an indicator for vertical motion during the evening time. In case of GAIA model simulations, the vertical component of plasma drift due to the zonal component of the electric field E at the magnetic equator is derived using the electric field and magnetic field data (in the eastward, southward and upward direction). The observation period (01-16 March 2011) is classified in two categories: EPB occurrence day (8 days) and non-EPB occurrence day (7 days). It is observed that the vertical drift obtained using ionosonde ranges between 50-55 m/s on the EPB occurrence day and 10-30 m/s during the days with no EPB. In the GAIA model simulations, the vertical drift varies from 40-50 m/s during the days with EPB while it ranges between 30-40 m/s during the non-EPB days. The detailed outcomes of the study will be presented.

GNU Radio Beacon Receiver 2 (GRBR2) の開発 –衛星打上げ後の状況報告–

山本 衛 [1]; Tsunoda Roland T.[2]
[1] 京大・生存圏研; [2] SRI International

Development of GNU Radio Beacon Receiver 2 (GRBR2) – Progress after the satellite launch –

Mamoru Yamamoto[1]; Roland T. Tsunoda[2]
[1] RISH, Kyoto Univ.; [2] SRI International

GNU Radio Beacon Receiver (GRBR) is the very successful digital receiver developed for dual-band (150/400MHz) beacon experiment. We were successfully conducted observations of total-electron content (TEC) of the ionosphere over Japan and in southeast Asia. However, many beacon satellites is now aging, and its number is decreasing. We now have a project to start new satellite-ground beacon experiment with new satellite constellations. One of them is TBEx (Tandem Beacon Explorer), a project by SRI International, to fly a constellation of two 3U cubesats with triband beacon transmitters. Another one is a project of FORMOSAT-7/COSMIC-2 by Taiwan/USA. Well-known mission of COSMIC-2 is GNSS occultation experiment, but the satellites carry triband beacon transmitters. All of these satellites were placed into low-inclination orbits by one launch vehicle flight on June 25, 2019. Now intitial checkout of the satellites are underway. We have developed a new digital receiver, GRBR2, for these new satellite beacon. GRBR2 receive four channels of 150/400/965/1067MHz, and realizes many TEC measurement with the new satellites. We started install of GRBR2 in Thailand, Vietnam, Indonesia, and Taiwan since March 2019. In the presentation, we will report current status of this new experiment.

GNU Radio Beacon Receiver（GRBR）はデュアルバンド（150/400MHz）ビーコン実験用に開発された非常に成功したデジタル受信機であった。日本および東南アジアにおいて、電離圏全電子数（TEC）の観測に成功してきた。しかし多くのビーコン衛星は老朽化してきており、その数は減少している。いま、新しい衛星群を用いた衛星＝地上ビーコン実験が始まろうとしている。それらの 1 つは、SRI International による TBEx（Tandem Beacon Explorer、3U サイズの cubesate 2 機）であり、もうひとつは、台湾/米国による FORMOSAT-7/COSMIC-2 のプロジェクトである。6 機編隊で構成される COSMIC-2 の第 1 の任務は GNSS 波の掩蔽観測であるが、多周波数のビーコン送信機も搭載している。これら 2 種類の衛星は 2019 年 6 月 25 日に Falcon Heavy ロケットの 1 回のフライトによって、それぞれ所定の低軌道傾斜角の軌道に打上げられた。現在は衛星のチェック作業が進行中である。これらの衛星計画に対応して開発してきたビーコン受信機 GNU Radio Beacon Receiver 2 (GRBR2) についても、2019 年 3 月ごろからタイ・ベトナム。インドネシア・台湾への配備を進めている。GRBR2 は、周波数が 150/400/965/1067MHz の 4 バンドの信号を同期して受信し、多数の TEC 観測を実現する予定である。発表では、衛星打上げ後の観測状況について報告する。

S-310-44 号機観測ロケットによって観測された Sq 電流系における VLF 帯波動の解析

中村 龍一郎 [1]; 三宅 壮聡 [1]; 石坂 圭吾 [2]; 阿部 琢美 [3]; 熊本 篤志 [4]; 田中 真 [5]
[1] 富山県大; [2] 富山県大・工; [3] ＪＡＸＡ宇宙科学研究所; [4] 東北大・理・地球物理; [5] 東海大・情教セ

Analysis of VLF Band Waves in the Sq Current System Observed by S-310-44 Sounding Rocket

Ryuichiro Nakamura[1]; Taketoshi Miyake[1]; Keigo Ishisaka[2]; Takumi Abe[3]; Atsushi Kumamoto[4]; Makoto Tanaka[5]
[1] Toyama Pref. Univ.; [2] Toyama Pref. Univ.; [3] ISAS/JAXA; [4] Dept. Geophys, Tohoku Univ.; [5] Tokai Univ.

The Sq current system is one of the ring current which occurs in the lower ionosphere in the winter daytime. It is caused the specific plasma phenomena such as electron heating and strong electron density disturbance. S-310-44 sounding rocket was launched from Uchinoura Space Center at 12:00 LT on January 15th to clarify the special phenomena. The rocket passed through the Sq current focus, and all the scientific instruments onboard the rocket worked successfully. In this experiment, Electric Field Detector (EFD) observed the VLF band AC electric fields up to 6.4 kHz in the altitude from 100km to 160km. We made the altitude profile of the electric field spectra, and found clear VLF band waves with the frequencies from 2kHz to 3kHz at the altitude about 100km, which are observed during the rocket ascent. The Fast Langmuir Probe(FLP)observed that the electron temperature increase about 150K larger than the background in this region, and the frequency variation of the VLF band waves shows good correlation with the electron temperature. According to the polarization analyses, the electric fields of the VLF band waves are almost perpendicular to the magnetic field. In addition, the frequency range of this VLF band waves is consistent with the ion cyclotron frequency. These results suggest that the VLF band waves observed in this experiment are one of the ion cyclotron harmonic waves whose frequencies vary with the temperature ratio of the electron and the ion(T_e/T_i). On the other hand, the frequency variation of the VLF band waves also shows good correlation with the electron density. We are going to investigate this correlation, and clarify the heating mechanism of the electrons near the Sq current focus.

Sq 電流系は，冬季の昼間に電離圏下部領域で発生する環電流である．この Sq 電流系の中心付近では，電子加熱や強い電子密度擾乱といった特異な現象が引き起こされる．これらの現象を解明するため，S-310-44 号機観測ロケットが 2016 年 1 月 15 日 12 時 00 分（JST）に内之浦宇宙空間観測所から打ち上げられた．ロケットが Sq 電流系中心付近を通過し，搭載された観測機器はすべて正常に動作した．電場観測装置（EFD）は高度 100km から 160km にかけて 6.4kHz までの VLF 帯交流電界を観測した．電界スペクトル高度分布から、上昇時の高度 100km 付近で 2-3kHz の周波数帯の VLF 帯波動が確認された．また，高速ラングミューアプローブ（FLP）が観測した電子温度は高度 100km 付近で 150K ほど上昇しており，電子温度上昇と周波数変化に良い相関が見られた．偏波解析の結果，観測された VLF 帯波動は磁場に対してほぼ垂直であり，さらに周波数帯がイオンサイクロトロン周波数と一致することがわかった．これらの解析結果から，この VLF 帯波動は電子温度とイオン温度の比（T_e/T_i）によって周波数が変化するイオンサイクロトロン高調波である可能性が考えられる．一方，この VLF 帯波動の周波数変化は電子密度変化との相関も見られる．この相関関係について調査するとともに，Sq 電流系中心付近に発生する高温電子領域の発生メカニズムの解明を目指す．

Lower hybrid resonance (LHR) waves around the Sq current focus in the winter lower ionosphere

Atsushi Kumamoto[1]; Takumi Abe[2]; Keigo Ishisaka[3]; Makoto Tanaka[4]
[1] Dept. Geophys, Tohoku Univ.; [2] ISAS/JAXA; [3] Toyama Pref. Univ.; [4] Tokai Univ.

The plasma waves around lower hybrid resonance (LHR) frequency around Sq current focus in the winter lower ionosphere was investigated based on the data obtained by sounding rocket S-310-44. In order to clarify electron heating phenomena in the center of Sq current focus in the winter ionosphere, the sounding rocket experiment S-310-44 was launched at 21:00 UT on January 15, 2016 at Uchinoura Space Center (USC). Plasma Wave Monitor (PWM) onboard the S-310-44 was successfully measured plasma waves in a frequency range from 300 Hz to 22 MHz along the rocket trajectory with apex altitude of 160 km, which is also confirmed to be near the Sq current focus by using data from magnetometer chain on the ground. During the flight, harmonic emissions of LHR were found in a frequency range from several hundred Hz to several kHz. Their frequencies changes depending on the ambient plasma density and likely on the ion compositions. They are enhanced at altitude around 100 km in ascent but not enhanced at the same altitude in descent.

The LHR waves in the ionosphere can be generated by various energy inputs. Baker et al. [2000] reported that LHR emissions were found in the sounding rocket experiment, and suggested that they are caused by the whistler waves from the thunderstorms on the ground. At S-310-44 launch, however, the nearest weather front was farer than 1000 km distance, and clear inducing impulsive emissions of lightning were not found with LHR emissions. Cattel and Hudson [1983] suggested that perpendicularly heated ions, which were found in cusp and auroral regions, can cause flute mode waves near LHR frequency. Several studies suggested that lower hybrid drift instability (LHDI) can be caused in the inhomogeneous plasma in the ionosphere [Huba and Ossakow, 1981] and thin cross field current sheet in the magnetosphere [Yoon et al., 2008]. So, we can consider several candidates for causing LHR waves found in S-310-44 experiment: (a) Localized cross field current around the Sq current focus, (b) ions heated by the interhemispheric field aligned current (IHFAC) around Sq current focus, and (c) inhomogeneous plasma in the ionosphere. In the presentation, we will also verify the candidates using other data such as electron number density and temperature (FLP), DC and AC electric field (EFD), and magnetic field (MGF) onboard S-310-44.

中・低緯度で Swarm 衛星が観測する磁場および電子密度変動微細構造の比較

家森 俊彦 [1]; 青山 忠司 [2]; 横山 佳弘 [3]
[1] 京大; [2] 京大・理; [3] 京大理

A comparison between electron and magnetic fluctuations as observed by Swarm satellites in low- and mid-latitudes

Toshihiko Iyemori[1]; Tadashi Aoyama[2]; Yoshihiro Yokoyama[3]
[1] Kyoto Univ.; [2] Graduate School of Science, Kyoto Univ.; [3] Grad school of Science, Kyoto Univ.

When we apply high-pass filter to magnetic and electron density data obtained by polar orbiting low-altitude satellites such as the Swarm satellites, small scale magnetic and electron density fluctuations appear in low and middle latitudes. These fluctuations typically have the period about 10-30seconds along satellite orbit, i.e., about 70-210 km. They are mostly the spatial structure of electron density and small-scale field-aligned current effects called 'magnetic ripples', respectively. Magnetic ripples are supposed to be generated in lower ionosphere by dynamo mechanism caused by neutral atmospheric waves from lower atmosphere. If we trace down to the dynamo layer around 120km altitude from magnetic ripples and compare the electron density fluctuations observed on the orbit at the latitude traced down to 120km, in some cases, they correspond better than the correspondence on the orbit. This indicates vertical propagation of atmospheric waves which causes both magnetic ripples and electron density fluctuations. However, their wave forms of fluctuations are different. In this presentation, we compare the structure of the fluctuations considering their geographical and seasonal distributions.

Swarm 衛星のような低高度極軌道衛星で測定された磁場および電子密度データにハイパスフィルターをかけると、小規模な変動がほぼ常に見られる。これらの変動の軌道に沿う時間スケールは通常 10-30 秒程度で、空間距離では約 70-210km になる。それらは主として軌道に沿う空間構造で、磁場については磁気リップルと呼んでいる。磁気リップルは、下層大気から伝搬した大気波動による電離層ダイナモ作用で生成した電流が発散した沿磁力線電流の効果であると考えられる。磁気リップルから磁力線沿いに高度 120km のダイナモ層にトレースした時の緯度に対応する電子密度変動を比較すると、それらが一致する場合がしばしば存在する。これは、大気波動が鉛直上方に伝搬しつつ、磁気リップルと電子密度変動を発生させたことを示している。しかし、それらの波形あるいは構造は異なる。この発表では、主としてそれら変動の構造を、地理的・季節的分布も考慮して比較する。

電離圏最下部の電子密度構造について

阿部 琢美 [1]
[1] ＪＡＸＡ宇宙科学研究所

On the electron density structure in the lowest region of the nightside ionosphere

Takumi Abe[1]
[1] ISAS/JAXA

Electron density structure in the ionosphere has been observed by in-situ and the ground-based instruments for many decades. We have used Langmuir probe and fixed-bias probe on the sounding rocket to measure the local electron density in the ionospheric D, E, and F regions. As a result of analyzing several altitude profiles derived from the sounding rocket data, we notice that a ledge structure of the electron density is observed to exist at the altitude of 80-85 km on the nightside. In this talk, characteristic feature of the ledge structure will be presented.

It is well known that the ionospheric D region disappears at night because there is no direct irradiation by the sun light. Therefore, the electron density below 90 km altitude is remarkably lower at night than at daytime. In fact, the sounding rocket observation shows that electron density in the nightside ionosphere is lower than $3x10^3$ cm^{-3} below 90 km altitude. In addition, it is significant that the electron density profile has a very steep positive gradient at a certain altitude, *i.e.*, it abruptly increases by more than 10 times in a narrow altitude range. For example, altitude profile of the electron density observed at 23:48 LT on December 19, 2011 by S-310-40 rocket abruptly increases by about 70 times at the altitude of 92 km. Similar increase was also observed during S-520-26 experiment, which was conducted at 05:51 LT on Jan 12, 2012. In these data set, the electron density was estimated from Langmuir probe measurement. Thus, it is noticeable that the altitude profile has a ledge structure where the density abruptly increases by more than a factor of 10 at a certain altitude. Such a ledge structure is found only at night but not at daytime.

Such an electron density structure was also observed by other sounding rocket experiments in US (Dickinson et al., 1980). They suggested that the ledge structure of the electron density at night is related to the abrupt fall to undetectable levels in the atomic oxygen density with decreasing height around 83 km altitude because the atomic oxygen density profile had a similar spatial structure as seen in the electron density. The common feature is attributed to chemical reaction in the lower D region in which atomic oxygen, metal, metallic ion, and other primary species play an important role.

In this talk, we present the detail structure of the electron density in the lowest region of the ionosphere and discuss a possible implication of the ionospheric chemistry.

Reference

Dickinson, P.H.G. et al., The determination of the atomic oxygen concentration and associated parameters in the lower ionosphere, Proc. R. Soc. London, 369, 379-408, 1980

Comparison of daytime medium-scale traveling ionospheric disturbance between GPS observation and GAIA simulation

Sivakandan Mani[1]; Yuichi Otsuka[2]; Priyanka Ghosh[1]; Hiroyuki Shinagawa[3]; Yasunobu Miyoshi[4]; Atsuki Shinbori[5]; Takuya Tsugawa[3]; Michi Nishioka[3]
[1] ISEE, Nagoya Univ.; [2] ISEE, Nagoya Univ.; [3] NICT; [4] Dept. Earth & Planetary Sci, Kyushu Univ.; [5] ISEE, Nagoya Univ.

Traveling ionospheric disturbances (TIDs) are wave-like perturbations of the ionospheric plasma. Depending on the wave parameters such as wavelength, phase speed and period TIDs are categorised into medium and large scale TIDs. Medium scale traveling ionospheric disturbances (MSTIDs) have wavelength, phase speed and period in the range of 100-500 km, 100-250 m/s and 15-90 minutes respectively. Most often, the MSTIDs propagate towards southeast or south during daytime and southwest during nighttime, which gives an evidence showing that generation mechanisms are different between daytime and nighttime. Though the observational results show that occurrence of daytime MSTID is maximum during the winter, the day-to-day and longitudinal variation of occurrence are not yet explored well.

We have analysed total electron content (TEC) data obtained from more than 1,200 GPS receivers in Japan in 2011. To obtain perturbation component of TEC, which could be caused by MSTID, we have subtracted 1-hour running average from the original TEC time series for each pair of satellites and receivers, and converted the slant to vertical TEC. We have defined MSTID activity as dI/I, where dI is the standard deviation of the perturbation component within 1 hour, and I is 1-hour average absolute vertical TEC. MSTID activity is found to be higher in winter than in other seasons. We have compared the observed MSTID activity with the MSTID activity obtained from TEC simulated by the GAIA (Ground-to-topside model of Atmosphere-ionosphere for Aeronomy). To estimate the MSTID activity from the GAIA TEC data, we obtained detrended TEC by subtracting 2-hour running average from the TEC, and calculated standard deviation of the detrended TEC in 2 hours. MSTID activity was obtained as a ratio of the standard deviation to the 2-hour averaged TEC. Present analysis shows that daytime MSTID activities simulated by the GAIA are also higher in winter (December-February) than in other season, indicating that the GAIA succeeded to reproduce seasonal variation of the MSITD activity during daytime. In addition to this, day-to-day and longitudinal-latitudinal variation of daytime MSTID activity will also be detailed in the presentation.

Seasonal differences in fine structures of the Es layer observed by a Ca+ resonance scattering lidar

Mitsumu K. Ejiri[1]; Takanori Nishiyama[1]; Katsuhiko Tsuno[2]; Takuo Tsuda[3]; Makoto Abo[4]; Takuya Kawahara[5]; Satoshi Wada[6]; Takuji Nakamura[1]
[1] NIPR; [2] RIKEN; [3] UEC; [4] System Design, Tokyo Metropolitan Univ.; [5] Faculty of Engineering, Shinshu University; [6] ASI, RIKEN

Calcium ion (Ca^+) is only metallic ion in the mesosphere and lower thermosphere (MLT) region that can be measured by resonance scattering lidar. Metallic ions, including Ca^+, originating from meteors are gathered in a narrow layer by vertical shear of horizontal neutral wind in the lower thermosphere, forming sporadic E (E_s) layers. Temporal variation of the Ca^+ density profiles observed by a Ca^+ resonance scattering lidar with high time and height resolutions can detect fine structure and time evolution of plasma irregularities in the E_s layer. A frequency tunable resonance scattering lidar to install and operate it at Syowa, Antarctica had been developed by the National Institute of Polar Research (NIPR). The lidar has a capability to observe the MLT temperature profiles and the density variations of minor constituents such as Fe, K, Ca^+, and aurorally excited N_2^+ in the MLT region. In August 2014, it received the first light from Ca^+ in E_s layer. After that, we increased the resolution of the Ca^+ observation and have succeeded in getting the Ca^+ profile with time/height resolution of 5 sec/15 m. Also, background noise was reduced using narrower band-pass filter in an optical receiving system after December 2015. In this study, we show fine structures of the Ca^+ layer corresponding to some E_s layer events observed in March, August, September and December in 2015 and 2016 and will discuss differences between summer and winter and some characteristics seen around equinox.

中緯度域スポラディックE層の有する様々な構造の発生メカニズムに関するシミュレーション

安藤 慧 [1]; 齊藤 昭則 [2]; 品川 裕之 [3]; 江尻 省 [4]; 宮崎 真一 [1]
[1] 京大・理; [2] 京都大・理・地球物理; [3] 情報通信研究機構; [4] 極地研

Simulation on formation mechanisms of various structures of sporadic E layer

Satoshi Andoh[1]; Akinori Saito[2]; Hiroyuki Shinagawa[3]; Mitsumu K. Ejiri[4]; Shinichi Miyazaki[1]
[1] Earth and Planetary Sciences, Kyoto Univ.; [2] Dept. of Geophysics, Kyoto Univ.; [3] NICT; [4] NIPR

We have developed a three-dimensional numerical model for ionosphere to investigate formation mechanism of sporadic E. Sporadic E is a highly dense plasma layer and often appears in the E-region of the ionosphere. The layer is a critical phenomenon for ionospheric dynamics because it is affected by both atmospheric waves from the lower region and electrodynamics coupling effect in the ionosphere. The physics of the sporadic E formation is described through the Wind Shear theory. According to the theory, ions are gathered in the thin layer by the vertical wind shear driven by large-scale atmospheric waves in the thermosphere, for example diurnal tides and semi-diurnal tides. Moreover, characteristics of sporadic E reflected shorter period tides and gravity waves are also observed, but these characteristics have not been investigated fully.

We have used neutral winds data of GAIA model for background parameters in our model, and have succeeded to simulate multiple structures of sporadic E observed before. Additionally, we have found the variety structures depending on the date of neutral winds data. In this presentation, we are going to introduce the formation mechanisms of these structures.

中緯度におけるスポラディックE層 (以下 Es 層) の生成・発達・消滅のメカニズムを解明するための 3 次元数値モデルを開発した。Es 層は電離圏 E 領域に発生するプラズマの高密度層である。Es 層は熱圏・中間圏から伝播してくる大気波動や電離圏 E-F 領域の電磁気学的結合によって影響を受けるため、超高層大気の物理を理解するうえで重要な現象である。現在、Es 層の発生機構は Wind Shear 理論が通説となっており、水平方向中性風の鉛直シアーが Es 層の形成には重要であることが示唆されている。この鉛直シアーは熱圏下部で振幅が特に大きい日周期と半日周期の潮汐波によって形成されると考えられているが、それに加えて、半日よりも短い周期の潮汐波や内部重力波などの Es 層への影響を示す先行研究も多数ある。現在のところ、これらの短い周期の潮汐波や内部重力波が Es 層の構造に対してどのように、どの程度の影響を与えているかの議論はいまだ深くなされていない。

今回、我々の開発した中緯度域電離圏モデルに対して、NICT が開発を進める GAIA モデルの中性風データを入力することにより、Es 層の二層構造を再現することに成功した。また、入力に用いた中性風データの日付によって様々な Es 層の構造が生じることも見出した。発表では中性風と再現された多様な Es 層の構造との関係性について、いくつかの事例を取り上げて紹介する。

航空航法用 VHF 帯電波の異常伝搬と GPS-ROTI を組み合わせたスポラディック E 層 2 次元空間構造の広域可視化

木村 康択 [1]; 細川 敬祐 [1]; 坂井 純 [1]; 斎藤 享 [2]; 津川 卓也 [3]; 西岡 未知 [3]; 石井 守 [3]; 冨澤 一郎 [4]
[1] 電通大; [2] 電子航法研; [3] 情報通信研究機構; [4] 電通大・宇宙電磁環境

Visualization of two-dimensional structure of Sporadic-E in a wide area by using air-band VHF radio observations and GPS-ROTI

Kotaku Kimura[1]; Keisuke Hosokawa[1]; Jun Sakai[1]; Susumu Saito[2]; Takuya Tsugawa[3]; Michi Nishioka[3]; Mamoru Ishii[3]; Ichiro Tomizawa[4]
[1] UEC; [2] ENRI, MPAT; [3] NICT; [4] SSRE, Univ. Electro-Comm.

Sporadic-E (Es) is one of the outstanding phenomena in the mid-latitude ionosphere, during which the electron density in the bottom of E region extremely increases often greater than that in the F region. It is generally known that Es reflects the VHF radio waves for the Analog TV broadcasting and FM radio broadcasting. Recently, it was suggested that VHF radio waves assigned for the aircraft navigation system (108-118 MHz) can also be reflected by Es and propagate in a long distance (anomalous propagation).

Since the beginning of May, 2019, we have been observing VHF radio waves in the air-band frequency range (VOR and ILS) at Chofu, Kure, Oarai, Sugadaira, Onna, and Sarobetsu in Japan. By using these data, we aim at estimating the occurrence of Es in a wide area. In addition, we also attempted to detect electron density irregularities within Es using ROTI (Rate of TEC index) routinely derived from GPS-TEC observations. We combined these two datasets in the same geographic coordinate system and tried to visualize the two-dimensional structure of Es in a wide area.

During the summer months in 2019, we detected an event of intense Es on July 4th, 2019 in the ROTI map. The Es first appeared in the south of the mainland of Japan, and then moved northward. ROTI visualized that the Es maintained its spatial structure elongating in the east-west direction for about 3 hours. In addition, the reflection points of air-band VHF radio waves well matched the structure visualized by ROTI. This result shows that the monitoring of air-band VHF anomalous propagation is an effective way to visualize the spatial structure of Es. In the presentation, we will introduce the strong point of the combination of ROTI and air-band VHF radar observations for visualizing the two-dimensional spatial structure of Es. We also discuss how the increase of the observation points affects the coverage of the Es visualization.

電離圏 E 領域の下部において、電子密度が F 領域を超えるほど増大する現象をスポラディック E 層 (Es) と呼ぶ。日本上空では夏季の昼間に集中して発生するという季節的特徴がある。Es が発生した際には、アナログ放送や FM 放送に割り当てられた VHF 帯の電波が反射され異常伝搬することがよく知られていたが、近年の研究によって、航空航法用通信に割り当てられた VHF 帯の電波 (108-118 MHz) も Es によって反射されていることが統計的に示された。

我々は、2019 年 5 月から、調布、呉、大洗、菅平、恩納、サロベツの 6 地点において、Es 反射によって異常伝搬した航空航法用 VHF 帯電波 (VOR) の広域観測を開始した。受信信号から受信局、日付、時刻 (時間分解能 10 秒)、受信周波数、受信信号強度を抽出し、観測データを準リアルタイムで公開している。本研究では 6 地点の受信局で取得された航空航法用 VHF 帯電波の異常伝搬データと、GPS 衛星の電離圏全電子数 (TEC: Total Electron Content) の 5 分間での変動値の標準偏差を取った電子密度擾乱指数 ROTI (Rate of TEC Index) を組み合わせることによって、広域での Es の 2 次元空間構造の可視化を試みた。

2019 年の夏季の観測において、2019 年 7 月 4 日に特に大規模な Es の発生が確認できたため、この事例について ROTI と異常伝搬データを組み合わせた解析を行った。ROTI のデータでは、本州南部で発生した Es が約 3 時間にわたって東西に伸びた構造を保ったまま、南から北へと移動する様子が検出された。また同時刻の異常伝搬データに基づいて算出された航空航法用 VHF 帯電波の Es による反射点が ROTI によって可視化された Es の空間構造と一致することが分かった。この結果から、航空航法用 VHF 帯電波の異常伝搬データから反射点のマッピングを行うことが、 Es の 2 次元空間構造を可視化する上で有効な手段となりうることが示された。発表では、他の観測手法と比較して、ROTI と航空航法用 VHF 帯電波の異常伝搬データを組み合わせることがどのようなメリットを持つのかを示し、異常伝搬データを取得するための受信局の数を増やすことによって Es 空間構造可視化の精度がどのように変化するのかについて議論する。

高緯度電離圏擾乱の SAR イメージング

佐藤 博厚 [1]; Kim Jun Su[1]; 小川 泰信 [2]; Haggstrom Ingemar[3]
[1] DLR; [2] 極地研; [3] EISCAT Headquarters

High latitude ionospheric disturbances in space-born Synthetic Aperture Radar images

Hiroatsu Sato[1]; Jun Su Kim[1]; Yasunobu Ogawa[2]; Ingemar Haggstrom[3]
[1] DLR; [2] NIPR; [3] EISCAT HQ

We present space borne L-band Synthetic Aperture Radar (SAR) observation of small-scale plasma density irregularities over Tromsoe, Norway. Low-frequency SAR systems have been suggested to achieve mapping of ionospheric density distributions in terms of Total Electron Content (TEC) at a finer resolution than do GPS/GNSS measurements. This study uses Advanced Land Observation Satellite 2 (ALOS-2)/Phase Array type L-band Synthetic Aperture Radar-2 (PALSAR-2) system and simultaneous ground observations. The SAR system detects local change of TEC down to sub-kilometer scale in in 70 km x 50 km acquisition frame. Such images are compared with European Incoherent Scatter (EISCAT) UHF radar measurement and 558 nm all sky images. The irregular electron density is typically characterized by tens of kilometers of band-like structures aligned in the east-west direction with small patch-like structures. We present a method for estimating the local change of TEC gradient and the height of ionospheric irregularities by using single-image sub-band data. The results suggest that these observed small scale density structures are likely to be associated with precipitating electrons in auroral ionosphere.

GNSS-TEC と SuperDARN レーダー観測に見られる SED の時間・空間発展について

新堀 淳樹 [1]; 大塚 雄一 [2]; 惣宇利 卓弥 [3]; 津川 卓也 [4]; 西岡 未知 [4]; Bristow William A.[5]; Ruohoniemi John M.[6]; Shepherd Simon G.[7]; 西谷 望 [8]
[1] 名大・宇地研; [2] 名大宇地研; [3] 名大　ISEE; [4] 情報通信研究機構; [5] アラスカ大; [6] バージニア工科大; [7] Dartmouth College; [8] 名大 ISEE

Temporal and spatial evolutions of storm enhanced density (SED) as seen in the GNSS-TEC and SuperDARN radar observations

Atsuki Shinbori[1]; Yuichi Otsuka[2]; Takuya Sori[3]; Takuya Tsugawa[4]; Michi Nishioka[4]; William A. Bristow[5]; John M. Ruohoniemi[6]; Simon G. Shepherd[7]; Nozomu Nishitani[8]
[1] ISEE, Nagoya Univ.; [2] ISEE, Nagoya Univ.; [3] ISEE, Nagoya Univ.; [4] NICT; [5] UAF; [6] ECE, Virginia Tech; [7] Dartmouth College; [8] ISEE, Nagoya Univ.

Temporal and spatial evolutions of storm enhanced density (SED) in the low and midlatitudes during a geomagnetic storm that occurred on 27-28 September 2017 have been investigated using GNSS (Global Navigation Satellite System)-TEC (Total Electron Content) and midlatitude SuperDARN radar data. The GNSS-TEC data analysis results show that the TEC enhancement related to the storm enhanced density (SED) first occurs in the American sectors (11:00-15:00 MLT: magnetic local time) at high latitudes within one hour after the southward turning of interplanetary magnetic field (IMF). The enhanced TEC region moves to the mid- and low-latitude regions extending into both the latitudinal and longitudinal directions as the geomagnetic storm develops. The midlatitude trough with a latitudinally narrow structure is also observed in the higher latitude of the TEC enhancement. The signature of the TEC enhancement is not only observed in the American sector but also in the, European, Japanese, and Australian sectors. During the late main phase of the geomagnetic storm, another TEC enhancement related to the equatorial ionization anomaly (EIA) occurs in equatorial and low latitudes and extends to higher latitudes. The two prominent TEC enhancements due to the SED and EIA finally meet each other at low latitudes. On the other hand, the midlatitude ionospheric plasma flow observations taken by the SuperDARN radars at Adak Island East (ADE), Adak Island West (ADW), Blackstone (BKS), Christmas Valley East (CVE), Christmas Valley West (CVW), Fort Hays East (FHE), Fort Hays West (FHW), Hokkaido West (HKW), and Hokkaido East (HOK) show that large poleward and westward flows with a speed of more than 1000 m/s appear in the noon to evening sectors (12:00-23:00 MLT) after the southward turning of IMF. The intense ionospheric plasma flows exist near the high-latitude boundary of SED and inside the midlatitude trough. The location of the plasma flows moves equatorward together with the SED and midlatitude trough as the geomagnetic storm develops. Sometimes, the large westward flow is observable in the TEC enhancement related to SED. From these analysis results of the GNSS-TEC and SuperDARN radar data, it can be considered that the mid-latitude TEC enhancement related to SED is not generated by the high-latitude expansion of the EIA, but by the uplifting and westward transportation of ionospheric plasma in the sunlit region due to localized intense electric field drifts associated with storm-time enhanced ionospheric convection.

気象再解析データ中の気温・オゾンに現れる太陽プロトンイベントの影響

冨川 喜弘 [1]
[1] 極地研

Responses of temperature and ozone to solar proton events in the latest reanalysis data

Yoshihiro Tomikawa[1]
[1] NIPR

Solar proton events (SPEs) have some impacts on the middle atmosphere through NOx/HOx formation, its subsequent ozone destruction, and Joule heating. Several observational and simulation studies have reported their impact on temperature and circulation in the middle atmosphere. However, their impact has never been captured in the meteorological reanalysis data. The latest meteorological reanalyses have been developed to assimilate satellite radiance and ozone observations in the upper stratosphere and lower mesosphere, so that they have a potential to reproduce atmospheric impacts of SPEs in those regions. This study examines whether the SPEs' impacts on the middle atmosphere can be captured in the latest reanalysis data or not.

大型大気レーダー PANSY で観測される中間圏エコー強度のオーロラ活動依存性

村瀬 清華 [1]; 片岡 龍峰 [2]; 西山 尚典 [2]; 西村 耕司 [2]; 橋本 大志 [3]; 田中 良昌 [4]; 門倉 昭 [5]; 冨川 喜弘 [2]; 堤 雅基 [2]; 佐藤 薫 [6]; 三好 由純 [7]
[1] 総研大・極域科学; [2] 極地研; [3] 京大・情報学・通信情報システム; [4] 国立極地研究所/総研大; [5] ROIS-DS/極地研; [6] 東大・理; [7] 名大 ISEE

Auroral activity dependence of mesospheric echo power observed by PANSY radar

Kiyoka Murase[1]; Ryuho Kataoka[2]; Takanori Nishiyama[2]; Koji Nishimura[2]; Taishi Hashimoto[3]; Yoshimasa Tanaka[4]; Akira Kadokura[5]; Yoshihiro Tomikawa[2]; Masaki Tsutsumi[2]; Kaoru Sato[6]; Yoshizumi Miyoshi[7]
[1] Polar Science, SOKENDAI; [2] NIPR; [3] Communications and Computer Eng., Kyoto Univ.; [4] NIPR/SOKENDAI; [5] ROIS-DS/NIPR; [6] Graduate School of Science, Univ. of Tokyo; [7] ISEE, Nagoya Univ.

The PANSY radar is the largest atmospheric radar in Antarctica, installed at Syowa Station in 2011, and has been operated in full-system since 2015. It has observed various atmospheric phenomena in the polar region. One of the interesting aspects of such phenomena is the effect of auroral activity on neutral atmosphere, which provides an important clue to understanding the possible links between the space environment and terrestrial environment. Even the middle mesosphere is ionized by energetic electrons during an auroral breakup event as recently reported by Kataoka et al. (2019, EPS), in which the PANSY radar detected transient enhancement of the VHF echo power, called polar mesospheric winter echo (PMWE). In this study, we statistically investigate the similar kind of echo power enhancement in the mesosphere using the continuous data of the PANSY radar in winter seasons during 2017-2018. The auroral activity is categorized by the amplitude of the southward excursion of the local magnetic field data at Syowa station, which is a proxy of the amplitude of auroral electrojets. More specifically, the minimum values of north-south magnetic field component at evening-to-midnight sector are used as the peak time of auroral activity, and the altitude-resolved mesospheric echo powers are superposed to the peak times to find the averaged picture. As a result, a positive dependence of the superposed echo power of PMWE is found against auroral activities. Another interesting finding is the simultaneous enhancement of a noise level covering wide altitude ranges, which can be interpreted by the contamination of the side-lobe echoes from field-aligned irregularities (FAIs). The rapid growth of the FAIs may be a result of current-convective instability associated with auroral field-aligned currents. Although we obtained the averaged pictures against auroral activity, our understanding is still far from prediction. We sometimes find no echoes during high auroral activity, and we sometimes find strong noise without active auroras. We therefore examine such exceptional events in more detail to understand other possibilities of the origins of echo power enhancement and the noise enhancement by using other observation data sets at Syowa Station as well as satellite data sets. We also apply a new method to clearly differentiate the noise using the original PANSY echo data to understand the fundamental properties of FAIs related to auroral activities.

2012 年 5 月、南極昭和基地において本格運用が開始された PANSY（Program of the Antarctic Syowa MST/IS）レーダーは、VHF 帯でのドップラー観測によって、大気圏での気象現象から電離圏の擾乱まで、広い高度域の大気現象を観測できる最新の大型大気レーダーである。PANSY レーダーによって観測されている極域特有のエコーの一つに、冬季に中間圏で見られる PMWE（Polar Mesospheric Winter Echo）がある。PMWE は、中性大気の乱流と日照による大気の電離によるものに加え、オーロラ活動による影響を含んでいるため、宇宙から大気へのインパクトを理解する上で重要な現象である。近年、PANSY の観測から、磁気嵐や太陽プロトン現象に関連して PMWE の観測率が上昇すること（Nishiyama et al., 2018, JGR）や、オーロラ爆発に伴う相対論的電子の降り込みによって中間圏の電離度が増加し PMWE が検出されたこと（Kataoka et al., 2019, EPS）が報告されている。この他、オーロラ活動に伴ってエコーのノイズレベルが上昇することが知られているが、その主な原因としては、メインビームではなくアンテナサイドローブによる遠方の沿磁力線不規則構造（FAI）からのエコーの混入が考えられている。本研究では、もし以上に挙げた事項が主要因であれば、オーロラ活動が活発になるほど PMWE やノイズレベルが強まるはずではないかと考え、フルシステムの連続観測から得られた 2017～2018 年の 2 年分の冬季の中間圏エコーデータについて統計解析を行った。オーロラ活動の指標としては、オーロラジェット電流に伴って大きな変化を示す磁場観測データの南北成分を用いた。より具体的には、各晩での昭和基地における磁場の南北成分の最小値によってオーロラ活動の大小を分類し、最小となる時刻を基準としてエコー強度の時間変化を重ね合わせることで、各オーロラ活動度におけるエコー強度の高度分布の平均像を得た。この統計解析の結果、オーロラ活動が活発なほど PMWE の強度が平均的に強くなり、またノイズレベルも高まる傾向が得られた。これらの結果は、オーロラ活動による相対論的電子の降り込みが普遍的に起こっているものであるということ、また同様のオーロラ活動が FAI の生成を通して PANSY のエコー観測のノイズ源にもなることを示唆している。ただし、オーロラ活動が活発でも PMWE の見られないイベントや、オーロラ活動では説明が難しいノイズ増大イベントも複数見つかっているため、それぞれの現象の予測が可能なレベルの理解には至っていない。本発表では、ノイズを積極的に抽出する新しい PANSY エコーの分析手法も用いて、また昭和基地の様々な拠点観測データや衛星データとの比較から多面的に現象を把握することで、そのような個々の特徴的なイベントについて詳細に解析した結果も含めた研究の現状を報告する。

国際宇宙ステーションからのデジタルカメラ観測を用いた脈動オーロラ時空間特性の広域可視化

南條 壮汰 [1]; 穂積 裕太 [1]; 細川 敬祐 [1]; 片岡 龍峰 [2]; 三好 由純 [3]; 大山 伸一郎 [3]; 尾崎 光紀 [4]; 塩川 和夫 [5]; 栗田 怜 [3]
[1] 電通大; [2] 極地研; [3] 名大 ISEE; [4] 金沢大; [5] 名大宇地研

Visualizing Large-Scale Distribution of the Pulsating Aurora Periodicities: Digital Camera Observations from the ISS

Sota Nanjo[1]; Yuta Hozumi[1]; Keisuke Hosokawa[1]; Ryuho Kataoka[2]; Yoshizumi Miyoshi[3]; Shin-ichiro Oyama[3]; Mitsunori Ozaki[4]; Kazuo Shiokawa[5]; Satoshi Kurita[3]
[1] UEC; [2] NIPR; [3] ISEE, Nagoya Univ.; [4] Kanazawa Univ.; [5] ISEE, Nagoya Univ.

Various ground-based and space-based imagers have enable us to capture the dynamical characteristics of aurorae. However, it still remains difficult to observe their fine-scale structures in a wide area with a reasonable temporal resolution. For example, the THEMIS All-Sky Imagers (ASI) network succeeded in capturing aurora in a wide area. But, since the temporal resolution of the ASIs is 3 seconds, they are not good at observing rapidly varying aurorae such as pulsating aurora (PsA). In addition, since ground-based observations are affected by the weather, it is rare to be able to observe auroras at all the stations. Space-based ultraviolet imagers such as ones onboard the IMAGE and DMSP satellites can observe the large-scale structure, but it is, in turn, difficult to observe their fine structures, as they do not have sufficient temporal resolutions.

The photographs taken with a digital single-lens reflex cameras from the International Space Station (ISS) have sensible spatial and temporal resolutions and a wide field-of-view that can overcome the limitation mentioned above. In recent years, with the remarkable development of digital imaging technology, it is possible to capture aurorae from the ISS with a temporal resolution less than 1 second. Besides, the high spatial resolution, that is one of the big advantages of digital camera images, enables us to distinguish the spatial structure of aurora within 1 km. However, since these photographs are not taken for scientific research, accurate imaging parameters, such as camera orientation or angle-of-view, are unknown. It is required to estimate them in order to map the photographs onto the geographic coordinate system. At the JpGU meeting, we presented methods for calibrating these imaging parameters and mapping the images. By showing that we confirmed that the accuracy of mapping is sufficient for studies of PsA. In this presentation, we will present several case studies to show the spatial distribution of the PsA periodicities in a wide area. We discuss what factor controls the temporal variations of PsA based on the wide area visualization of their periodicities.

地上や宇宙機からの様々な光学イメージング観測がオーロラの時空間特性の解明に用いられてきた。しかし，オーロラの詳細な時空間特性を広域に観測することは依然として難しいままである。たとえば，微細な構造を押さえながらある程度広い領域を撮像できる地上全天イメージャとして THEMIS ASI ネットワークが存在するが，撮像の時間分解能が 3 秒であるため，脈動オーロラのような数秒から数十秒での変動を起こすオーロラの観測には不向きである。EMCCD カメラは高い時間分解能を有するが，その高価さゆえに広い経度域をカバーするように設置することは難しい。また，地上観測は天候の影響を受けるため，実際に広域での観測が成立する可能性が低いという問題点もある。宇宙機に搭載された広域イメージャとして，IMAGE 衛星や DMSP 衛星の紫外撮像装置が挙げられるが，時間分解能が不十分であるだけでなく，紫外光での観測であるために微細構造を観測することは難しい。

国際宇宙ステーションからデジタル一眼レフカメラを用いて撮像されている画像は，地上観測と衛星観測の弱点を同時に克服できる広い視野と高い時空間分解能を持ち合わせている。昨今の目覚ましいデジタル撮像技術の発展に伴い，近年は 1 秒以下の時間分解能が達成されている。また，デジタルカメラの特徴である高い空間分解能は，オーロラの 1 km 以下の構造を区別することができる。ただし，これらのデジタルカメラ画像は科学研究用途で撮像されたものではないため，画像を地理座標上にマッピングするためには，撮像視野を決定するイメージングパラメータ（カメラの向きや画角など）の正確な推定（較正）が求められる。先の JpGU では，これらのパラメータの較正手法，またそのパラメータを用いたマッピング手法を紹介し，その時空間精度が脈動オーロラの解析に耐えうるものであることを報告した。今回はこれらのデータセットを用いて，脈動オーロラの明滅周期の空間分布を広域に調べた結果を報告する。特に，数秒から数十秒であると言われている脈動オーロラの周期性が，緯度や磁気地方時にどのように依存しているのかを，広域を観測できる長所を活かし，シングルイベントでスナップショットとして可視化した結果を示す。その依存性の有無によって，周期性を決定している要因について議論する予定である。

しらせ船舶搭載オーロラ・大気光の観測全天イメージャーの開発

八木 直志 [1]; 坂野井 健 [2]; 穂積 裕太 [3]; 津田 卓雄 [3]; 齊藤 昭則 [4]; 江尻 省 [5]; 西山 尚典 [5]; 解良 拓海 [6]
[1] 東北大・理・地物; [2] 東北大・理; [3] 電通大; [4] 京都大・理・地球物理; [5] 極地研; [6] 東北大・理・PPARC

The development of all-sky imagers on Shirase for aurora and airglow observations

Naoshi Yagi[1]; Takeshi Sakanoi[2]; Yuta Hozumi[3]; Takuo Tsuda[3]; Akinori Saito[4]; Mitsumu K. Ejiri[5]; Takanori Nishiyama[5]; Takumi Kera[6]
[1] Geophys. , Tohoku Univ.; [2] Grad. School of Science, Tohoku Univ.; [3] UEC; [4] Dept. of Geophysics, Kyoto Univ.; [5] NIPR; [6] PPARC, Tohoku Univ.

We developed an All Sky Imager (ASI) which will be installed on Antarctic research ship Shirase to observe aurora and airglow. In this presentation, we report the development of ASI.

Optical observation with all-sky imager so far has been limited only to the ground. In North America, THEMIS All Sky Imager Array, which consists of 20 all sky imagers made much progress in understanding of auroral phenomena. On the other hand, in the Southern hemisphere, while some imagers are working at Syowa Station (S69°, E39°), from East of Syowa station to South of Australia, there are huge blank area of ground-based observations under the aurora and sub-aurora regions due to the lack of lands. Moreover, a research on propagation of atmospheric gravity wave associated with polar winds in a latitude direction, which is supported by ANtarctic Gravity Wave Instrument Network (ANGWIN) on the Antarctica, can be better understood from that blank area on the sea.

In order to cover this blank area of ground-based observations, we developed the high-sensitivity ASI system which will be installed on Antarctic research ship Shirase. The ASI on Shirase can cover the blank area with optical observation. The ASI can also detect the faint emission of airglow with exposure time of a few minutes. During the time of a few minute exposure, the shake of Shirase is designed to be canceled by using a 3-axis controlled gimbal. The ASI consists of bandpass filter (central wavelength: 630nm), fisheye lens (field of view: 185° x185°, focal length: 2.7mm, F-number: 1.8), 1-inch cooling CMOS camera (ZWO/ASI-183MMPro 5496x3672pix) and 3-axis controlled gimbal. The camera is operated with LINUX pc, named LIVA-Q2. Automatic camera operation system has been built in the pc. This system achieves automatic adjustment of camera operational parameters such as time period and interval of taking images, exposure time and gain of image sensor, depending on its geological coordinates which can be obtained from GPS. All the observation equipments are stored inside of box with an acrylic dome on top of that. The box is going to be installed on the 06th left deck and data logger while data logger system will be built in the observation room of Shirase.

The calibration test of ASI was conducted at National Institute of Polar Research on July 26th and 27th, 2019, by using integrating sphere. From the result of calibration tests, we confirmed that ASI can detect emissions from 400R to 200kR with S/N >100 by adjusting its exposure time to 10s, 30s, and 120s.

In addition, we conducted ground test observation with the ASI at Zao observatory of Tohoku University (N38°, E140°), from 1am to 3am on June 13th, 2019 (JST). From images taken with 2-minute exposure and 30 second frame intervals, subtracting 1-hour averaged image as background emissions, we concluded that OI 630nm emission of airglow was detected with the ASI. After 2am, striped structure of airglow with the wavelength of 300km moved to south-westward and the TEC data from GPS satellites at corresponding time shows good similarity in the structure. From those characteristics, that striped structure indicated the existence of Medium-scale traveling ionospheric disturbance at that time.

After the installation to Shirase on September and operation verification at the shakedown cruise from the end of September to October, whole observation system will be completed. From the departure on November and to the return to Japan on March, 2020, the observation of airglow and aurora in wavelength of 630nm will be continuously conducted by the ASI. Although the observation data will be collected on March 2020, a part of the data will be sent on the internet as a thumbnail.

Moreover, additional imagers for N2 1PG emission and Na airglow is going to be installed in 2020 and 2021 respectively so more quantitative and multiple observations will be conducted.

我々はオーロラ・大気光観測を目的とし、南極観測船しらせ船舶に搭載される全天イメージャーを開発した。今回はその開発状況と初期成果を報告する。

これまでの地上オーロラ・大気光観測は陸域上に限られていた。例えば北米 THEMIS All-Sky Imager Array では約 20 台の全天イメージャーが、上空のオーロラ帯・サブオーロラ帯のオーロラ発光現象を観測しており [Donovan et al., 2006]、多くの成果を上げている。一方南半球では昭和基地（南緯 69 度、東経 39 度）がオーロラ帯に位置しているが、その東側のオーロラ帯は海洋があり、観測の空白域となっている。さらに南極大陸で近年盛んに研究されている、極夜ジェットに伴う大気重力波の伝搬に関する観測研究は、ANtarctic Gravity Wave Instrument Network (ANGWIN) プロジェクトによって南極大陸上空がサポートされているが、大気重力波の緯度方向伝搬を効率よく捉えるためには、観測の空白域である海洋上観測点が不可欠である。

我々は、この観測空白域を補うことを目指し、船舶上からの高感度全天イメージャーシステムの開発を進めている。本研究では南極観測船しらせに搭載する全天イメージャーを開発した。国立極地研究所の南極地域研究活動を担う南極観測船しらせは、日本を 11 月に出航し同年 12 月末に昭和基地に到着した後、翌年 2 月初旬に昭和基地を出発、4 月に

日本に帰港する。特に、12 月から 2 月にかけたしらせの航路上でオーロラ帯を通過するためオーロラ観測が期待される。この全天イメージャーは、露光時間を数分に設定することで大気光を観測できる性能を持つ。数分間の露光中に生じ得る船舶の揺れは、ジャイロと駆動モータによる 3 軸制御ジンバル機構を用いることで打ち消すことができる設計である。

我々が開発した全天イメージャーは、中心波長 630nm バンドパスフィルター、魚眼レンズ（視野 185x185 度、焦点距離 2.7mm、F 値 1.8）、冷却 1 インチ CMOS カメラ（ZWO/ASI-183MMPro 5496x3672 ピクセル）、そして 3 軸制御ジンバル（DJI Ronin-S）から構成される。カメラは LINUX 搭載小型 PC の LIVA-Q2 で制御され、データ取得、ビニング処理、データ送信を自動で行うシステムが構築されている。カメラ自動運用システムは、しらせが供給する GPS データから、地理座標、標準時間を取得し、そこから適切な撮像モード（撮像する時間帯、撮像間隔、露光時間、ゲイン）を設定することができる。観測装置一式は、アクリルドームを有する耐候性の観測箱に格納され、しらせ 06 甲板左舷側に設置される。また、データロガー等はしらせ観測室に設置する。

我々は、2019 年 6 月 26 日、27 日に国立極地研究所の積分球を用いてカメラの校正実験を行なった。校正実験の結果から、対象物の明るさに応じて露光時間を 5 秒、10 秒、30 秒、120 秒に設定することで、400R から 200kR の発光に対して S/N>100 でデータ取得できることを確認した。

また、大気光の試験観測を、2019 年 6 月 13 日に東北大学蔵王観測所（北緯 38 度、東経 140 度、海抜 685m）で行なった。2 分の露光時間で 30 秒おきに撮像を行った画像から、前後 30 分に平均した画像を背景光として差し引くことで、大気光の OI630nm 発光を確認した。午前 2 時 JST 以降は南西方向に伝播するおよそ波長 300km の縞構造を観測した。この構造は GPS 衛星 Total Electron Content(TEC) データが示す構造とも良い対応があり、中規模伝搬性電離圏擾乱（MSTID）と考えられる。

今後 9 月にしらせへの設置、9 月末から 10 月にかけて試験航海による船舶上観測による動作実証を行い、観測システムを完成させる。11 月のしらせ出航以降 2020 年 3 月に日本に帰港するまで、630nm 大気光とオーロラ発光観測の連続観測を継続して行う。観測データは 3 月に帰国後収集するが、インターネットで一部少量の観測結果を配信する。また、2020 年度にはオーロラ N2 1PG 発光や Na 大気光を観測するイメージャーを追加し、より定量的・多角的な科学観測を実施する計画である。

カスプ領域における中性大気質量密度異常の数値モデリング

大井川 智一 [1]; 品川 裕之 [2]; 田口 聡 [1]
[1] 京大理; [2] 情報通信研究機構

Numerical modeling of the neutral mass density anomaly in the cusp region

Tomokazu Oigawa[1]; Hiroyuki Shinagawa[2]; Satoshi Taguchi[1]
[1] Grad school of Science, Kyoto Univ.; [2] NICT

http://www-step.kugi.kyoto-u.ac.jp/

The thermosphere and ionosphere in the polar region have been studied for a long time. Recent results of the ground and satellite measurements have suggested that polar thermospheric and ionospheric dynamics are extremely complicated. In particular, in the auroral region, various processes, such as ion-neutral drag, Joule heating, heating and ionization by particle precipitation, chemical processes, and diffusion, are strongly coupled. In the auroral region, particularly in the cusp, previous observations have shown the neutral mass density anomaly, where the neutral mass density is several tens of percent larger than that of ambient regions. Previous modeling studies are partially successful in reproducing it under geomagnetically disturbed conditions, whereas it is also observed under quiet conditions. It is considered that soft electron precipitation and local heating in the F region play significant roles. However, we still have not understood how such processes contribute to the mass density anomaly in detail. In order to study the mesoscale density anomaly in the cusp, we employ a high-resolution numerical model including various physical and chemical processes. In contrast to previous studies, it is shown that not only Joule heating but also particle heating caused by electron precipitation is important for thermospheric heating. We will report how thermospheric processes such as electron precipitation and Joule heating contribute to the mass density anomaly using a two-dimensional numerical model.

極域の熱圏・電離圏は長年にわたって研究がなされてきたが、近年の地上や衛星からの観測により、そのダイナミクスはきわめて複雑であることが明らかになりつつある。特にオーロラ領域においては、イオンと中性気体のドラッグ、Joule 加熱、降下粒子による加熱と電離、化学反応、拡散等の様々な過程が相互作用していることが知られている。このオーロラ領域の、特にカスプで特徴的なメソスケールの現象として、中性大気の質量密度が周囲よりも数 10%以上大きい質量密度異常が挙げられる。これまでの数値計算による研究では、磁気的に擾乱の強い場合についてはこの現象をある程度再現できているが、実際には静穏時においても質量密度異常は観測されている。また、この現象の発生には低エネルギーの電子の降り込みや F 層の局所的な加熱が重要な役割を担っていると考えられているが、それぞれの過程がどの程度寄与するのかについても未だ詳細は明らかでない。本研究では、このようなメソスケールの密度異常を調べるために、様々な物理・化学過程を含んだ高分解能な数値モデルを使用した。その結果、熱圏加熱の過程として、先行研究とは異なり Joule 加熱だけでなく降下電子による粒子加熱も重要であることが明らかになってきた。本講演では、2 次元数値モデルを用いて、このような降下電子や Joule 加熱等の過程が質量密度異常の発生にどのように寄与するのかを定量的に評価した結果を報告する。

電離圏電気伝導度を算出するための衝突周波数

家田 章正 [1]
[1] 名大宇宙地球研

Ion-neutral collision frequencies for calculating ionospheric conductivity

Akimasa Ieda[1]
[1] ISEE, Nagoya Univ.

http://www.isee.nagoya-u.ac.jp/~ieda/

Molecular oxygen collides with its first positive ion in the earth's ionosphere. The collision frequency of this particle pair is used to calculate the electric conductivity. However, for this parental pair there are two collision types, resonant and nonresonant, and the selection of the collision type has been different among previous studies in calculation of conductivity. In the present study we clarify that the nonresonant collision is essential for this pair because relevant temperatures are low. That is, the peak of the ionospheric conductivity is located at altitudes between 100 and 130 km, where the temperatures of ions and neutral particles are usually lower than 600 K, for which nonresonant collision is dominant. The collision frequency would be underestimated by 30% if the resonant collision was assumed at 110-km altitude (where the temperature is 240 K). The impact of this difference on the conductivity is estimated to be small (3%), primarily because molecular nitrogen is much more abundant than molecular oxygen. Although we have confirmed that the nonresonant collision is essential, we also include the resonant type, primarily in case of possible elevated temperature events. A set of ion-neutral collision frequency coefficients for calculating the conductivity is summarized, including other particle pairs, in the Appendices. Small corrections to the classical coefficients are made.

地球電離圏ではプラズマと中性大気が共存している。両者の衝突は、電離圏電流・電気伝導度を支配しており、衝突周波数として表現される。衝突周波数モデルは、論文によって大小さまざまな相違があり、その根拠は不明であることが多い。本研究では特に、酸素分子と酸素分子イオンの衝突について、衝突周波数モデル間の相違と意味を明らかにし、どのモデルを採用すべきかを議論した。

古典的な衝突周波数モデルでは、遷移温度 (800 K) を境に衝突のメカニズムが異なる。(1) 低温では中性粒子が分極することによる nonresonant 衝突、(2) 高温では電子移動による resonant 衝突が支配的であると考えられている。一方、近年採用されている衝突周波数モデルでは、(A) 北欧のレーダーコミュニティは温度に依らず (1) のみを用い、(B) 米国のモデリングコミュニティは温度に依らず (2) のみを用いるなど、さまざまであり、その根拠は不明であった。また遷移温度が 800 K である根拠も不明であった。

本研究では、まず、電気伝導度が集中する E 層 (高度 90-150 km) では、イオンや中性大気の温度は典型的には 200-600 K と、遷移温度より低温であるために、(1)nonresonant 衝突が支配的であることを確認した。従って、(B) は誤解である。次に、遷移温度は 800 K と教科書に記されてきたが、これは誤解であり、正しくは 600 K、すなわち、(1) と (2) が等しくなる温度であることを明らかにした。遷移温度が下がったために、(2) は E 層付近でも重要となり、無視しにくくなった。さらに、擾乱時など温度上昇した場合は (2) が必要である。従って、(A) は静穏時の E 層には概ね妥当だが、温度上昇時には特に不適切である。まとめると、(A) や (B) は一般性がなく、電気伝導度の算出には遷移温度 600 K を境として (1) と (2) の両方を用いることが適切である。

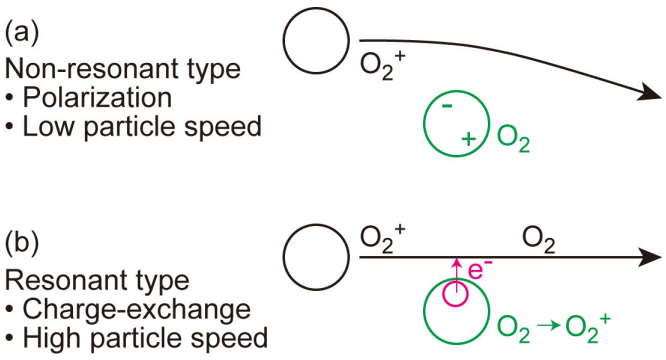

下層大気起源のプラネタリー波が電離圏変動に及ぼす影響について

三好 勉信 [1]; 山崎 洋介 [2]; 陣 英克 [3]; 藤田 茂 [4]; 吉川 顕正 [5]; 阿部 修司 [6]
[1] 九大・理・地球惑星; [2] 九大・理・地惑; [3] 情報通信研究機構; [4] 気象大; [5] 九州大学地球惑星科学専攻; [6] 九大・ICSWSE

Effect of planetary wave on short-term variability in the ionosphere

Yasunobu Miyoshi[1]; Yosuke Yamazaki[2]; Hidekatsu Jin[3]; Shigeru Fujita[4]; Akimasa Yoshikawa[5]; Shuji Abe[6]
[1] Dept. Earth & Planetary Sci, Kyushu Univ.; [2] Earth and Planetary Sciences, Kyushu Univ.; [3] NICT; [4] Meteorological College; [5] ICSWSE/Kyushu Univ.; [6] ICSWSE, Kyushu Univ.

Effect of the 6-day planetary wave on short-term variability in the ionosphere has been studied using satellite observation (CHAMP and SWARM) and numerical simulation (GAIA). Our analysis indicates that the amplitudes of the diurnal and semidiurnal tides fluctuates with about 6-day period through the nonlinear interaction between the 6-day planetary wave and the tides. This 6-day modulation of the diurnal and semidiurnal tides produces 6-day oscillation of the Equatorial Electro Jet (EEJ) and Total Electron Content (TEC) through the E-region dynamo process. Moreover, the satellite observation shows that the 6-day oscillation of EEJ and TEC has strong longitudinal variability. Mechanism for the longitudinal variability of EEJ and TEC also examined using the GAIA simulation. The relation between the 6-day wave and the geomagnetic variability is also studied.

下層大気起源のプラネタリー波により、どの程度の電離圏変動が引き起こされるかについて、CHAMP/SWARM による衛星観測と大気圏電離圏結合モデル（GAIA）による数値シミュレーションにより調べてみた。今回は、周期約 6 日のプラネタリー波の影響に注目して解析を行った。衛星観測により、赤道エレクトロジェット（EEJ）や全電子数（TEC）が、6 日波の出現時に約 6 日周期で変動していることが明らかになりつつある。そこで、GAIA を用いて、6 日波に伴う中性大気変動がどのような過程を経て電離圏に影響しているかについて調べてみた。解析の結果、6 日波と 1 日潮汐波・半日潮汐波の非線形相互作用により、中間圏上部から下部熱圏領域での潮汐波の振幅が 6 日周期で変動していることが分かった。潮汐波の 6 日周期変動が、E 層ダイナモを介して、電場分布に影響を与え、結果として赤道エレクトロジェットや全電子数（TEC）が 6 日周期で変動することが分かった。さらに、EEJ や TEC の 6 日周期変動には、強い経度依存性がみられるが、経度依存性を引き起こす原因についても GAIA を用いた解析により明らかにする予定である。さらに、6 日波と地上磁場変動との関係についても明らかにしていきたい。

Vertical Structure of Terdiurnal Tides in the Antarctic MLT Region: 15-Year Observation Over Syowa

Liu Huixin[1]; 堤 雅基 [2]
[1] 九大・理・地惑; [2] 極地研

Vertical Structure of Terdiurnal Tides in the Antarctic MLT Region: 15-Year Observation Over Syowa

Huixin Liu[1]; Masaki Tsutsumi[2]
[1] None; [2] NIPR

The terdiurnal tide (TDT) in the Antarctic mesosphere and lower thermosphere region
is poorly known. This study examines TDT using neutral wind observations at Syowa during years of 2004–2018. TDT is found to be a significant tidal component with distinct vertical structures and seasonal evolution. (1) It shows a prominent height-dependent seasonal variation with phase reversal at 94 km. (2) The vertical wavelength in summer is ∼40 km shorter than in winter. These features differ largely from those in the Arctic, indicating hemispheric asymmetry. The phase structure reveals a dominant upward propagating mode in local summer but superposition of more than one mode in other seasons. A downward propagating mode above 94 km in winter suggests Joule heating/ion drag as additional tidal sources to lower atmosphere ones. These results provide new constrains and benchmarks for model simulations that seek to understand terdiurnal tidal forcing mechanisms in polar regions. We also examine the possible influence of auroral heating on the tides using WACCM-X model.

The terdiurnal tide (TDT) in the Antarctic mesosphere and lower thermosphere region
is poorly known. This study examines TDT using neutral wind observations at Syowa during years of 2004–2018. TDT is found to be a significant tidal component with distinct vertical structures and seasonal evolution. (1) It shows a prominent height-dependent seasonal variation with phase reversal at 94 km. (2) The vertical wavelength in summer is ∼40 km shorter than in winter. These features differ largely from those in the Arctic, indicating hemispheric asymmetry. The phase structure reveals a dominant upward propagating mode in local summer but superposition of more than one mode in other seasons. A downward propagating mode above 94 km in winter suggests Joule heating/ion drag as additional tidal sources to lower atmosphere ones. These results provide new constrains and benchmarks for model simulations that seek to understand terdiurnal tidal forcing mechanisms in polar regions. We also examine the possible influence of auroral heating on the tides using WACCM-X model.

赤道成層圏を介した南北半球間結合

安井 良輔 [1]; 佐藤 薫 [1]; 三好 勉信 [2]
[1] 東大・理; [2] 九大・理・地球惑星

Interhemispheric coupling through the equatorial stratosphere

Ryosuke Yasui[1]; Kaoru Sato[1]; Yasunobu Miyoshi[2]
[1] Graduate School of Science, Univ. of Tokyo; [2] Dept. Earth & Planetary Sci, Kyushu Univ.

http://www-aos.eps.s.u-tokyo.ac.jp/~yasui/

Stratospheric Sudden Warmings (SSWs) often occur in the winter northern hemisphere (NH). This is accounted for breaking of the stationary Rossby waves in the stratosphere to form meridional circulation and the adiabatic heating in the polar region (Matsuno, 1970). On the other hand, it is shown that warming appears in the mesosphere and lower thermosphere (MLT) of the southern hemisphere (SH) after an Arctic SSW based on the model simulation (Karlsson et al., 2009). A scenario has been proposed to explain the interhemispheric coupling, by considering the modulation of the meridional circulation driven by gravity wave forcing in the MLT region (Koernich and Becker, 2010; KB10).

However, another scenario can be considered. While the warm anomaly is formed in the high latitudes of NH stratosphere, the cold anomaly is formed across the equator to the low latitude of the SH stratosphere (Semeniuk and Shephard, 2001). Quasi 2-day waves which probably give the second-largest wave forcing after gravity wave forcing (Sato et al., 2018) develop in such a situation during SSW (e.g., McCormack et al., 2009). The processes also result in warming in the SH upper mesosphere (France et al., 2018). This is a different interhemispheric coupling scenario from the KB10. In this study, we focus on events that arise cold anomaly in the equatorial stratosphere, reexamine the interhemispheric coupling from the viewpoint of wave forcing including both gravity waves and Rossby waves, and elucidate the warm anomaly formation in the SH MLT region.

We use the simulation data from a whole atmosphere model (i.e., Ground-to-topside model of Atmosphere and Ionosphere for Aeronomy (GAIA)). The analyzed period is 19 seasons from December to March of 1996-2015. The cold anomaly events in the equatorial stratosphere are extracted, and the central day (Day = 0) is defined as the date when the temperature anomalies from climatology at (0N,4.5hPa) and (20S,4.5hPa) are coldest and lower than 2sigma. The results are shown by composite analysis for the anomaly from the climatology.

The large Rossby wave forcing in the NH stratosphere strengthens the meridional circulation and builds cold anomaly in the SH stratosphere extending to ~40S. On the other hand, the warming in the SH first appears in the lower thermosphere after the occurrence of the cold anomaly in the equatorial stratosphere. Second, the warming is observed in the upper mesosphere. These warm anomalies are formed by resolved gravity waves in the lower thermosphere, and by Rossby waves especially by quasi 2-day waves in the upper mesosphere, respectively. Furthermore, it is also shown that quasi 2-day waves and resolved gravity waves causing the warm anomalies in the MLT region are generated from mesospheric barotropic/baroclinic instability and shear instability. These instabilities are caused by primary gravity wave forcing in the SH mesosphere, and these changes of gravity wave forcing are responsible to the formation of the easterly wind anomaly associated with the cold anomaly in the equatorial stratosphere. This simulated interhemispheric coupling occurs due to a different mechanism from the KB10 scenario. Longitudinal structures of the interhemispheric coupling which have not examined by previous studies will be also shown.

北半球冬季成層圏では、成層圏突然昇温（Stratospheric Sudden Warming; SSW）がしばしば発生する。これは、北半球成層圏において定在ロスビー波が砕波することで、子午面循環を形成し、その下降（上昇）流域で断熱圧縮（膨張）に伴って北極（赤道）成層圏が昇温（降温）する現象である（e.g., Matsuno, 1971）。一方、南半球中間圏及び下部熱圏（MLT）では、北極 SSW 後に高温偏差が現れることが数値シミュレーションによって示され（Karlsson et al., 2009）、この結果に基づいて中間圏重力波強制による北半球成層圏から北半球中間圏、南半球中間圏を通した気候値からの気温偏差の南北間半球結合のシナリオが提唱された（Koernich and Becker, 2010; KB10）。

しかし、SSW に伴い赤道を越えて南半球低緯度成層圏まで低温偏差が形成されること (Semeniuk and Shepherd, 2001) や南半球中間圏で重力波強制に次いで大きい波強制を与える準 2 日波（Sato et al., 2018）が、SSW 時に発達し（e.g., McCormack et al., 2009）、南半球上部中間圏で昇温をもたらすこと (France et al., 2018) から、KB10 シナリオとは異なる南北半球間結合が発生する可能性がある。したがって本研究では、赤道成層圏に大きな低温偏差をもたらすイベントに注目し、重力波およびロスビー波を両方含めた波強制の観点から南北半球間結合を見直し、南半球 MLT 領域の温度偏差形成の要因の解析を行なった。

本研究では、中性大気電離大気結合モデル Ground-to-topside model of Atmosphere and Ionosphere for Aeronomy (GAIA) による現実大気再現実験データを用いた。解析期間は、1996 年 12 月から 2015 年 3 月までの 19 シーズンである。大きな赤道低温偏差イベントは、4.5 hPa における赤道および 20S の気候値からの気温偏差が 2sigma 以上低くなる期間のうち最も気温偏差の小さくなる日を中心日（Day = 0）として抽出した。結果については、気候値からの偏差から 90 日の移動平均を取り除いたもの（以下、偏差と呼ぶ）についてコンポジット解析を行なった。

東西平均場では、北半球成層圏で大きな波強制によって、南半球成層圏では南緯 40 S 付近まで大きな低温偏差が現れ

ることがわかった。一方、南半球 MLT 領域の高温偏差は、赤道成層圏の低温偏差発生後、まず下部熱圏が昇温し、その後上部中間圏が昇温する様子が見られた。これらの高温偏差は、重力波およびロスビー波のそれぞれの波強制の偏差と比較すると、それぞれ下部熱圏は解像される重力波、上部中間圏はロスビー波、特に準 2 日波による波強制によって形成されることが分かった。したがって、この南北半球間結合は KB10 シナリオとは異なる要因で生じることがわかる。さらに、これらの上部中間圏および下部熱圏に高温偏差をもたらす準 2 日波および重力波はともに中間圏の順圧/傾圧不安定、シア不安定から発生することも明らかになった。これらの順圧/傾圧不安定やシア不安定は、南半球中間圏における重力波強制によって生じており、その重力波強制の変化は赤道成層圏の低温偏差に伴う東風強化によって形成される可能性がある。発表では、南北半球間結合の経度構造も併せて示す。

火山性成層圏エアロゾルをトレーサとした赤道域における物質の水平並びに鉛直輸送の観測

阿保 真 [1]; 柴田 泰邦 [1]; 長澤 親生 [1]
[1] 首都大・システムデザイン

Observations of horizontal and vertical transport of substances in the stratosphere using volcanic aerosols over equatorial region

Makoto Abo[1]; Yasukuni Shibata[1]; Chikao Nagasawa[1]
[1] System Design, Tokyo Metropolitan Univ.

The transport of substances between stratosphere and troposphere in the equatorial region makes an impact to the global climate change, but it has a lot of unknown behaviors. We have performed the lidar observations for survey of atmospheric structure of troposphere, stratosphere, and mesosphere over Kototabang (100.3E, 0.2S), Indonesia in the equatorial region since 2004. We investigate the transport of substances between stratosphere and troposphere in the equatorial region by data which have been collected by the polarization lidar, the Equatorial Atmosphere Radar(EAR) ground-based at Kototabang and the CALIOP over nearby Kototabang.

We derived extinction coefficients for ash particles and sulfate aerosol from the polarization lidar data. Volcanic sulfate over 20km were transported upward with branch of the Brewer-Dobson circulation. Large ash particles below 20km descended by sedimentation.

In June 2014 (4 months after the eruption), aerosol transport in the stratosphere were observed by the polarization lidar at Kototabang. At the same time, strong downward winds were observe by the EAR.

A typical vertical wavelength of the Kelvin wave in the equatorial lower stratosphere is about 10km and the phase of fluctuations propagates eastward and downward with time. Periods are about 15days. Typical Kelvin wave structure was found in the time-height cross sections of temperature anomalies over Padang and longitude-time cross sections of equatorial temperature anomalies at 50 hPa (˜21km).

赤道域における成層圏－対流圏間の物質輸送は気候変動に大きなインパクトを与えるが、その直接観測の事例は少ない。2014 年 2 月 13 日に噴火したインドネシアジャワ島のケルート火山（7.9S, 112.3E）の多くの火山ガスは高度 19˜20km 付近の成層圏に注入された。衛星ライダーである CALIOP データからは火山起源のエアロゾルが噴火後緯度方向に広がり 5 日で赤道に達し、その後赤道上空では QBO に伴う顕著な強い東向きの風により経度方向に輸送され、約 1ヶ月で地球を 1 周し、3 周まで周回する様子が見られた。4 周目に入る 6 月になると東向きの風が弱まり経度方向の動きは明瞭でなくなった。

成層圏に注入されたエアロゾルを偏光ライダーデータより球形で粒径の小さい硫酸液滴と非球形で粒径の大きい ash particle に分類し、その鉛直方向への輸送を調べた。小さい粒径の硫酸液滴は Brewer-Dobson 循環により、赤道上空では上方に輸送される様子が確認出来た。一方粒径の大きい ash particle は重力沈降により成層圏から対流圏に下方輸送される様子が確認出来た。

6 月には高度 21km 付近の成層圏でエアロゾルが下方に輸送される様子が赤道ライダーにより観測され、この時の EAR の鉛直風観測では強い下降流が観測された。当該期間の気温偏差の時間高度プロット並びに時間経度プロットから、鉛直波長約 10km、周期約 15 日で東向き並びに下方に位相が伝搬する典型的な赤道ケルビン波の存在を確認した。これらの考察より。赤道ケルビン波に伴い下降流が生じ、成層圏内でエアロゾルが鉛直輸送された様子を地上ライダーにより観測したものと考えられる。

火山性成層圏エアロゾルは、赤道域において水平並びに鉛直輸送の有用なトレーサとなることが明らかとなった。講演では 2019 年 6 月 26 日に噴火した赤道域のパプアニューギニア Ulawun 火山（5.1S, 151.3E）の解析速報についても紹介する。

民間会社が運用する観測ロケット Momo シリーズを用いた高層大気中音波伝搬の計測

山本 真行 [1]
[1] 高知工科大

Measurement of sound wave propagation in middle atmosphere by using Momo series sounding rockets operated by a private company

Masa-yuki Yamamoto[1]
[1] Kochi Univ. of Tech.

http://www.ele.kochi-tech.ac.jp/masayuki/

Sound propagation in middle and upper atmosphere has been investigated experimentally since 1950-1960's when the early stage of sounding rocket development in the world. After recognizing characteristics of altitude profile of the sound speed, namely, temperature profile in middle and upper atmosphere in more basic sense, atmospheric model studies have been carried out into the present era. More recently, importance of sound propagation from the ground to the thermosphere, or vise versa, has gradually been focused on among many topics of the Earth's atmospheric studies, especially some studies on physics of atmospheric gravity waves (AGW) or infrasound to be propagated upward/downward in these atmospheric spheres. However, experimental studies are extremely limited in these areas because we need high altitude balloons or sounding rockets for in-situ observation in these altitude ranges.

In 2012, we conducted an experiment with using S-310-41 sounding rocket of ISAS/JAXA and altitude profile of sound attenuation process was investigated. After the early dates of sounding rocket development in Japan, it was the first experiment of investigating sound propagation process in middle and upper atmosphere mainly because the affinity between sound and vacuum space is poor, especially in case of higher altitude in thermosphere to be reached with high altitude rockets of ISAS/JAXA S-310/S-520 series.

In 2017, Momo series sounding rockets opened a new page of Japanese space exploration as the first sounding rocket developed totally by a private company, Interstellar Technologies Co. (IST). In 2018, we installed two infrasound sensors with a buzzer for sound source aboard Momo-2 sounding rocket and tried the similar experiment for sound attenuation and propagation, but the rocket was exploded just after the launch. At that time, we measured the shock wave of rocket explosion with the onboard sensors as well as high accuracy pressure sensors deployed on ground.

In 2019, we also installed the same instruments onboard Momo-3 sounding rocket. In the experiment we operated 10 fireworks on ground, before and after the rocket launch, making loud pressure wave impulses to be propagated from the troposphere to stratosphere, mesosphere, and lower thermosphere. The launch of the Momo-3 was successful and it became the first private company's rocket reached 100 km altitude border. The apex was 113.4 km and we successfully recorded the sound/infrasound signals until 282.5 s from the launch. Moreover, in July 2019, Momo-4 flight is on-going situation within 3 months after the Momo-3 experiment. Such rapid repetition as well as low-cost launch is considered as significant advantage of the private company's rockets.

In this presentation, we will introduce the most recent activities with using the Momo series sounding rockets operated by IST and its first result of interesting sound propagation characteristics found in the datasets with showing situation of Momo series operation process as well as current environment of a new rocket launch pad in Taiki town, Hokkaido.

Study of oscillations of atmospheric electric field during snowfall at Chiba, Japan, using W- and X-band cloud radars

Hiroyo Ohya[1]; Kota Nakamori[2]; Masashi Kamogawa[3]; Tomoyuki Suzuki[4]; Toshiaki Takano[5]; Kazuomi Morotomi[6]

[1] Engineering, Chiba Univ.; [2] Electrical and Electronic, Chiba Univ.; [3] Dept. of Phys., Tokyo Gakugei Univ.; [4] Education, Gakugei Univ.; [5] Chiba Univ.; [6] Japan Radio Co., Ltd.

It is known that cloud-to-ground lightning and precipitations generated from thunderclouds are a generator of global electric circuit (e.g., Williams, 2009). In the fair weather, the atmospheric electric field at the ground is generally 100 V/m and downward (positive). The atmospheric electric field varies during not only lightning/thunderstorms, but also snowfall/blizzard (e.g., Minamoto and Kadokura, 2011). Wave pattern of the atmospheric electric field with the periods of several tens of minutes during snowfall was first observed in England (Simpson, 1948). The wave pattern of the atmospheric electric field occurred, when the snow clouds were nimbostratus (Kawamura, 1961). The oscillations with the period of 20 minutes during snowfall were observed in Hokkaido, Japan, on 16 January, 1978 (Kikuchi and Inatsu, 1979). When the polarity of the snow particles at the ground was positive (negative), the atmospheric electric field was negative (positive), which was called as "mirror image relation". Based on balloon observations, the mirror image relation became weak with increasing height (Asuma et al., 1988). As the cause of the oscillations, the polarity of snow particles arrived at the ground became opposite to that in the bottom of snow clouds due to corona discharges at the ground (Asuma et al., 1988). However, the mechanism of the oscillations has not been revealed yet. In this study, we investigate the oscillations of the atmospheric electric field during snowfall of 23-24 November, 2016, using a field mill, the 95 GHz cloud radar, FALCON (FMCW Radar for Cloud Observations)-I that was originally developed by our group, Chiba University, and a X-band radar (9.4 GHz). We have observed the atmospheric electric field with a Boltek field mill, and cloud reflectivity and the Doppler velocity with the FALCON-I in Chiba University, Japan, (CHB, 35.63N, 140.10E). At 16.2 km southeast from the CHB, a phased array X-band radar operated by Japan Radio Co., Ltd. observed precipitations/cloud. During the snowfall of 23-24 November, 2016, periodic oscillations in the atmospheric electric field with periods of 70-90 minutes were observed at four observation sites; CHB, Kakioka (KAK, 36.23N, 140.19E), Tokyo Gakugei University (KGN, Kokubunji, Tokyo, 35.71N, 139.49E), and Seikei High School (MSN, Musashino, Tokyo, 35.72N, 139.57E). The distances of CHB-KAK, CHB-TGU, and CHB-SHS are 64.8 km, 55.9 km, and 49.0 km, respectively. This is the first observations of similar oscillations in the atmospheric electric field with the periods of 70-100 minutes at different observation sites separated by a long distance of 50-65 km. The coherence between the atmospheric electric field and FALCON-I reflectivity was highest (0.98) at 0-1 km height with the same periods (39.0, 54.6, and 78.0 min.) of the oscillations. The FALCON-I reflectivity preceded the oscillations at 0.8 km height by 40 min. The phase difference decreased with decreasing the height. At the same time, various snow crystals (with/without cloud particles and hail) were observed in Kanto region, which means conductive snow clouds (Araki, 2018). We consider that the oscillations with the period of 78 minutes were caused by that positive/negative snow particles fell down from the bottom of the snow clouds to the ground alternately. The origin was internal vertical cells in the snow clouds. In the presentation, we will discuss the cause of the oscillations in the atmospheric electric field.

北西太平洋域雷検出網で観測された雷活動と 2018 年の台風の強度発達との関係

佐藤 光輝 [1]; 高橋 幸弘 [2]; 久保田 尚之 [3]; 山下 幸三 [4]; 濱田 純一 [5]; Marciano Joel[6]
[1] 北大・理; [2] 北大・理・宇宙; [3] 北大・理; [4] 足利大・工学部; [5] 首都大・都市環境・地理; [6] ASTI, DOST

Relation between Lightning Activities Measured by the V-POTEKA Network and Intensity Development of 2018 Pacific Typhoons

Mitsuteru SATO[1]; Yukihiro Takahashi[2]; Hisayuki Kubota[3]; Kozo Yamashita[4]; Jun-ichi Hamada[5]; Joel Marciano[6]
[1] Hokkaido Univ.; [2] Cosmosciences, Hokkaido Univ.; [3] Faculty of Science, Hokkaido Univ.; [4] Engineering, Ashikaga Univ.; [5] Geography, Tokyo Metropolitan Univ.; [6] ASTI, DOST

Lightning activity is a good proxy representing the precipitation and updraft intensities in thunderclouds. Recent studies suggest that the monitoring of the lightning activities enables us to easily predict the maximum wind speed and minimum sea-level pressure of the tropical cyclone by one or two days before, though the prediction error of typhoon intensities by the recent meteorological model is getting worse in the past 30 years. Many countries in the northwest Pacific region suffer from the attack of tropical cyclone (typhoon) and have a strong demand to predict the intensity development of typhoons by means of a cost-effective way. Thus, we have developed a new automatic lightning observation system (V-POTEKA) and installed this system in the Philippines, Guam, Palau, Jakarta, Okinawa, and Sapporo since September 2017. Using the V-POTEKA data, lightning locations are estimated by using the time-of-arrival geolocation software. We have compared the relation between the lightning activities measured by the V-POTEKA network and the intensity variation of the 2018 Pacific typhoons. In 2018, a total of 29 typhoons occurred. We selected 11 of 29 typhoon events and conducted cross-correlation analysis between lightning activities and typhoon intensities. We confirmed that the time variations of the detected lightning event numbers and typhoon intensities (maximum wind speed and center pressure) are highly correlated. Especially, there is clear time lag (~2 days) between lightning activities and typhoon intensities in category 1-3 typhoons.

雷放電は強い上昇気流に伴い発達した雷雲内で生じるため，雷雲活動度，降水量，鉛直対流強度などに対し良い指標となりうると指摘されている。中でもシビア気象の 1 つである台風に関して，最新の気象モデルでは進路予測精度は年々向上しているが，強度発達の予測精度は年々悪化しているという報告がある。これに対し，台風内部で発生する雷放電の発生数を計測すると，台風の最大風速と気圧の発達度を 1-2 日前に予測できるという先行研究も示されている。北西太平洋域では，台風やそれに関連したシビア気象による災害が毎年のように発生しているが，一部の地域を除いて気象観測網や雷観測網が十分に整備されている状態にはない。海洋から大気へのエネルギー流入と台風発達過程において雷雲が重要な役割を果たしていると考えられることから，この地域での雷放電活動のリアルタイム監視体制を構築し，簡易的な手法で速報的に台風強度発達を予測する体制の確立が急務となっている。そのため我々は，新たな雷観測システム (V-POTEKA) を開発し，2017 年 9 月から北西太平洋域に設置・展開してきた。2019 年 7 月現在，フィリピン国内に 4 箇所，パラオ・グアム・ジャカルタ・沖縄・札幌の各地に 1 箇所の，合計 9 箇所で稼働しており，得られた雷電波観測データから到来時間差法 (TOA) を用いて雷放電発生位置を推定できる体制が整っている。2018 年は 29 個の台風が発生したが，そのうち解析可能であった 11 個の台風に対して，最大風速・中心気圧と，V-POTEKA による雷データとの比較を行った。11 個の台風の強さの内訳は，カテゴリー (1, 2, 3, 4, 5) のそれぞれで (2, 2, 3, 0, 4) 個であった。台風の中心から半径 500km の円内で発生した雷の発生数を 6 時間毎に計数し，台風の最大風速と中心気圧との比較を行った結果，両者には高い相関が見られ，特にカテゴリー 1-3 の低・中規模の台風では雷数の変化が台風強度発達に約 2 日ほど先行する様子が明確であった。講演では，これらの解析で得られた相関性について詳しく紹介する。

SuperDARN近距離エコーの再評価(2)

行松 彰 [1]
[1] 国立極地研究所/総研大

Reassessment of SuperDARN/SENSU near range echoes (2)

Akira Sessai Yukimatu[1]
[1] NIPR/SOKENDAI

SuperDARN is a powerful and unique tool primarily contributed to space weather research by providing global (polar and mid-latitude) ionospheric plasma convection and electric field potential map in high temporal resolution of ~1-2 min in quasi real time with its global coverage of international HF radars' FOVs. It also contributes to vertical coupling of ionised and neutral atmosphere in middle and upper atmosphere by observing TIDs (traveling ionospheric disturbances), neutral winds, and PMSE/PMWE etc in MLT (mesosphere and lower thermosphere) or MTI (mesosphere, thermosphere and ionosphere) regions.

SuperDARN near range echoes are important targets especially for lower altitude echoes like those in D and E regions and those in MLT region. As typical range resolution of SuperDARN radars is rather coarse and HF ray paths bend in ionosphere, obtaining precise height/altitude information is key to understand the physics in the region correctly.

These years SuperDARN community has tried to improve and re-establish the method of interferometer calibration in success. Some radars have also started to try higher range resolution using imaging (SDI/FDI) and pulse coding technique etc.

We here try to re-calibrate the interferometer and elevation angles in our Antarctic Syowa SuperDARN SENSU radars data and to reassess the height information of the near range echoes.

Some recent papers related to this issue proposed near range echoes in summer midday obtained with Canadian SuperDARN radars seem not from mesopause region altitude but from slightly higher altitude so those echoes might not be PMSEs. Results of reassessment of near range echoes in Syowa SENSU radars in more detail and possible potential origins of the echoes will be shown and discussed.

Ion temperature and velocity variations in the D- and E-region polar ionosphere during stratospheric sudden warming

Yasunobu Ogawa[1]; Satonori Nozawa[2]; Masaki Tsutsumi[1]; Yoshihiro Tomikawa[1]; Chris Hall[3]; Ingemar Haggstrom[4]
[1] NIPR; [2] ISEE, Nagoya Univ.; [3] TGO, UiT; [4] EISCAT HQ

We analyzed ion temperature and velocity observed by the European Incoherent Scatter (EISCAT) UHF radar at Tromsoe (69.6 deg N, 19.2 deg E) during a stratospheric sudden warming (SSW) that occurred in January-February 2017. The zonal ion velocities at 85-100 km height reversed approximately 8 days earlier than the zonal wind reversal in the upper stratosphere. Ion temperature at 85-95 km decreased simultaneously with the zonal ion velocity reversal at the same altitude, and vertical ion velocity changes of about +/-2 m/s were also seen from ˜8 days before the SSW onset. Downward propagation speed of the vertical ion velocity variation was ˜0.01 m/s, as well as that of ion temperature variation. We also found that the ion temperature variations in the daytime were close to those of ambipolar diffusion coefficients derived from the the Nippon/Norway Tromsoe Meteor Radar (NTMR) data at the same altitude even when geomagnetic activity is moderate. We will discuss energy and momentum exchanges between ions and neutrals at 85-95 km based on the observational results during SSW.

南極昭和基地 PANSY レーダーによる電離圏沿磁力線不規則構造のイメージング観測

香川 大輔 [1]; 橋本 大志 [2]; 齊藤 昭則 [3]; 西村 耕司 [4]; 堤 雅基 [4]; 佐藤 亨 [2]; 佐藤 薫 [5]
[1] 京大・理・地惑; [2] 京大・情報学・通信情報システム; [3] 京都大・理・地球物理; [4] 極地研; [5] 東大・理

Imaging observation of Ionospheric Field Aligned Irregularities by the PANSY radar at Antarctic Syowa Station

Daisuke Kagawa[1]; Taishi Hashimoto[2]; Akinori Saito[3]; Koji Nishimura[4]; Masaki Tsutsumi[4]; Toru Sato[2]; Kaoru Sato[5]
[1] Earth and Planetary Sciences, Kyoto Univ.; [2] Communications and Computer Eng., Kyoto Univ.; [3] Dept. of Geophysics, Kyoto Univ.; [4] NIPR; [5] Graduate School of Science, Univ. of Tokyo

PANSY radar is a large atmospheric and VHF-band radar located at the Antarctic Syowa Station. This radar has the capability of a MST radar which observes mesosphere, stratosphere, and troposphere, furthermore it is capable of observing plasma quantities in an altitudinal range from 100km to 500km using the ionospheric incoherent scatter (IS). In 2015, the PANSY radar performed the first ionospheric IS observation in the Antarctica. PANSY radar has a frequency of 47MHz, so it is capable of observing the echoes of field aligned irregularities (FAI) in E region. If FAI has a space scale of half wavelength of radio waves they are coherently backscattered, so PANSY radar observes the coherent echoes from 3-m-scale FAI.

Signal processing using adaptive beamforming has been developed, because IS observation of PANSY radar is affected by the FAI echoes. PANSY radar has the FAI array of 24 antennas in addition to the main array of 1045 antennas. FAI array comprises of a pair of peripheral linear arrays of 12 antennas, and it can separate the signal from various angles using the directionally-constrained minimization of power (DCMP) algorithm. In fact, by this algorithm, we can observe not only electron density in the background but also FAI and its motion.

In the presentation, we will show the temporal and spatial variation of FAI by the imaging observation using the PANSY radar, and will figure out a physical process of FAI generation by comparing these variation to the observation of geomagnetic field or satellite.

PANSY レーダーは南極の昭和基地に設置されている大型 VHF 帯大気レーダーである。本レーダーは対流圏や成層圏、中間圏を観測対象とする MST レーダーとしての機能に加え、電離圏非干渉性散乱 (IS) を用いて地表 100km から 500km におけるプラズマ物理量を観測することが可能である。2015 年には南極で初となる電離圏 IS 観測が開始された。また、PANSY レーダーは周波数 47MHz を用いており、E 領域の沿磁力線不規則構造 (Field Aligned Irregularity: FAI) エコーの観測が可能である。FAI がレーダー電波の半波長の空間スケールを持つとき電波はコヒーレント散乱を起こすため、PANSY レーダーでは約 3m スケールの FAI からのコヒーレント・エコーの観測が行われる。

この FAI からのエコーの混入による PANSY レーダーの IS 観測への影響に対処するため、適応的ビーム形成技術を用いた信号処理法が開発された。PANSY レーダーには 1045 本のアンテナからなるメインアレイに加え、24 本のアンテナからなる FAI アレイがある。 FAI アレイには 12 本ずつ直線状に配置されたアレイアンテナが 2 組あり、方向拘束付き出力電力最小化法に基づいた手法を用いて異なる角度からの信号を分離できる。つまり、この手法により、背景の電子密度だけでなく FAI やその運動を観測することも可能である。

本発表では、PANSY レーダーによる FAI のイメージング観測において測定された FAI の時間変化及び空間変化について考察し、またそれらを磁場観測や衛星観測など、他の観測と比較することによって FAI 生成の物理過程を解明する。

近赤外波長における北欧2地点光学観測：昼側へのオーロラ・大気光観測の拡張

西山 尚典 [1]; 鍵谷 将人 [2]; 小川 泰信 [1]; 坂野井 健 [3]; 田口 真 [4]
[1] 極地研; [2] 東北大・理・惑星プラズマ大気研究センター; [3] 東北大・理; [4] 立教大・理・物理

Near infrared optical observations in the Northern Europe: Extension of dayside aurora and airglow measurements from the ground

Takanori Nishiyama[1]; Masato Kagitani[2]; Yasunobu Ogawa[1]; Takeshi Sakanoi[3]; Makoto Taguchi[4]
[1] NIPR; [2] PPARC, Tohoku Univ; [3] Grad. School of Science, Tohoku Univ.; [4] Rikkyo Univ.

Dayside aurora, polar patch, and airglow are key phenomena for the understanding of dayside magnetosphere, ionosphere, and neutral atmosphere coupling process. Those phenomena have been mainly monitored by active/passive radio remote sensing such as HF/VHF/UHF radar, GNSS receiver, and imaging riometer, but spatial and temporal resolutions by those measurements are basically not so good in comparison to optical measurements. Near infrared (NIR) wavelength are crucially important because lower background sky radiation by Rayleigh scattering may allow us to conduct ground-based optical observation even in dayside. However, NIR aurora has a total lack of its spectral information with enough resolutions to make a feasibility study in comparison to that in visible wavelength.

We are planning to install two different type of imaging spectrometers at two observatories in the Northern Europe to evaluate and establish optical measurements in NIR for dayside aurora and airglow. The detail of the spectrographs is as follows.

Czerny-Turner type imaging spectrometer at Kiruna (67.85^{o}N, 20.21^{o}E):

It is a narrow field spectrometer with medium-high spectral resolution that mainly consists of a Czerny-Turner type imaging spectrometer (HORIBA, iHR320) with a gold coated off-axis parabolic mirror, a NIR long-pass filter, two blazed gratings (600 and 150 gr/mm) and 1D InGaAs array (1024 pixels). Spectral range and that per pixel with a 600 gr/mm grating are 119 nm and 0.11 nm/pixel, respectively. It is going to be installed at IRF Kiruna in the end of August 2019. This spectrometer focuses on continuous measurements of aurora (N_2^+ Meinel) and airglow (OH 3-1 band) spectrum around 1.5 microns. Although auroral emissions in this wavelength is thought to be not so strong compared to airglow, its detailed spectral feature is not fully understood. On the other hand, P1(2) and P1(4) emissions in OH 3-1 band allow us to estimate OH rotational temperature near mesopause. Additionally, the airglow measurement has a possibility to collaborate with an all-sky monochromatic OH imager planned by IRF/Kiruna and MATS satellite founded by Swedish National Space Agency, which is scheduled for launch late 2019.

Meridional imaging spectrometer at Longyearbyen (78.21^{o}N, 15.55^{o}E):

We have designed a new imaging spectrometer for NIR wavelength ranging from 1.09 to 1.25 microns that covers strong auroral emissions in N_2^+ Meinel band (1.1 microns) and N_2 1st Positive band (1.2 microns). It mainly consists of three camera lenses, a few selectable slits, a NIR long-pass filter, a volume phase holographic grating (950 gr/mm) and 2D InGaAs array (640 x 512 pixels). Fast CCTV lenses (F1.4) for security purpose are used as two objective and one collimating lens. FOV and angular resolution are 55 degree and 0.11 degree per pixel, respectively. If a 30-microns slit is used, wavelength resolution at 1.17 microns is 2230, and signal-to-noise ratio for 1 kR emissions can get larger than 1.0 in a few seconds exposure time. Therefore, we can investigate temporal variability of dayside phenomena such as dayside reconnection and pulsating auroras in sufficient sampling rates of a few seconds. After development and calibration, this spectrograph will be installed at The Kjell Henriksen Observatory/The University Centre in Svalbard. Taking a great advantage of its location, 24-hours continuous observations can be expected (solar zenith angle lager than 96 degrees) near the winter solstice. Additionally, collaborative studies with active/passive radio remote sensing such as EISCAT ESR and GNSS receiver network will be done in near future to evaluate spatial and temporal characteristics of dayside aurora.

ノルウェーのトロムソで観測された脈動オーロラ発光の波長特性

李 成宇 [1]; 津田 卓雄 [1]; 細川 敬祐 [1]; 野澤 悟徳 [2]; 川端 哲也 [2]; 水野 亮 [2]; 大山 伸一郎 [3]; 栗原 純一 [4]
[1] 電通大; [2] 名大・宇地研; [3] 名大 ISEE; [4] 北大・理・宇宙

Spectra of pulsating aurora emissions observed by an optical spectrograph at Tromsoe, Norway

Chengyu Li[1]; Takuo Tsuda[1]; Keisuke Hosokawa[1]; Satonori Nozawa[2]; Tetsuya Kawabata[2]; Akira Mizuno[2]; Shin-ichiro Oyama[3]; Junichi Kurihara[4]
[1] UEC; [2] ISEE, Nagoya Univ.; [3] ISEE, Nagoya Univ.; [4] Cosmosciences, Hokkaido Univ.

Pulsating auroras are a diffuse-type aurora, and are characterized by a repetition of brighter (on-phase) and darker (off-phase) auroral emissions with periods of a few to a few tens of seconds. Optical observations for pulsating auroras have been widely performed for many years. Recent major activities in the optical imaging observation would be, for example, high-speed observations for faster modulations (3-Hz or higher) in the emission intensity of pulsating auroras and ground network observations in association with satellites in the magnetosphere for investigating source regions of pulsating auroras. While such imaging observations equipped with some bandpass or cutoff filters are useful for observing some auroral emission lines and bands of specific atoms and molecules. There is relatively less information on optical spectra of pulsating auroras.

In this study, we have been investigating optical spectra of pulsating auroras observed by an optical spectrograph at Tromsoe, Norway (69.6˚N, 19.2˚E). The spectrograph is capable of measuring optical emission intensity in mainly visible range from 480 to 880 nm with a resolution of 1.6 nm. The aperture, i.e. F-number, is 4. The field-of-view (FOV) of spectrograph is 0.03x2.00 degrees, which is pointed at magnetic field-aligned direction. The time resolution is 1 second, and thus, pulsating auroras, which have periods from a few to a few tens of seconds, are well detectable.

Here, we present a pulsating aurora event from 03:13 to 03:50 UT on 6 March 2017. The event is a relatively long-lasting event within the FOV of spectrograph, and it allows us to make more data integrations to enhance signal-to-noise ratios. After such data integrations, auroral emission lines, such as OI 557.7 nm, OI 630 nm, and OI 844.6 nm, as well as emission bands, such as N2 1PG, were clearly found in both integrated-optical spectra of the on- and off-phases. Then, we calculated a difference spectrum between the optical spectra of on- and off-phases to compare these spectra. In the difference spectrum, clear line-like shapes were found for the emission lines of OI 557.7 nm and OI 844.6 nm. On the other hand, a shape of the difference spectrum around 630 nm does not seem to be a line-like shape due to OI 630 nm, and it seems to be a part of band-like shape of the emission band of N2 1PG. In the presentation, we will show these results, and give a discussion on the optical spectra of on- and off-phases in more detail.

脈動オーロラはディフューズオーロラの一種であり、数秒から数十秒の周期で明るい発光 (ON) と暗い発光 (OFF) が繰返すように明滅するオーロラ発光現象である。脈動オーロラの光学観測は長年にわたって行われているが、近年では、イメージャー観測の発展に伴い、発光強度のより速い変調成分（3 Hz 変調等）に注目した高速観測やソース領域の調査の為の磁気圏衛星と連携した地上ネットワーク観測などが進展している。これらのイメージャー観測で用いられるバンドパスフィルタやカットオフフィルタによる分光観測は、特定の原子・分子の輝線・バンド発光を対象とするものであり、脈動オーロラ発光スペクトルの全体的な描像はあまりよく知られていない。

本研究では、ノルウェー、トロムソ（69.6˚N、19.2˚E）の欧州非干渉散乱（EISCAT）レーダー観測に設置した光学スペクトログラフを用いて脈動オーロラの発光スペクトルの調査を進めている。スペクトログラフの波長分解能は 1.6 nm、480-880 nm の波長範囲の発光強度を測定することができる。F 値は 4、視野角は 0.03x2.00 度、視線方向は磁力線方向に向けている。時間分解能は 1 秒であり、数秒から数十秒の周期をもつ脈動オーロラの観測に有効である。

本発表では、2017 年 3 月 6 日 03:13-03:50 UT に観測された脈動オーロライベントを紹介する。スペクトログラフの視野内で比較的長時間継続したイベントであり、スペクトルデータの時間積算によって比較的 SNR の良いスペクトルデータを得ることができる。発光強度の時系列データを元にスペクトルデータを脈動オーロラの ON と OFF の時間帯に分類して各々のデータセットを時間方向に積算し、ON と OFF のスペクトルデータを得た。その結果、OI 557.7 nm、OI 630 nm、OI 844.6 nm などの輝線発光や N2 1PG のようなバンド発光が ON と OFF のそれぞれのスペクトルではっきりと確認できた。ON と OFF のスペクトルの比較のために、両スペクトルの差分を求めた。求めた差分スペクトルにおいて、OI 557.7 nm、OI 844.6 nm は輝線の形状をしていた。一方で、630 nm 付近の差分スペクトルでは、OI 630 nm を示すような輝線の形状は確認できず、N2 1PG の発光バンドの一部のような形状が見られた。以上の結果を示し、脈動オーロラの ON と OFF の発光スペクトルについてより詳細に議論することを予定している。

Characteristics of the ionospheric variations in the dayside polar region

Hitoshi Fujiwara[1]; Satonori Nozawa[2]; Yasunobu Ogawa[3]; Yasunobu Miyoshi[4]; Hidekatsu Jin[5]; Hiroyuki Shinagawa[5]; Chihiro Tao[5]
[1] Faculty of Science and Technology, Seikei University; [2] ISEE, Nagoya Univ.; [3] NIPR; [4] Dept. Earth & Planetary Sci, Kyushu Univ.; [5] NICT

Some observations have revealed existence of the significant ionospheric variations in the polar cap region. Since the steep density gradients in the polar cap ionosphere may cause severe problems in radio wave communications, e.g. GPS navigation for trans polar flights, it should be one of important space weather issues to understand variations of the polar cap ionosphere.

The origins of the disturbances are thought to be transport of plasma produced by the solar EUV and/or auroral processes from the lower latitude (namely, polar cap tongue of ionization, polar cap patches, and blobs) and/or insitu particle precipitation and heating in the polar cap region. We have observed spatio-temporal variations of the dayside polar cap ionosphere with the European Incoherent Scatter (EISCAT) radar system to investigate characteristics of the ionospheric variations in the dayside polar region and their origins. The EISCAT observations enable us to understand variations of the electron density, electron and ion temperatures, and ion drift motion, simultaneously. In addition, simultaneous observations with the EISCAT UHF radar (at Tromsoe) and EISCAT Svalbard radar (ESR) (at Longyearbyen) are extremely helpful to compare the ionospheric variations in the polar cap with those in the auroral regions.

In the present study, we will report on our recent observations with the EISCAT UHF radar (at Tromsoe) and ESR at Longyearbyen in March 2019. The geomagnetic activities during the periods were almost quiet (Kp =1-2). Significant ionospheric disturbances were observed in the dayside polar region at around or higher than 80 deg latitude with the ESR 32 m antenna (elevation angle of 30 deg) on March 18 and 19, 2019, while the quiet ionosphere was observed in the same periods with ESR 42 m antenna (field-aligned direction) and the EISCAT UHF radar (at Tromsoe). Enhancements of the ion drift velocity and ion temperature were simultaneously observed with the ESR 32 m antenna during the disturbed periods. These features seem to be similar to those seen in the ionospheric data during geomagnetically quiet periods in our previous observations (e.g., March 2014, 2015, and 2018). On the other hand, we observed ionospheric variations during geomagnetically disturbed periods in March 2017. Significant disturbances were observed with the ESR 32 m and 42 m antennas and the EISCAT UHF radar. The ESR 32 m antenna observed interesting features of the ionospheric variation during the periods. When enhancements of the ion temperature were observed (more than 2000 K), the ion drift velocity was not so large with changing the direction of the motion. When enhancements of the ion velocity were observed (more than 1000 m/s), the ion temperature was small (about 1000 K).

We will clarify the variations of the dayside polar cap ionosphere during the geomagnetically quiet periods and those during geomagnetically disturbed period.

長期計算に向けたGAIA極域入力の改良

垰 千尋 [1]; 陣 英克 [1]; 品川 裕之 [1]; 三好 勉信 [2]; 藤原 均 [3]
[1] 情報通信研究機構; [2] 九大・理・地球惑星; [3] 成蹊大・理工

Improvement of GAIA polar input for long-term simulation

Chihiro Tao[1]; Hidekatsu Jin[1]; Hiroyuki Shinagawa[1]; Yasunobu Miyoshi[2]; Hitoshi Fujiwara[3]
[1] NICT; [2] Dept. Earth & Planetary Sci, Kyushu Univ.; [3] Faculty of Science and Technology, Seikei University

GAIA, Ground-to-Topside Model of Atmosphere and Ionosphere for Aeronomy, is the whole atmosphere model including interaction with ionized plasma under solar EUV variation and a various waves input using a meteorological reanalysis data. The purpose of this study to extend the GAIA to include the magnetospheric variation via electric field deposition at polar region and auroral electron precipitation using empirical models. We input polar electric potential map based on Weimer model driven by solar wind and interplanetary magnetic field parameters including saturation effect of cross-polar-cap potential for large potential case. Variable auroral precipitation is considered based on emission observation. Estimated Joule heating is comparable with the observation for the quiet condition. Enhancement of total electron content during the magnetospheric storm event is produced due to penetration electric field. Application to extreme events and long-term simulation will be discussed in the presentation.

GAIA(Ground-to-Topside Model of Atmosphere and Ionosphere for Aeronomy) は、大気下層に気象再解析データを入力し、対流圏から熱圏までの大気圏と電離圏の大気物理・化学過程を解くモデルである。極域から大気圏へインプットされる電場・電流は太陽風および磁気圏の状況に応じて大きく変化し、変化の大きさによっては全球の大気圏・電離圏に影響を及ぼす。この変動の効果をGAIAに含めるために、太陽風変動に依存するWeimer電場経験モデルの導入と、オーロラ粒子降り込みが磁気圏活動度に応じて変化するモデルの改良を実施している。静穏時にモデルで求まるジュール加熱率の観測との整合性を確認した。また、中低緯度への電場侵入による、磁気嵐時の中低緯度の全電子数増大の再現性も確認された。発表では、極端イベントへの適用や、長期計算に向けた安定化について、議論する。

GAIAモデルを用いた、二酸化炭素増加によるF2ピークの変動

阿部 宇宙 [1]; Liu Huixin[2]; 垰 千尋 [3]
[1] 九大・理・地惑; [2] 九大・理・地惑; [3] 情報通信研究機構

The variation of F2-peak due to CO2 increase: experiment with GAIA model

Takamichi Abe[1]; Huixin Liu[2]; Chihiro Tao[3]
[1] Kyushu Univ.; [2] None; [3] NICT

In recent years, the upper atmosphere has been cooling because of long-term increase of carbon dioxide. The ionosphere also contracts due to CO_2 cooling. Trends in the E- and F_1-region have been revealed by previous studies, with a con-sistent increase of the peak density, but drop in peak height. The trends of F_2-peak (NmF_2, hmF_2), however, has been found to vary from location to location and no consensus view has been reached. This is mainly due to the fact that trend caused by CO_2 in F_2-peak is weak compared to the strong solar and geomagnetic activity, and thus difficult to be separated from observations. Therefore here we investigate the effects of CO_2 cooling on F_2-peak with the GAIA model containing from surface to the ionosphere.

The results show that the response of NmF_2 de-pends strongly on season and local time, with both positive and negative changes. On the other hand, such dependence in hmF_2 is small, with hmF_2 decreasing globally. The atmospheric composition (O/N_2) shows a similar perturba-tion pattern to hmF_2. This indicates that the response of NmF_2 evolves more complicated processes than hmF_2. In particular, we investigate various plasma transport processes.

Utilizing 4D-var technique to image South African regional ionosphere

Nicholas Ssessanga[1]; Yong Ha Kim[2]; Mamoru Yamamoto[1]; John Bosco Habarulema[3]
[1] RISH, Kyoto Univ.; [2] Chungnam National University; [3] SANSA

In an endeavor to characterize and model a time-space variant ionosphere through which trans-ionospheric signals propagate, we have developed a strong constraint four dimensional variational data assimilation (4D-var) technique, and used the same to more accurately estimate the South African regional ionosphere (bound latitude 20deg S - 35deg S, longitude 20deg E - 40deg E and altitude 100 -1336 km). The altitude was capped to the JASON-1 satellite orbital altitude for the purpose of eliminating the plasmasphere contribution hence reducing the computation expense. Background densities were obtained from an empirical internationally recognized ionosphere model (IRI-2016), and propagated in time using a Gauss-Markov filter. Ingested data were STECs (slant total electron content) obtained from the South African GNSS (Global Navigation Satellite System) receiver network (TrigNet). The vertically integrated electron content was validated using GIMs (Global ionosphere Maps) and JASON-3 data over the continent and ocean areas, respectively. Further, vertical profiles after assimilation were compared with data from a network of ground based regional ionosondes (Hermanus (34.25S, 19.13E), Grahamstown (33.3S, 26.5E), Louisvale (21.2S, 28.5E) and Madimbo (22.4S, 30.9E). Results show that assimilation of STEC data has a profound improvement on the estimation of both the horizontal and vertical structure during quiet and storm periods. Accuracy of the horizontal structure decreases from the continent towards the ocean area where GPS receivers are less abundant. Superiority of assimilating STEC is best pronounced during day time especially when estimating maximum electron density of the F2 layer (NmF2), with a 60% RMSE improvement over the background values.

Calculation of the ray paths and propagation times of HF radio waves using the simulator of HF-START project.

Ryo Nakao[1]; Hiroyuki Nakata[2]; Hiroyo Ohya[3]; Toshiaki Takano[4]; Kornyanat Hozumi[5]; Takuya Tsugawa[6]; Susumu Saito[7]; Mamoru Ishii[6]
[1] Graduate school of Chiba Univ; [2] Grad. School of Eng., Chiba Univ.; [3] Engineering, Chiba Univ.; [4] Chiba Univ.; [5] NICT; [6] NICT; [7] ENRI, MPAT

HF simulator Targeting for All user's Regional Telecommunications (HF-STRAT) is a collaborative project with NICT, ENRI and Chiba University to provide the information of nowcast of radio propagation. In this project, propagation of HF radio waves is calculated by ray-tracing. Using the results of ray-tracing, we have determined whether HF radio wave travels between any two points. To confirm the results of ray-tracing, we have observed the differences of the propagation time of the HF radio waves transmitted from Nagara transmitter, RadioNIKKEI (35.46N, 140.20E). HF receivers are located at Chiba University (Chiba, 35.62N, 140.10E), Sarobetu (Hokkaido, 45.16N, 141.74E), Numata (Gunma, 36.62N, 139.02E), Yamagawa (Kagoshima, 31.20N, 130.61E), Ogimi (Okinawa, 26.68N, 128.15E). In the ray-tracing calculation, therefore, we have calculated propagation paths and times between transmitter and the receivers. In comparing the propagation time between Chiba and the other receivers, it is found that there was a difference of the propagation time between the ray-tracing results and the observations. This is because it is assumed that ground waves are propagated from Nagara to Chiba. By calculating the loss of electric field strength between Nagara and Chiba, we found out that the loss of sky wave that is reflected by ionosphere was almost same as that of ground wave. Thus, it is possible that the radio wave propagation between Nagara and Chiba is not ground wave but sky wave that is reflected by ionosphere or both ground wave and sky wave signals are received simultaneously by receiver at Chiba. As for further calculation, we plan to use the electron density distributions determined by GAIA and GNSS tomography in the ray-tracing calculation.

イオノゾンデの受信アレイを用いた電離圏エコー到来方向の推定

西岡 未知 [1]; 前野 英生 [2]; 近藤 巧 [2]; 津川 卓也 [1]
[1] 情報通信研究機構; [2] NICT

Arrival directions of ionospheric echo received by ionosonde antenna array

Michi Nishioka[1]; Hideo Maeno[2]; Takumi Kondo[2]; Takuya Tsugawa[1]
[1] NICT; [2] NICT

National Institute of Information and Communications Technology (NICT) has been observing ionosphere by ionosondes for over 70 years in Japan. In 2017, we replaced the previous ionosondes with Vertical Incidence Pulsed Ionospheric Radar 2 (VIPIR2) ionosondes, which is mainly developed in NOAA. VIPIR2s are automatically operated at four stations at Wakkanai (Sarobetsu), Kokubunji, Yamagawa, Okinawa (Ogimi). The biggest advantage of VIPIR2 is the multiple spaced receiving antenna. This antenna array makes it possible to estimate arrival directions of received echo. Methodology of deriving arrival directions are confirmed using radio waves which is transmitted from already-known locations, such as HF radio broadcasting or VIPIR2 transmission at other stations. Arrival directions of ionospheric echo of sporadic E-layers (Es) are also derived. In the presentation, preliminary results of the arrival direction derivation will be shown and possible collaborations will be discussed.

情報通信研究機構では、70年以上にわたってイオノゾンデによる電離圏観測を継続実施しており、その観測結果は、電離圏研究の基礎データとして、また、短波帯無線通信等の重要な情報源として活用されている。イオノゾンデ観測システムは幾多の変遷を重ねてきている。2017年度からは、主に米国で開発されてきたVertical Incidence Pulsed Ionospheric Radar 2 (VIPIR2)を用いて国内4観測点（サロベツ、国分寺、山川、大宜味）で定常観測を行っている。VIPIR2の最大の特徴は、複数のアンテナで受信アレイを構成している点である。受信アレイデータを用いると、受信電波の到来方向を推定することができる。本講演では、発信源の明確な放送波や、他観測点からのイオノゾンデ送信波等を用いて、電波到来方向推定手法の妥当性を確認する。また、スポラディックE層からのエコー到来方向を推定し、イオノゾンデを用いたスポラディックE層マップの作成の実現可能性を議論する。更に、今後のVIPIR2のデータ活用方法についても議論する。

イオノグラムから電子密度分布の full wave 計算による推定手法

深見 哲男 [1]; 長野 勇 [2]; 東 亮一 [1]
[1] 石川高専; [2] 金沢大

Estimated technique of electron density profile from ionogram using the full wave calculation

Tetsuo Fukami[1]; Isamu Nagano[2]; Ryoichi Higashi[1]
[1] NIT Ishikawa Col.; [2] Kanazawa Univ.

It is difficult to investigate the lower ionosphere directly as the altitude is lower than satellite orbit. Ionograms are effective data to know the lower ionospheric conditions from the ground. The ionogram is made by pulse wave intensities of the ionosonde and shows frequency characteristics of the virtual height *h'* calculated by time delay of the pulse wave received after traveling in the ionosphere. So, the ionograms have information of both virtual heights and reflection coefficients on observation frequencies. With the textbook, only the virtual height *h'* derived by the ray theory is considered in relation to the electron density profile [1]. We suggest a method that estimate the virtual height from the electron density profile and the collision profile by the full wave calculation [2]. Our method can simultaneously obtain the reflection coefficients. We checked the availability of our method from the simultaneous experiment of the rocket and the ionogram at Kagoshima Space Center [3].

On the other hand, The International Reference Ionosphere (IRI) can give the electron density profile at latitude, longitude and time [4]. We investigated difference between measured ionogram at the Kokubunji site [5] and theoretical ionogram calculated by the IRI profile for one example [6]. The theoretical *h'* values of the E and F2 layer is nearly agreement with the observed *h'* values, but the theoretical *h'* values of the F1 layer is not agreement.

In this presentation, we show estimated technique of the electron density profile from ionogram using the full wave calculation for this example.

[1] Budden, K. G.: The propagation of radio waves, Cambridge Univ. Press (1985).
[2] Fukami, T., I. Nagano and J. MacDougall: Proc. of ISAP 1996, 685-688 (1996).
[3] Fukami, T., I. Nagano and R. Higashi: Proc. of PIERS 2018 in Toyama, pp.2129-2133 (2018).
[4] International Reference Ionosphere 2016, https://ccmc.gsfc.nasa.gov/modelweb/models/iri2016_vitmo.php
[5] Ionospheric Sounding Data in JAPAN, http://wdc.nict.go.jp/ISDJ/ionospheric-signal.html
[6] Fukami, T., I. Nagano and R. Higashi: SGEPSS 144 in Nagoya, R005-P23 (2018).

衛星の高度より低い下部電離層は，直接探査が困難な領域であるが，HF 周波数帯以下を反射する重要な役割を持っている．イオノグラムは，イオノゾンデによって下部電離層を地上から定常観測する有効な資料である．イオノグラムは，周波数毎のパルス電波の見掛け高さ (*h'*) と反射強度を測定した図である．教科書では ray theory によって得られた見掛け高さだけを使って電子密度分布との関係が検討されている [1]．我々は，電子密度分布と衝突回数分布を与えれば full wave 計算法を用いて見掛け高さ (*h'*) を算出する理論計算法を提案した [2]．この方法では，同時に反射強度も見積もることができる．そして，見掛け高さの有効性をイオノグラムとロケットによる同時実験で確かめた [3].

他方，IRI モデルは，希望場所と時間の電子密度分布を与える [4]．ただし，IRI 電子密度モデルには，Es 層はない．我々は，情報通信研究機構の電磁波研究所が行っている国分寺の測定イオノグラム [5] と IRI 電子密度モデルによる理論イオノグラムを，2017 年 5 月 20 日 15:00LT の例に関して比較調査した．その結果，E 層と F2 層では，ほぼ合っているが，F1 層付近では，合っていなかった [6].

本報告では，この例で反射強度も考慮しながら IRI 電子密度モデルをもとにして，イオノグラム測定値に合うような電子密度分布を推定した．その手順を含めて発表する．

機械学習を用いたイオノグラムにおけるスプレッドF自動検出

清水 淳史 [1]; 中田 裕之 [2]; 大矢 浩代 [1]; 鷹野 敏明 [3]
[1] 千葉大・工・電気; [2] 千葉大・工・電気; [3] 千葉大・工

Automatic detection of Spread-F on ionogram using Machine Learning

Junji Shimizu[1]; Hiroyuki Nakata[2]; Hiroyo Ohya[1]; Toshiaki Takano[3]
[1] Engineering, Chiba Univ.; [2] Grad. School of Eng., Chiba Univ.; [3] Chiba Univ.

Ionospheric irregularities referred to as equatorial spread-F are very important phenomena in terms of radio wave propagation because their spatial scales are from centimeters to tens of kilometer and they affect wide-band radio waves. Therefore, they influence the reliability of satellite-ground communications, navigation systems and so on. The ionogram is one of the important observation system of spread-F. If spread-F in the ionogram is detected automatically by developing an excellent machine learning system, real time detection of spread-F could be replaced with automatic detection by developing an excellent machine learning system. Therefore, we have developed an automatic detection of spread-F in the ionogram using machine learning.

In this study, we prepare ionograms observed at 4 observatories (Wakkanai, Kokubunji, Yamagawa, Okinawa) utilized by National Institute of Information and Communications Technology. As for learning data in preparing the classifier, we use 200 events of spread-F observed at Okinawa in May, 2018. We made classifiers using feature quantities obtained by HOG(Histogram of Oriented Gradients) feature extraction.

Using the classifier to detect spread-F in the nest of ionograms of Okinawa in May 2019 which are not used as learning data, a detection rate at about 90%. In the presentation, we will present the comparison with another observation point at the same period and another period at the same observation point.

赤道スプレッドFと呼ばれる電離圏の不規則性は、電波の伝播という観点から非常に重要な現象である。スプレッドFに伴う電離圏擾乱の空間スケールはセンチメートルから数十キロメートルであり、広帯域の電波に影響を与える。したがって、それらは衛星地上通信、ナビゲーションシステムなどの信頼性にも影響を与える。

イオノグラムは、スプレッドFの重要な観測システムの1つである。従来イオノグラム内のスプレッドFの検出は手動で行われているので、優れた機械学習システムを開発することによってスプレッドFの検出を自動検出に置き換えることができれば、リアルタイムのスプレッドFの検出も可能になる。そこで、機械学習を用いてイオノグラム中のスプレッドFを自動検出する手法を開発した。

本研究では、情報通信研究機構が運用している4つの観測所（稚内、国分寺、山川、沖縄）で観測されたイオノグラムから周波数型とレンジ型のスプレッドFが現れているイオノグラムを用意した。今回の発表では、スプレッドF発生が多く見られる2018年5月の沖縄にて観測されたスプレッドF　200事例をデータとして用いた。この画像群に対してHOG(Histogram of Oriented Gradients)と呼ばれる輝度の勾配方向の分布を特徴量として機械学習を適用し分類器を作成した。この分類器を用いて学習に用いなかった2019年5月の沖縄のイオノグラムに対して検出を行ったところ9割程度の検出率が得られた。発表では同時期の別の観測点や同観測点の別の時期との比較結果について報告を行う予定である。

Xilinx社ZYNQ-7000 SoCを用いたFMCWイオノゾンデ・プロトタイプの開発

石橋 弘光 [1]; 近藤 巧 [2]; 津川 卓也 [1]; 石井 守 [1]
[1] 情報通信研究機構; [2] NICT

The development of the FMCW ionosonde prototype system based on the Xilinx ZYNQ-7000 SoC

Hiromitsu Ishibashi[1]; Takumi Kondo[2]; Takuya Tsugawa[1]; Mamoru Ishii[1]
[1] NICT; [2] NICT

NICT's portable and low-power FMCW (Frequency Modulated Continuous Wave) ionosonde system has been under operation for over 10 years as part of the SEALION (Southeast Asia Low-latitude Ionospheric Network) project. Because of system deterioration and frequent lightning damages in Southeast Asia monsoonal region, it becomes difficult to maintain the system and keep observations. Therefore, the development of a new ionosonde system is urgent issue for us to improve the SEALION.

The first attempt has been already presented at the SGEPSS 2016 fall meeting: we successfully got ionograms using a hybrid system that incorporates current FMCW ionosonde and Ettus Research USRP N210. After that, for the purpose of the control of current peripheral units, we also tried X300 USRP which has the GPIO interface (SGEPSS 2017 fall meeting). However, because we found some fatal technical problems, we were forced to abandon our FMCW ionosonde replacement plan using the USRP.

This presentation is a subsequent follow-up report for these past 2 years. We will show the newly developed prototype of FMCW ionosonde system based on the Xilinx ZYNQ-7000 SoC with hardware and software programmability. In addition, we will present the self-built transmitting module with the control PC of Raspberry Pi 2 which successfully functions as the replacement of current FMCW ionosonde transmitting system.

Statistical study of the growth rates of Medium-Scale TID observed with GPS-TEC

Takafumi Ikeda[1]; Akinori Saito[1]; Takuya Tsugawa[2]; Hiroyuki Shinagawa[2]
[1] Dept. of Geophysics, Kyoto Univ.; [2] NICT

We think two mechanism, E-F coupling and Perkins Instability, will relate to growth for nighttime-MSTID in mid-latitude [Tsunoda and Cosgrove., 2001 ; Perkins., 1973]. Linear growth rate of perturbation intensity of Pedersen conductivity expected from E-F coupling is around 15 minutes [Yokoyama et al., 2009], which is far shorter than one expected from Perkins Instability [Fukao and Kelley, 1991 ; Miller et al., 1997 ; Shiokawa et al., 2003]. However, Es layers spatial and temporal scale is less than 100km and 15min [Maeda et al., 2013 ; S.Saito et al., 2007].They are diffrent drom MSTID’s ones, which are 200-400 km and around 2hours [Otsuka et al., 2011].To decide which instability is responsible for growth of nighttime MSTID, the growth rate of MSTID was observationally determined with ground-based GPS network data.

We statistically investigated the growth rate of nighttime-MSTID in Japan in 2014 observed with GPS-TEC. The growth rate of nighttime -MSTID observed was 1.0 - 6.0 × 10-4 s-1 during 1800LT-2400LT in summer.Linear growth rate of Perkins instability in summer was 1.0 - 6.0 × 10-4 s-1 during 1800LT - 2400LT, so they were less than one of the E-F coupling instability.In presentation, we talk the detail about the relation between growth rates and two mechanisms, also growth rate and solar activity.

GNSS受信機によって観測された全電子数の緯度変化

大塚 雄一 [1]; 新堀 淳樹 [2]; 津川 卓也 [3]; 西岡 未知 [3]
[1] 名大宇地研; [2] 名大・宇地研; [3] 情報通信研究機構

Latitudinal Variation of Total Electron Content Observed by a World-Wide GNSS Receiver Network

Yuichi Otsuka[1]; Atsuki Shinbori[2]; Takuya Tsugawa[3]; Michi Nishioka[3]
[1] ISEE, Nagoya Univ.; [2] ISEE, Nagoya Univ.; [3] NICT

Latitudinal variation of the plasma density in the F region is characterized by Equatorial Ionization Anomaly (EIA), which is a phenomenon that the ionospheric plasma density is lager around +/-15 deg. than at magnetic equator. In this study, we investigate latitudinal variation of Total Electron Content (TEC) observed with Global Navigation Satellite System (GNSS) receivers. Using carrier phase and pseudorange data of dual frequency Global Navigation Satellite System (GNSS) signals, total electron content (TEC) along ray paths between satellites and receivers are obtained. We have analyzed the GNSS data provided by the International Geoscience Services (IGS), the University NAVSTAR Consortium (UNAVCO), Scripps Orbit and Permanent Array Center (SOPAC), and other global and regional data centers (more than 50 data providers in all). Absolute values of TEC are obtained from removing the inter-frequency biases from the original TEC by a method of Otsuka et al. (2002). In 2018, in the solar minimum conditions,

桜島噴火の規模とGPS-TEC変動との相関

庄子 聖人 [1]; 中田 裕之 [2]; 大矢 浩代 [3]; 鷹野 敏明 [4]; 津川 卓也 [5]; 西岡 未知 [5]
[1] 千葉大・工・電気電子; [2] 千葉大・工・電気; [3] 千葉大・工・電気; [4] 千葉大・工; [5] 情報通信研究機構

Relationship between the magnitude of Sakurajima eruptions and the disturbance of GPS-TEC

Kiyoto Shoji[1]; Hiroyuki Nakata[2]; Hiroyo Ohya[3]; Toshiaki Takano[4]; Takuya Tsugawa[5]; Michi Nishioka[5]
[1] Electrical and Electronic, Engineering, Chiba Univ; [2] Grad. School of Eng., Chiba Univ.; [3] Engineering, Chiba Univ.; [4] Chiba Univ.; [5] NICT

It is reported that ionospheric disturbances are caused by ground and atmospheric perturbations, e.g. earthquakes, typhoons and volcanic eruptions. Even though the volcanic eruptions excite the atmospheric waves, there is little reports of ionospheric disturbances caused by volcanic eruptions. Therefore, in this study, we analyzed the ionospheric disturbances caused by volcanic eruption using Total Electron Content (TEC) determined by GNSS system. And we estimate the propagation energy caused by the volcanic eruption from the data of the infrasound meter and estimate the TEC disturbance.

We analyzed TEC data observed in GNSS Earth Observation Network (GEONET) which is maintained by Geospatial Information Authority of Japan. Considering the effect of the difference in the direction between the propagation direction of atmospheric waves and geomagnetic field/the sight direction from GNSS receiver to the satellite, there is a positive relation between the magnitude of the eruption and TEC disturbances. An inverse correlation between the distance from the crater and the TEC disturbance was also appeard.

In this study, we have also tried to estimate the TEC disturbance from the magnitude of the eruption. Assuming that the propagation of the acoustic wave by the volcanic eruption is a spherical wave, the amplitude of the acoustic wave can be estimated from the infrasound data of Higashi-Korimoto and the distance from the crater. The amount of TEC disturbance is estimated from the amplitude of the acoustic wave and the electron density in the pierce points. In the presentation, we will show the result of this estimation.

地震や台風、火山噴火などの下層の現象に伴い、大気波動が生じ、これによって電離圏擾乱が引き起こされることが知られている。火山噴火に伴い、大気波動が生じることは知られているが，火山噴火に伴う電離圏擾乱の観測事例はそれほど多くない。そこで本研究では、火山噴火に伴う電離圏の変動について、全電子数 (Total Electron Content(以下 TEC)) を用いて解析した。また、空振計の値から火山噴火による伝搬エネルギーを推定し、TEC の変動量の推定を試みた。

火山噴火による電離圏変動として，桜島で発生した火山噴火 4 事例 (2007 年 1 月 2 日 9 時 5 分 (UT)、2009 年 10 月 3 日 7 時 45 分 (UT)、2012 年 9 月 19 日 1 時 7 分 (UT)、2014 年 2 月 12 日 20 時 21 分 (UT)) に伴う TEC 変動について解析した。大気波動の伝搬方向と，磁場，GPS の視線方向のずれによる影響を補正した結果，火山噴火の規模と TEC 変動との間には相関関係が見られた。さらに，火口からの距離と TEC 変動との間にも逆相関関係が見られた。

次に，解析した 4 事例について火山噴火で発生した大気波動の伝搬による TEC の変動量の推定を試みた。火山噴火による音波が球面波として同心円状に伝搬すると仮定し、空振計データ（東郡元）と火口からの距離より貫通点での音波の振幅が推定できる。この振幅の大きさと電離圏電子密度分布より TEC の変動量を推定する。発表では，その結果について述べる予定である。

HF ドップラー観測による H-IIA ロケット打ち上げに伴う電離圏変動の解析

山崎 淳平 [1]; 中田 裕之 [2]; 大矢 浩代 [3]; 鷹野 敏明 [4]; 細川 敬祐 [5]
[1] 千葉大; [2] 千葉大・工・電気; [3] 千葉大・工・電気; [4] 千葉大・工; [5] 電通大

Examination of the ionospheric perturbations associated with H-IIA rocket launching using HF Doppler sounding

Junpei Yamazaki[1]; Hiroyuki Nakata[2]; Hiroyo Ohya[3]; Toshiaki Takano[4]; Keisuke Hosokawa[5]
[1] Chiba Univ.; [2] Grad. School of Eng., Chiba Univ.; [3] Engineering, Chiba Univ.; [4] Chiba Univ.; [5] UEC

Since rocket launches generate the atmosphere waves, it is reported that passage and exhaust plumes associated with rocket launches generate TEC perturbations observed by GEONET data (e.g. Furuya and Heki 2008; Lin et al., 2014, 2017). On the other hand, there are few studies about ionospheric perturbations associated with rocket launches away from rockets' trajectories. Because of the disturbances due to exhaust plumes don't appear in the distance from the trajectories, we can extract those due to the atmospheric waves. Using HF Doppler sounding, therefore, we analyzed ionospheric perturbations associated with H-IIA (No.25 and 26) whose trajectories are relatively far from the Japanese islands. The Doppler sounding system is utilized by the University of Electro-Communications. In this system, the radio waves of 5 MHz and 8 MHz are transmitted from Chofu campus of University of Electro-Communications and those of 6 MHz and 9MHz are from Nagara transmitter of Radio NIKKEI. In this study, the Doppler shifts data observed at Sugadaira, Oarai, Kakioka, Fujisawa and Kyoto were used. In those data, the perturbations of Doppler shifts associated with H-IIA (No.25 and 26) were observed about 35 minutes after the launches. It is confirmed that this delay corresponds to the propagation time of the infrasound wave from the rocket to observation points once reflected on the ground. In both event, the periods of the disturbance of Doppler shift were 100˜200 s(5˜10 mHz). The Doppler shift perturbations were clear when the infrasound wave reached the observation point after reflection on the ground as compared to the case where the infrasound wave reached the observation point directly. The time of the perturbations of Doppler shifts at high altitude were faster than that of at low altitude. Therefore, it denoted that infrasound wave propagated from high altitude to low altitude.

テポドンなどのロケット打ち上げに伴う大気波動や排気煙により TEC 変動が発生することが GEONET データによる解析結果として報告されている (e.g. Furuya and Heki 2008; Lin et al., 2014, 2017)。テポドンは日本上空を通過したが、日本上空を通過しないロケットについて軌道から離れた位置における電離圏の変動は極めて報告例が少ない。遠方では排気による変動が現れないため、大気波動に伴う変動のみを抽出できる利点もある。そこで、本研究では HF ドップラー観測を用いて、H-IIA ロケット (25 号,26 号) 打ち上げに伴う、ロケット軌道から比較的離れた位置での電離圏の変動を解析した。本研究で使用した HF ドップラー観測システムは電気通信大学で運用されているもので、送信点は電気通信大学調布キャンパス (5 MHz, 8 MHz) とラジオ日経長柄送信所 (6 MHz, 9 MHz) である。また本研究では、調布キャンパスより送信された 5 MHz と 8 MHz、ラジオ日経長柄送信所より送信された 6 MHz と 9 MHz をそれぞれ、菅平、大洗、柿岡、藤沢、京都の各観測点で受信した際のドップラーデータを用いた。その結果、ロケット打ち上げから約 35 分後にドップラーシフトに変動が確認された。この時刻はロケットにより生じた音波が地面で 1 回反射後に観測点に到達した時刻と一致したことが、音波のレイトレイシングより確認された。また、これらの変動は 100〜200 秒 (5〜10 mHz) の帯域で変動強度が上昇していることが、どちらのイベントでも確認された。ドップラーシフトの振幅は、ロケットからの音波が直接観測点に到達した変動よりも、1 回地面に反射して観測に到達した変動のほうが大きかった。また、変動の到達時間から、低高度よりも高高度の変動のほうが、約 10〜20 秒早いことが確認できた。このことから、ロケットに伴う変動は高高度から低高度へ伝搬していると考えられる。

H-IIAロケットにより生じた電離圏TEC変動解析

武川 毅 [1]; 中田 裕之 [2]; 大矢 浩代 [3]; 鷹野 敏明 [4]; 津川 卓也 [5]; 西岡 未知 [5]
[1] 千葉大院・理工・基幹工学; [2] 千葉大・工・電気; [3] 千葉大・工・電気; [4] 千葉大・工; [5] 情報通信研究機構

Analysis of ionospheric TEC fluctuation excited by H-IIA rocket launches

Tsuyoshi Takegawa[1]; Hiroyuki Nakata[2]; Hiroyo Ohya[3]; Toshiaki Takano[4]; Takuya Tsugawa[5]; Michi Nishioka[5]
[1] Chiba Univ.; [2] Grad. School of Eng., Chiba Univ.; [3] Engineering, Chiba Univ.; [4] Chiba Univ.; [5] NICT

It is known that atmospheric waves arisen by massive earthquakes, typhoons and volcanic eruptions cause the ionospheric variation. In recent years, ionospheric fluctuations excited by rocket launches have been confirmed (e.g., Furuya and Heki, 2008; Lin et al., 2014, 2017). In association with Taepodong 2 launch, TEC fluctuations were appeared due to the chemical reaction with ionospheric plasmas and the exhaust of the rocket about 5 minutes after the launch (First wave). Subsequently, TEC fluctuations were observed about 30 minutes after the launch (Second wave). To examine the ionospheric disturbances apart from the trajectories of rockets, in this study, TEC fluctuation due to the launches of H-IIA rocket No.25 and No. 29 were examined using GEONET data. The first waves of the TEC fluctuations were confirmed around hundred kilometers from the rocket trajectory 5 minutes after launch of both of H-IIA rockets, as was the case for Taepodong 2. The first waves appeared as large decreases in TEC, while the second waves were fastly oscillating patterns.

Calculating the propagation time of the sound waves from the points on the trajectories of the rockets, the time of first wave correspond to the arrival times of directly acoustic wave from the trajectories of rocket.

The second waves of the TEC fluctuations which have higher frequency than first waves were confirmed around hundred kilometers from the rocket trajectory 30 minutes after launch of both of H-IIA rockets. The time of second wave correspond to the propagation times of the acoustic wave reflected once on the ground from the trajectories of the rockets.

先行研究より，巨大地震や台風，火山噴火といった地表付近の現象に伴って大気波動が生じ、これにより電離圏変動が引き起こされることが知られている。近年ではロケットによっての電離圏変動が確認されており、先行研究でもテポドン 2 号による電離圏変動が報告されている (e.g., Furuya and Heki, 2008; Lin et al., 2014,2017)。発射から約 5 分後に電離圏変動の第一波としてロケットの排気によっての化学反応から電子が減少、そして発射から約 30 分後に第二波が確認されている。そこで本研究では H-IIA ロケット 25 号 29 号の打ち上げに伴う TEC 変動の解析を、GEONET データを用いて行った。その結果、H-IIA ロケットの発射から 5 分後にロケット軌道より約 100 km の距離に、TEC の大きな減少として電離圏変動の第一波が観測された。また音波のレイトレーシングにより変動が観測された時間は、ロケットの軌道上の点から TEC 貫通点まで直接音波が伝搬する時間と一致することが確認された。また、ロケット発射から 30 分後に第一波に比べ変動周期の早い第二波が先行研究と同様に確認された。また第二波の到達時間を第一波と同様に計算したところ、地面に 1 回反射した波の到着時間と一致したことが明らかになった。

LF帯標準電波観測とGPS-TECによるTID同時観測

町 康二郎 [1]; # 中田 裕之 [2]; 大矢 浩代 [3]; 鷹野 敏明 [4]; 津川 卓也 [5]; 西岡 未知 [5]
[1] 千葉大・融合理工; [2] 千葉大・工・電気; [3] 千葉大・工・電気; [4] 千葉大・工; [5] 情報通信研究機構

Simultaneous observation of traveling ionospheric disturbances using LF radio wave observation and GPS-TEC

Kojiro Machi[1]; # Hiroyuki Nakata[2]; Hiroyo Ohya[3]; Toshiaki Takano[4]; Takuya Tsugawa[5]; Michi Nishioka[5]
[1] Grad. School of Sci. and Eng., Chiba Univ.; [2] Grad. School of Eng., Chiba Univ.; [3] Engineering, Chiba Univ.; [4] Chiba Univ.; [5] NICT

We had observed the LF Standard Time and Frequency Transmission to determine the height variation of the lower Ionosphere. The Standard Time and Frequency Transmission at the frequency of 60 kHz, which is transmitted from Mt. Hagane station, were observed by crossed loop antenna at Sugadaira, Nagano Prefecture. Separating the sky wave and the ground wave from the received wave, the variation of the ionospheric height was estimated from the phase variation of the sky wave.

In this study, we analyzed the height variation of the ionosphere whose frequency is about 0.3 mHz. This frequency corresponds to that of Traveling Ionospheric disturbances (TID). Using the wavehop method, the LF wave is considered to propagate from Mt. Hagane to Sugadaira with a single reflection at the ionosphere. We examined the TEC variations in the mid-point between Mt. Hagane and Sugadaira in association with the height variation in the lower ionosphere and found that the amplitudes of these variations have a linear relationship each other. Therefore, there is a relationship of ionospheric fluctuations between the lower and upper ionospheres.

HF ドップラー及び地震計を用いた地震に伴う電離圏擾乱の解析

大野 夏樹 [1]; 中田 裕之 [2]; 大矢 浩代 [3]; 鷹野 敏明 [4]; 細川 敬祐 [5]; 津川 卓也 [6]; 西岡 未知 [6]
[1] 千葉大・工・電気電子; [2] 千葉大・工・電気; [3] 千葉大・工・電気; [4] 千葉大・工; [5] 電通大; [6] 情報通信研究機構

Examination of ionospheric disturbances associated with earthquakes using HF Doppler and seismograph

Natsuki Ono[1]; Hiroyuki Nakata[2]; Hiroyo Ohya[3]; Toshiaki Takano[4]; Keisuke Hosokawa[5]; Takuya Tsugawa[6]; Michi Nishioka[6]
[1] Electrical and Electronic, Chiba Univ.; [2] Grad. School of Eng., Chiba Univ.; [3] Engineering, Chiba Univ.; [4] Chiba Univ.; [5] UEC; [6] NICT

It is reported that ionospheric disturbances occur after giant earthquakes. One of the reasons for these disturbances are the infrasound wave excited by ground motions.

The infrasound wave propagates upward and produces perturbations of the electron density in the ionosphere. Such perturbations are also detected by a network of ground-based GPS receivers as TEC perturbations. Using these TEC perturbations, horizontally propagation of the ionospheric disturbances from the epicenter is examined.

In this study, the coseismic ionospheric disturbances are examined using HF Doppler (HFD), GPS-TEC and seismometer data (F-net). The HF Doppler sounding system used in this study is enable to observe the vertical speed of the ionosphere in the midpoint between the transmitter and the receiver at four different altitudes.

We have found that the Doppler shift data obtained in Sugadaira observatory fluctuated in the events where the seismic intensity is larger than 6 lower and the magnitude is larger than M6. When the maximum ground velocity observed by Onishi seismometer, which is located closest to the reflection point, is larger than 2 mm/s, the long period fluctuation (3 - 20 mHz) dominates but decays as the distance between the observation point and the epicenter increases. In addition, in 3 cases where ionospheric disturbances in the different altitudes were observed by HFD, the long period fluctuation was dominant and the short period fluctuation (21 - 50 mHz) was attenuated as the reflection points become higher. This is because the acoustic wave excited by the seismic wave tend to attenuate at high altitudes.

大規模な地震の発生後に地面変動や津波により生じた音波や大気重力波が電離圏高度まで伝搬し電離圏擾乱が発生することが知られている．本研究で用いる HF ドップラー観測 (HFD) では，異なる送信周波数 (5.006，6.055，8.006，9.595 MHz) の電波を用いることで複数の高度での変動を観測することが可能である．また国土地理院の GNSS 連続観測システム (GNSS Earth Observation Network : GEONET) により導出される GPS-TEC のデータにも同様に地震に伴う変動が確認されることから，防災科学研究所の広帯域地震観測網 (F-net) の地震波形データ (速度) を合わせて，地面変動による電離圏擾乱への影響に注目し解析を行った．

2004 年以降に発生した震度 6 弱, M6 以上の地震 8 イベントで，菅平にて観測されたドップラーシフトデータに変動が確認された．さらにドップラーデータの周波数解析を行った．電波の反射点にもっとも近い鬼石地震計で観測された地面変動速度の最大値が 2mm/s よりも大きい地震では，ドップラーシフトの変動において長周期の変動成分 (3 - 20 mHz) が卓越し, 観測点と震央の距離が離れるにつれ，長周期の変動成分は減衰する傾向が確認された．また，複数の周波数において変動が観測できた 3 事例では，電波の反射高度が上がるにつれ，長周期変動成分は卓越し、短周期変動成分 (21 - 50 mHz) は減衰した．これは地震波が励起した音波は高い周波数ほど高高度で減衰するため，比較的高い高度で反射する電波 (8.006，9.595 MHz) のドップラーシフトデータでは変動が減衰したと考えられる．

現在地震計及び GPS-TEC データも合わせて周波数解析を行っており，発表ではその結果についても報告する予定である．

S-310-44号機観測ロケットによって観測されたSq電流系付近のDC電場の解析

森 俊樹 [1]; 石坂 圭吾 [2]; 阿部 琢美 [3]; 熊本 篤志 [4]; 田中 真 [5]
[1] 富山県大・工; [2] 富山県大・工; [3] ＪＡＸＡ宇宙科学研究所; [4] 東北大・理・地球物理; [5] 東海大・情教セ

Analysis of DC Electric Field in Sq current Observed by S-310-44 Sounding Rocket

Toshiki Mori[1]; Keigo Ishisaka[2]; Takumi Abe[3]; Atsushi Kumamoto[4]; Makoto Tanaka[5]
[1] Toyama Pref Univ.; [2] Toyama Pref. Univ.; [3] ISAS/JAXA; [4] Dept. Geophys, Tohoku Univ.; [5] Tokai Univ.

In the winter daytime, the Sq current system is generated in the ionosphere of about 100km at mid latitude. Unusual plasma phenomenon such as electron heating and strong electron density disturbance occur in the Sq current focus. In order to investigate, the S-310-44 rocket was launched in Japan in January 2016. The rocket passed through the Sq current focus, and all the on-board observation instruments were worked well. The rocket was equipped with Electric Field Detector (EFD), and the DC electric field (DC to 200 Hz) at the Sq current focus was observed.

The electric field observed by EFD is a mixed electric field of a natural electric field and an induced electric field generated when the rocket passes through the magnetic field. The rocket's attitude data is used to transform the induced electric field from the geographic coordinate system to the spin coordinate system, and the induced electric field is subtracted from the synthetic electric field obtained by EFD to calculate the natural electric field. The coordinate system of the natural electric field is converted from the spin coordinate system to the geographical coordinate system by transforming it again with attitude data. From these procedures, the DC electric field vector at the Sq current focus is estimated.

In this research, DC electric field vector was estimated at rocket ascent (altitude about 97km to 160km). The altitude at which the Sq current system is supposed to occur is around 97km to 107km. The natural electric field value at altitude of about 110km can be confirmed that the intensity is increased, because it is assumed that the electric field accelerates the electrons down, and collides with the neutral atmosphere around 100 km and electrons are heated.

We are going to investigate the generation mechanism of the high temperature electron region generated near the center of the Sq current system, by comparing the natural electric field vector to the electron density and the electron temperature.

冬季の昼間, 高度約 100km の電離圏中緯度にて Sq 電流系が発生し,Sq 電流系中心では電子加熱や強い電子密度擾乱等の特異なプラズマ現象が発生する. これらの特異なプラズマ現象を調査するために 2016 年 1 月に S-310-44 号機観測ロケットが打ち上げられた. ロケットは Sq 電流系中心を通過し, 搭載された観測機器はすべて正常に動作した. ロケットには電場観測装置 EFD が搭載されており,Sq 電流系中心の DC 電場 (DC~200Hz) を観測した.

EFD によって観測された電場は自然電場とロケットが磁場中を通過することで発生する誘導電場の合成電場である. そのため, 自然電場を求めるために, 磁場データとロケットの飛翔速度から誘導電場の値を導出する. そして, ロケットの姿勢データを用いて誘導電場を地理座標系からスピン座標系に変換する. そして,EFD 観測から得られた合成電場から誘導電場を減算し、自然電場を導出する. 自然電場の座標系を姿勢データを用いて再度変換することで, スピン座標系から地理座標系に変換する. これらの手順から,Sq 電流系中心の DC 電場ベクトルを導出する.

本研究では, ロケット上昇時 (高度約 97km-160km) における DC 電場ベクトルを導出した.Sq 電流系が発生するとされている高度は約 97km-107km 付近である. この付近の電場ベクトルを見ると,110km 近辺で電場の値が大きくなっていることが確認できた. これは電場が電子を下向きに加速させて, 電子が中性大気に衝突することで電子加熱が起こっていると推測する.

今後は, 得られた DC 電場ベクトルを電子密度や電子温度と比較し, より詳しい解析を行うことで Sq 電流系中心付近に発生する高温電子領域の発生メカニズムの解明を目指す.

S-520-27号ロケットより放出されたTMAの観測画像を用いた熱圏下部中性風プロファイルの解析と評価

大塚 祐樹 [1]; 山本 真行 [2]
[1] 高知工科大・工・基盤工学; [2] 高知工科大

Analysis and evaluation of the neutral wind profile in the lower thermosphere using images of TMA released from S-520-27 rocket

Yuki Otsuka[1]; Masa-yuki Yamamoto[2]
[1] Engineering, KUT; [2] Kochi Univ. of Tech.

1. Research background and purpose

The altitude profiles such as the plasma density or the neutral atmospheric density in the lower thermosphere varies with the solar activity, the season, and/or local time. Such fluctuation causes various problems that affect on telecommunication or orbits of the satellites. However, we do not understand the mechanism for causing these problems. Our laboratory has participated experiments of observing neutral window profiles in the lower thermosphere with JAXA and NASA in this decade.

In this study, our purpose is analyzing the neutral wind profile in the lower thermosphere by using sequential images of Trimethylaluminium (TMA)observed in the rocket experiment in July 2013. Also, we tried to calculate the wind profile by applying several methods and evaluate by comparing with each results.

2. Outline of rocket experiment

In July 20, 2013, JAXA conducted a sounding rocket campaign. The purpose of this experiment is investigating the electromagnetic interaction and the total picture of ionization, the neutral atmosphere interaction which act in the middle latitude ionosphere. Two rockets, S-310-42 and S-520-27, were launched at Uchinoura Space Center (USC). S-310-42 released TMA and S-520-27 released Lithium (Li). And luminous clouds of TMA and Li were observed at multipoint on ground and an airplane.

3. Method of wind profile calculation

We calculate wind profile with images of TMA observed in the rocket experiments. We analyze the images taken at the airplane (Fig. 1) and USC (Fig. 2)because TMA were clearly identified in these images and a sequence of long time optical observation was conducted at these observation points.

Process of wind profile calculation is as follows

1) Calculating the center axis of TMA illumination by polynomial approximation or skeleton extraction.
2) Calculating the relative azimuth/elevation changes between two images of the center axis of TMA.
3) Calculating the migration length of TMA from the relative azimuth/elevation changes and the trajectory information of the sounding rocket.
4) Calculating wind profile from the migration length of TMA and the passage of time between two images.

4. Results and consideration

The calculated result of the wind profile with observation images at USC is shown in the figure 3. The opened circles show the result by polynomial approximation and the closed circles show the results by skeleton extraction. The results are the averaged wind velocity between 23:05:24 (JST) and 23:06:20 (JST) in July 20th, 2013. We can find the strong windshear at an altitude range from 85 km to 100 km.

In the altitude range less than 90 km, there is a difference between the results by polynomial approximation and those by skeleton extraction. It is thought that the cause of the problem is in the applying program, and currently we are trying to make a revision of it.

5. Summary and future plan

In the analyses, we calculated wind profiles by using observation images taken at USC. In near future, we are going to correct the errors of lens distortion and tilt of the camera setting. Also, we are going to analyze not only the images taken at USC but also those at airplane. And we are going to calculate two dimensional wind profile by applying triangulation technique.

Reference

[1]Kihara Daiki, "Airborne observation of resonance scattering Lithium vapor released from sounding rocket in upper atmosphere and development of determination method of thermospheric neutral wind in daytime", Master thesis, Kochi University of Technology, 2015.

[2]Yokoyama,Yuki, "Multipoint observation of resonance scattering Lithium vapor released from S-520-23 rocket and high precision analysis of thermospheric neutral wind", Master thesis, Kochi University of Technology, 2009.

1. 研究背景・目的

電離圏における電離大気密度や中性大気密度等の高度プロファイルは、太陽活動・季節・昼夜の変化に伴い、変動する。こうした変動は地上での通信や人工衛星の軌道等に影響を与える様々な影響を引き起こすが、詳しい発生メカニズムは分かっていない。本研究室では、電離圏における中性大気風に関して、JAXA や NASA との共同実験・研究を実施してきた。

本研究では JAXA が 2013 年 7 月に実施した、夜間中緯度域におけるロケット実験時に観測されたトリメチルアルミニウム (TMA) の画像を用いて、電離圏における中性風の風速を算出することを目的とする。また複数の手法による風速算出を実施し、それぞれの結果を比較することで、算出した風速の評価も行っていく。

2. ロケット実験概要

中緯度電離圏に作用する電磁気的相互作用と電離・中性大気相互作用の全貌を明らかにすることを目的として、JAXA が 2013 年 7 月ロケット実験を実施した。内之浦宇宙空間観測所（USC）から S-310-42 号機と S-520-27 号機の計 2 機の観測ロケットが打ち上げられた。前者では TMA、後者からは Li（リチウム）が超高層大気中へと放出され、各観測地点及び航空機からの光学観測が実施された。

3. 風速算出方法

風速の算出には、2013 年 7 月のロケット実験で観測された TMA 発光雲の画像を用いる。各観測地点で観測された画像から、TMA が明瞭に写り、かつ長時間光学観測が実施された組み合わせとして、航空機からの画像（図 1）と USC での画像（図 2）を解析していく。

風速算出の手順

1. TMA の観測画像から多項式近似、または骨格抽出を用い、TMA の中心軸を算出する。
2. TMA 中心軸の相対方位角・相対仰角を算出する。
3. 2 で得られた相対方位角・相対仰角とロケットの軌道情報から TMA の移動距離を算出する。
4. 移動距離と経過時間から風速を算出する。

4. 結果・考察

USC での観測画像のみを用いての風速算出結果を図 3 に示す。風速は 2013 年 7 月 20 日 23:05:24(JST)～23:06:20(JST) の平均風速である。緑で示したものが多項式近似による中心軸算出を用いた風速算出結果、赤で示したものが骨格抽出による中心軸算出を用いた風速算出結果である。特に高度 85km～100km 付近において非常に強いウィンドシアがあることが分かる。

高度 90km 以下においてデータ数の差が出ている。これは骨格抽出のプログラムが原因と考えられるため、修正する必要がある。

5. まとめ・今後の予定

今回は USC での観測画像のみを用いての風速算出を行った。今後はレンズの歪み・カメラの傾き等による誤差の評価を行っていく予定である。また 1 地点での観測画像のみでなく、航空機からの観測画像も併用し、三角測量による解析も実施し、2 次元方向の風速算出結果も発表する予定である。

参考文献

[1] 木原大城,“観測ロケットより超高層大気中に放出したリチウム共鳴散乱光の航空機観測と昼間熱圏中性風測定手法の開発”平成 26 年度高知工科大学大学院 特別研究報告,2015.

[2] 横山雄生,“S-520-23 号ロケット放出 Li による共鳴散乱光の多地点観測と熱圏中性風の高精度解析”平成 20 年度高知工科大学大学院 特別研究報告, 2009.

Fig. 1 Observed TMA image at airplane

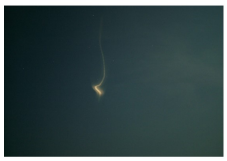

Fig. 2 Observed TMA image at USC

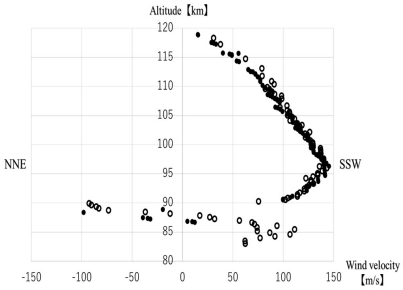

Fig. 3 The results of calculation wind profiles by two methods

Solar X-ray effects on the D-region ionosphere using tweek atmospherics

Kodai Yamanobe[1]; Hiroyo Ohya[2]; Hiroyuki Nakata[3]; Toshiaki Takano[4]; Kazuo Shiokawa[5]
[1] Chiba University; [2] Engineering, Chiba Univ.; [3] Grad. School of Eng., Chiba Univ.; [4] Chiba Univ.; [5] ISEE, Nagoya Univ.

It has been known that intensity and phase of very low frequency (VLF, 3 - 30 kHz)/low frequency (LF, 30 - 300 kHz) transmitter signals significantly change due to intense ionization by solar flare X-ray [e.g., Mitra, 1974; Thomson et al., 2005]. The duration of the D-region enhancements due to X-ray is easier to be estimated using the VLF/LF waves, because the relaxation time for recombination in the D-region ionosphere is short to be within ˜100 s [e.g., Ohya et al., 2015]. Tweek atmospherics are VLF/Extremely Low Frequency (ELF, 0.3-3 kHz) electromagnetic waves that are originated from lightning discharges and propagate for a long distance with reflecting between the Earth's surface and bottom of the ionosphere. It is possible to estimate the electron density at the reflection height in the lower ionosphere using the tweeks. The D-region electron density in wide area can be estimated by the tweeks compared with limited propagation paths of transmitter signals. In this study, we investigate solar X-ray effects on the D-region ionosphere using tweeks. We analyzed the daytime tweek atmospherics observed at Moshiri (44.37N, 142.27E), Japan. To investigate the X-ray effects on the D-region ionosphere in more detail, the observation time of the tweeks has been improved from four minutes every hour to 59 minutes every hour since 18 June, 2019. In addition, the sampling frequency was changed from 20 kHz to 40 kHz. During 00:00-06:00 UT on 1-5, 29 July and 12-14 September, 2013, the tweek reflection height had a weak negative correlation (the correlation coefficient: -0.42) with X-ray flux observed by the GOES-13/15 satellites, which suggests that electron density in the D-region ionosphere increased with increasing the X-ray flux. In this presentation, we show variations in the tweek reflection height before and after solar flares.

Sub-ionospheric effects of volcano eruptions using VLF/LF standard radio waves

Kei Maruyama[1]; Hiroyo Ohya[2]; Fuminori Tsuchiya[3]; Kenro Nozaki[4]; Kozo Yamashita[5]; Yukihiro Takahashi[6]; Hiroyuki Nakata[7]; Toshiaki Takano[8]
[1] Electrical and Electronic, Chiba Univ.; [2] Engineering, Chiba Univ.; [3] Planet. Plasma Atmos. Res. Cent., Tohoku Univ.; [4] NICT; [5] Engineering, Ashikaga Univ.; [6] Cosmosciences, Hokkaido Univ.; [7] Grad. School of Eng., Chiba Univ.; [8] Chiba Univ.

Several studies for the F-region ionosphere associated with volcano eruptions based on GPS-TEC data have been reported so far (e.g., Heki, 2006; Dautermann et al., 2009; Heki et al., 2010). These studies reported that acoustic waves excited by volcano eruptions reach up to the F-region ionosphere and caused F-region perturbations. After eruption of the Kelud Volcano, Indonesia, in February 2014, acoustic resonance between the Earth's surface and lower thermosphere was reported based on TEC data and the seismic wave data (Nakashima et al., 2015). However, little studies on the D-region ionosphere associated with volcano eruptions have been reported. In this study, we investigate the D-region effects of eruptions of Sakurajima volcano (31.59N, 130.66E), Japan, and Eyjafjallajokull (63.63N, 19.63W), Iceland, using intensity and phase of VLF/LF transmitter signals. The VLF/LF propagation paths used in this study were JJY60 kHz - TWN (Taiwan), JJI (22.2 kHz) - TWN, and NRK (37.5 kHz) - NYA (Norway). As for eruptions of Sakurajima volcano at 04:11 UT on June 6, 2014, based on wavelet spectra, the variations of both intensities (JJY60kHz - TWN and JJI - TWN) had a frequency of 2-6 mHz during 04:12-04:30 UT after the eruptions. We compared the VLF/LF variations with atmospheric pressure data obtained by an infrasonic meter observed by Sakurajima Volcano Research Center, Kyoto University, and seismic waves in the NIED F-net data (FUK, STM, and SBR) located close to the JJY-TNN path. The atmospheric pressure and vertical velocity of the seismic waves had the similar frequencies of 2-10 mHz during 04:12-04:47 UT. As for eruptions of Eyjafjallajokull at 05:55 UT on April 14, 2010, the intensity of transmitter signals (NRK- NYA) increased by about 2 dB after the eruption. Frequencies of 0.8-1.5 mHz and 2-10 mHz appeared during 06:12-06:18 UT. The variations in the VLF/LF intensity with the common frequencies of the 2-10 mHz for two eruption events could be caused by acoustic resonance between the Earth's surface and lower thermosphere, or by acoustic or atmospheric gravity waves generated by volcanic eruptions. However, variations in the VLF/LF intensity with the frequencies of 0.8-1.5 mHz have not been reported so far. In the presentation, we will show the results of these eruption events and discuss the cause of the VLF/LF variations in more detail.

Improvement of estimation method for propagation distance of tweek atmospherics

Masafumi Kanno[1]; Hiroyo Ohya[2]; Kazuo Shiokawa[3]; Hiroyuki Nakata[4]; Toshiaki Takano[5]
[1] Science and Engineering, Chiba Univ.; [2] Engineering, Chiba Univ.; [3] ISEE, Nagoya Univ.; [4] Grad. School of Eng., Chiba Univ.; [5] Chiba Univ.

Tweeks are very low frequency (VLF) / extremely low frequency (ELF) waves radiated from a lightning discharge and propagate in the Earth-Ionosphere waveguide for a long distance. As the most important characteristics, tweeks have frequency dispersion that the frequency rapidly falls down from 10 kHz to 2 kHz during several tens of milliseconds. So far, the cutoff frequency and the horizontal propagation distance of tweeks were estimated by curve fitting on dynamic spectra drawn by the maximum entropy method (MEM). However, the rapid variations in the frequency at the arrival time and overlapping tweeks caused the low estimation accuracy. The accuracy of the lightning location estimated from tweek atmospherics is low to be 60 km [Santolik and Kolmasova, 2017], while the accuracy of lightning location for the lightning discharges of world-wide lightning location (WWLLN) data is high to be less than 10 km [Rodger et al., 2005]. In this study, we propose a new method to estimate tweek propagation distances and compare the results from the new and previous methods. The new method uses conversion of non-linear dispersion equation to a linear equation. The linear equation would be more useful for estimating the propagation distance, even if attenuation around the cut-off frequency is large. As a result of evaluation by pseudo-tweeks using this method, the error of the propagation distance was estimated to be 6.8%. In this presentation, we show the new method for tweek propagation distance in detail and discuss its accuracy.

Diminished occurrence of afternoon counter electrojet in certain longitude sectors and seasons

Dupinder Singh[1]; Huixin Liu[2]
[1] Faculty of Science, Kyushu Univ.; [2] None

Dupinder Singh, Huixin Liu, S. Gurbubaran

Equatorial electrojet (EEJ) is a narrow band of current flowing eastward in the dayside ionosphere around the vicinity of the geomagnetic equator. Occasionally, the EEJ reverses from its normal eastward direction to westward during daytime. The reversed EEJ is known as counter electrojet (CEJ). CEJs occur mainly during morning and afternoon hours and is referred to as morning CEJ (MCEJ) and afternoon CEJ (ACEJ) respectively.

We derived the occurrence pattern of ACEJ from a chain of ground magnetic observations in the vicinity of the geomagnetic equator. It is found that the occurrence of ACEJ is diminished in certain longitude sectors and seasons. These results are discussed in context with the observed electrojet and tidal patterns from CHAMP satellite and TIMED Doppler Interferometer (TIDI) respectively. We also attempt to compare these observations with GAIA simulation results.

TBEx衛星・COSMIC-2衛星からの２周波ビーコン波による低緯度電離圏観測手法の開発

氏原 伸裕 [1]; 山本 衛 [2]
[1] 京大・情報・通信; [2] 京大・生存圏研

Development of low-latitude ionosphere observation technique with dual-band beacon experiment from TBEx and COSMIC-2 satellites

Nobuhiro Ujihara[1]; Mamoru Yamamoto[2]
[1] Communications, Kyoto Univ.; [2] RISH, Kyoto Univ.

In the low-latitude ionosphere, plasma bubbles are frequently generated, and it is known that they occur immediately after sunset of the ionospheric altitude in the equinox. Behavior of plasma bubbles is complex, and thus has been studied very much. From total electron content (TEC) observations with C/NOFS satellite (Orbit inclination: 13 degrees) revealed that the plasma bubble is associated with the ionospheric large-scale fluctuation of several 100 km wavelength in the east-west direction, which is called Large-Scale Wave Structure (LSWS). The plasma bubble is generated more often when the LSWS amplitude increases. As there was only one C/NOFSsatellite, the observation frequency was only every ˜90 minutes, which limited in capturing space-time structures of LSWS. On June 25, 2019, two new satellite, TBEx (constellation of two units) and COSMIC-2 (constellation of six units), were newly launched. If beacon TEC measurement is available from all these satellites, the observation frequency can reach every 15 minutes, which helps much to study the space-time structure of plasma bubbles and LSWS. The purpose of this study is a development of observation method using these two beacon satellites. We conducted orbital simulation of new satellites, the development of received signal analysis software, the design and installation of the receiver, and the examination of processing method of observation data. In the presentation, we will report on examination of processing method of observation data.

低緯度電離圏ではプラズマバブルが頻繁に発生する. プラズマバブルは春分・秋分の電離圏高度の日没直後に発生することが知られている. しかしながらその日々変化が複雑であって, 研究トピックとされている. プラズマバブルの前兆現象として, 電離圏に Large Scale Wave Structure (LSWS) と呼ばれる東西方向の波長数 100km に及ぶ大規模な変動が現れる. 低緯度の観測に特化した C/NOFS 衛星 (軌道傾斜角 13 度) から地上へのビーコン観測から電離圏 Total Electron Content (TEC) を求められ, LSWS とプラズマバブルの関連が明らかになり, さらに LSWS の振幅が増大するときにプラズマバブルの発生確率が増大することが分かった. しかし C/NOFS 衛星は 1 機のみであったため, 観測頻度が約 90 分毎と少なく, LSWS の時空間構造を捉えることに限界があった. 本年 6 月 25 日に新しく 2 種類の衛星, TBEx (2 機編隊) と COSMIC-2 (6 機編隊) が打上げられた. これら全ての衛星からビーコン波が送信されれば, 観測頻度は平均 15 分に 1 回程度になり, プラズマバブルと LSWS の時間・空間変化を観測することができる. 本研究では, この 2 種類のビーコン衛星を用いた観測手法の開発を目的とする. 現在までに新しい衛星の軌道シミュレーション, 受信信号解析ソフトウェアの開発, 受信機の設計・開発・設置, 観測データの処理方法についての検討を行った. 本発表では観測データの処理方法についての検討について報告する.

Current status of the project to investigate ionospheric effects on GNSS in Southeast Asia

Takuya Tsugawa[1]; Kornyanat Hozumi[2]; Punyawi Jamjareegulgarn[3]; Pornchai Supnithi[3]; Susumu Saito[4]; Yuichi Otsuka[5]; Shinichi Hama[6]; Takahiro Naoi[1]; Mamoru Ishii[1]
[1] NICT; [2] NICT; [3] KMITL; [4] ENRI, MPAT; [5] ISEE, Nagoya Univ.; [6] NICT

NICT have started a research project to investigate ionospheric impacts on GNSS positioning/navigation including precise positioning technique using quasi-zenith satellite (QZSS) since 2017. In this project, we have studied ionospheric effects on individual positioning techniques (single frequency, DGPS, and RTK-PPP) and consider methods to mitigate and/or prevent the positioning errors under severe ionospheric conditions such as large ionospheric storm and plasma bubble. In the low-latitude region such as Southeast Asia, one of the most important ionospheric phenomena is plasma bubble. Plasma bubbles can cause ionospheric scintillation on GNSS signals which pass through the plasma bubble structures due to ionospheric plasma irregularities inside the structures. The GNSS scintillation would result in the loss-of-lock on GNSS signals in the worst case. Therefore, it is important to precise observation of the plasma bubble structures and identify which satellite-receiver path suffers from the structures for verifying the plasma babble impacts on GNSS positioning.

In this project, we have proceeded to install a VHF radar at Chumphon (Thailand) and multi-GNSS receivers (TEC and scintillation monitors) at Chumphon, Bac Lieu (Vietnam), and Cebu (Philippines) at the magnetic equator. The VHF radar consisting of 18 Yagi antennas will use the frequency of 39.65MHz with 25kHz bandwidth. The radio license in Thailand has been approved in June 2019 and will be installed in November-December in 2019. The multi-GNSS receiver, Septentrio PolaRx5S, have been installed in Chumphon in June 2019. The other two receivers will be installed in Bac Lieu and Cebu in August-September in 2019. In this presentation, we will report the current status of the project.

Comparison of plasma bubble drift velocity observed by ground GPS and those simulated by GAIA model

Hiroto Takahashi[1]; Huixin Liu[2]; Yuichi Otsuka[3]; Hiroyuki Shinagawa[4]
[1] Earth and planetary science, Kyusyu Univ.; [2] None; [3] ISEE, Nagoya Univ.; [4] NICT

Knowledge of the zonal drift velocity of plasma bubbles is important for real-time forecast of plasma bubble occurrence. In the equatorial region, the ExB drift is responsible for the eastward motion of the background plasma. It is considered that the plasma bubble travels at the same speed as the background plasma. In this study, we estimate the drift velocity of irregularity associated with the equatorial plasma bubble using three single frequency GPS receivers at the equatorial atmospheric radar (EAR) site at Kototabang in Indonesia (0.20 S, 100.32 E; geomagnetic latitude 10.6 S). This velocity is then compared to the zonal drift velocity reproduced by the GAIA model, to examine the consistency of the two. If the consistency is good, the GAIA model can be used to predict the arrival time of plasma bubbles at locations eastern of Kototatabang. The predicted arrival time of plasma bubbles are verified by using the GPS scintillation observation at Pontianak (0.02 S, 109.3 E; geomagnetic latitude 9.8 S), located 800 km east of Kototabang.

プラズマバブル監視用地上設置型リアルタイム全天観測システムの開発

直井 隆浩 [1]; 坂口 歌織 [1]; 小川 泰信 [2]; 久保 勇樹 [1]
[1] 情報通信研究機構; [2] 極地研

Development of the ground-based real-time all-sky imager for plasma bubble monitoring

Takahiro Naoi[1]; Kaori Sakaguchi[1]; Yasunobu Ogawa[2]; Yuki Kubo[1]
[1] NICT; [2] NIPR

The development of the ground-based optical observation system for monitoring of equatorial plasma bubbles is shown. We manufactured the system with catalog items only, so that it was made much cheaper than the general products were. As degradation such as by the solar radiation at day time needs not mind for the low-cost product, the system is suitable for full-time monitoring observation. This system has been installed at YAMAGAWA radio observation facility of NICT (National Institute of Information and Communications Technology) on the 13th February 2019 and started observation.

Plasma bubbles are irregular and low-density regions generated locally in the equatorial and low-latitude ionosphere. Plasma bubbles usually begin to appear around sunset near the magnetic equator and propagate eastward having with structures aligned with the magnetic field. Plasma bubbles occasionally reach Japanese latitudes under high solar activity or certain geomagnetic storm conditions. Satellite communication and navigation are often disrupted by irregularities in the ionospheric plasma density. The evaluation and forecast of such plasma density irregularities are regarded as a critical issue for stable communication and precise navigation.

We chose 630.0 nm atomic oxygen emission to identify the plasma bubbles. The airglow has the brightness at the point about 50 km below the peak of the F layer. When plasma bubbles appear in ionosphere, the number of the atomic oxygen and electron are rapidly decrease. As a result, the intensity of the glow is weakened and the one like a dark shadow is recognized there. The propagation velocity and spatial change can be known by the consecutive imaging with high-sensitivity camera. Our new system was installed at the roof of the main two-story building, $31^d12^m17^s$N $130^d36^m58^s$E, in the YAMAGAWA facility, Ibusuki, Kagoshima, Japan. Because the geomagnetic latitude there is relatively low compare to the geographical latitude, plasma bubbles are observable from the facility.

The system includes optics, housing, and control parts. The optics consists of a color (WAT-221S2) and a monochrome (WAT-910HX) high-sensitivity cameras with wide field-of-view fish-eye lens (TV1634DC). As a 630.0 nm filter is mounted in the monochrome camera, we can distinguish easily between the bubbles and clouds. The exposure time is 1/60 sec and the number of the integration is 256 times, so that the cameras show the images about every 4.3 seconds which are sent to a video encoder (M7014). The encoder received the analogue data and send them to a control PC 14 times per minute through the internet. The data are captured at night time from 5 p.m. until 5 a.m. every day. Concerning the housing, we adopted a plastic box (PL20-44) for outdoor use. Two acrylic domes were attached on the top of the box and sealed for waterproofing. The camera sets, video encoder, and a power tap were installed in it. The PC saves the image data in the external HDD and transfers them to NICT at Koganei headquarters in real time. The transferred data are processed into movies automatically which enable us to recognize the bubbles easily. Besides, the calibration experiment for the monochrome camera with 630.0 nm filter was done at NIPR (National Institute of Polar Research). Here, we report the results of the observation at YAMAGAWA but also discussion about the absolute sensitivity and comparison among the similar observations.

本発表では、プラズマバブルの監視目的のため、地上設置型の光学観測システムの開発と最初の運用結果について示す。システムはカタログ品を組み合わせ低廉化することで、製造コストを低く抑えることに成功している。廉価カメラによる観測は月や日中の日射などを特に気にすることなく観測を続けることができるため、定常観測に適している。システムは、情報通信研究機構の山川電波観測施設に設置され、リアルタイム監視による定常観測運用を行っている。

プラズマバブルは、地表から高度 100km 以上の電離圏で発生する局所的にプラズマ密度が低い領域と考えられている。多くの場合、日没時刻頃に赤道域で発生し、南北に伸びた構造を保ちながら、背景大気の風の影響で東にゆっくり伝搬することがわかっている。プラズマバブルに伴う局所的なプラズマ密度の不規則構造が発生した場合には、電波の振幅や位相の急激な変動が生じる。これらは一般に擾乱（じょうらん）、もしくはシンチレーションと呼ばれ、測位衛星等を利用した電子航法に深刻な障害を及ぼすことが知られている。

この現象を捉えるため、本観測では、630.0nm の酸素原子大気光をターゲットとした。この大気光は F 層のピーク高度よりも 50km ほど下に発光のピークを持つと考えられている。電離圏でプラズマバブルが発生すると、その場の O+ と電子が急減するため、大気光発光強度も弱くなり、観測画像に黒い影のように認められる。高感度の光学観測機器を用いた連続観測で、この空間的な広がりと伝搬時間の変化を捉えることができる。システムは、鹿児島県指宿市にある情報通信研究機構山川電波観測施設（北緯 31 度 12 分 17 秒、東経 130 度 36 分 58 秒）の観測棟 2 階屋上に設置した。日本周辺は地理緯度に対して磁気緯度が比較的低くなっており、同施設から赤道電離圏擾乱現象のひとつであるプラズマバブルの観測が可能である。

観測システムはカメラ等の光学系、カメラを収納するハウジング、これらを制御するソフトウェアからなる。カメラはカラー (WAT-221S2) と白黒 (WAT-910HX) の 2 式を用意した。双方のカメラに魚眼レンズ (TV1634DC) を装着し、また白黒カメラには 632nm (FWHM=10nm) の光学フィルタをインストールしている。カラーカメラで同時に撮像すること

により、画像内の領域がプラズマバブルか雲かを区別しやすくしている。カメラは、シャッター速度 1/60 秒、256 積分により、およそ 4.3 秒に 1 度の割合で信号を切り替える。アナログ信号を受けたエンコーダ (M7014) は、1 分間に 14 回、ネットワーク経由で制御 PC へ信号を送っている。データは、現地時間で午後 5 時から午前 5 時までの、夜間のみの取得としている。ハウジングには、一般に屋外へ配電盤などを収納するためのプラスティックボックスを採用した (PL20-44)。天板を加工してアクリルドームを固定し、防水性を高めるためにシールした。ボックス内部の基盤取り付け板にカメラ用の雲台を固定し、他に電源とエンコーダを収納した。制御 PC には CentOS 7 をインストールし、自前の制御ソフトによりデータの保存と加工及び転送を行っている。データは準リアルタイムで小金井へも転送している。情報通信研究機構小金井本部へ送信された画像データは、通常画像の動画化と差分を取った画像の動画化を行い、バブルの動きを直感的にとらえやすくする加工施している。全自動で処理されたこれらの結果は、ブラウザ上で簡単に閲覧できるようにした。また、絶対放射強度を見積もるためのカメラの較正実験を行った。実験には、国立極地研究所の較正実験施設を利用した。発光の絶対強度を知ることは、類似の観測結果との比較に不可欠である。他の観測点や異なる波長での観測結果の比較は、水平方向のドリフトだけでなく、高度プロファイルの見積もりを可能とし、三次元構造の推定ができるようになる。

プラズマバブルを捉え可視化することで、空間的広がりの理解、伝搬時間の把握、本州への電波通信障害の予測への応用、が可能である。プラズマバブルが本州付近を通過する際の電波障害のリアルタイム予報に役立てられ、宇宙天気予報業務に貢献できる。

ハワイの大気光画像中に見られる中間圏・電離圏波動の水平位相速度・パワースペクトル密度分布の統計解析及びイベント解析

内藤 豪人 [1]; 塩川 和夫 [1]; 大塚 雄一 [1]; 坂野井 健 [2]; 齊藤 昭則 [3]; 中村 卓司 [4]
[1] 名大宇地研; [2] 東北大・理; [3] 京都大・理・地球物理; [4] 極地研

The horizontal phase velocity and PSD distribution of mesospheric and ionospheric waves observed in airglow images in Hawaii

Hideto Naito[1]; Kazuo Shiokawa[1]; Yuichi Otsuka[1]; Takeshi Sakanoi[2]; Akinori Saito[3]; Takuji Nakamura[4]
[1] ISEE, Nagoya Univ.; [2] Grad. School of Science, Tohoku Univ.; [3] Dept. of Geophysics, Kyoto Univ.; [4] NIPR

Atmospheric gravity waves (AGWs) and medium-scale traveling ionospheric disturbances (MSTIDs) are important wave phenomena in the upper atmosphere, since they can control global dynamics of the atmosphere and affect GNSS positioning. Matsuda et al. [JGR, 2014] proposed a method of deriving the horizontal phase velocity and propagation direction of the power spectral density of waves found in images using three-dimensional fast Fourier transform. However, there has been no report to apply this method to airglow images obtained at low latitudes near the equator. In this study, we applied the analysis method of Matsuda et al. [2014] to airglow images obtained at wavelengths of 557.7 nm and 630.0 nm during the three years from 2013 to 2016 at Haleakala (20.7oN, 203.7oE) in Hawaii. We clarified the statistical features of AGWs and MSTIDs near the equator, and compared them with features seen in Japan reported by Takeo et al. [JGR, 2017] and Tsuchiya et al. [JGR, 2018], where the latitude, longitude and orography are greatly different those of Hawaii.

The three-year average of the phase velocity spectra of AGWs observed in airglow images at wavelength of 557.7 nm shows that there was no difference in the zonal propagation between summer and winter. In Japan, however, it is known that the propagation direction is eastward in summer and westward in winter. We reported this result in JpGU2019 and discussed this difference due to latitudinal variation of mesospheric jet wind which controls AGW propagation through wind filtering effect.

The MSTIDs observed in airglow images at a wavelength of 630.0 nm shows that the power spectral density (PSD) was strongest and the waves propagate mainly in the east-west direction in winter. To explain this seasonal variation in power spectral density, we calculated maximum linear growth rate of Perkins instability [Perkins, JGR, 1973] with considering the effect of seasonal variation of thermospheric neutral wind in Haleakala and its magnetic conjugate point, as was done by Duly et al. [AnnGeo, 2013]. We found that the seasonal variation of PSD cannot be explained by the neutral wind. This seems to be consistent with the previous suggestion by Yokoyama et al. [JGR, 2009] and Narayanan et al. [JGR, 2018] that the sporadic E layer is more important to produce nighttime MSTIDs at middle latitudes. Regarding the east-west propagation of MSTIDs in winter, we made detailed event study using zonal keogram, and found that there is no plasma bubble mixed in the eastward propagation and the observed waves has larger wavelengths and less continuity compared with MSTIDs observed in Japan.

超高層大気の波動現象である大気重力波や伝搬性電離圏擾乱は、大気のグローバルな循環や衛星測位に大きな影響を与えることが知られている。夜間大気光の撮像を通して、これらの波動を可視化することができる。Matsuda et al. [JGR, 2014] は、3 次元高速フーリエ変換を用いて大気光画像中に見られる波のパワースペクトル密度の水平位相速度分布の導出手法を提案した。しかし、この手法を赤道近くで得られた大気光画像の解析に用いた例はない。本研究では、ハワイのハレアカラ観測点 (20.7oN, 203.7oE) で 2013 年から 2016 年の 3 年間に得られた波長 557.7 nm と 630.0 nm の大気光画像に Matsuda et al. [JGR, 2014] の解析方法を適用し、この赤道近くの低緯度域での大気重力波と MSTID の統計的な特徴を明らかにするとともに、日本で見られた同種の波動の統計的特徴 [Takeo et al., JGR, 2017; Tsuchiya et al., JGR, 2018] との比較を行った。

3 年間の位相速度スペクトルの平均から、波長 557.7 nm の大気光画像に見られた大気重力波において、夏と冬の比較で東西方向の伝搬に違いは見られなかった。しかし、信楽や陸別では、夏に東、冬に西と伝搬方向が反対になることが分かっている。これについては本年 5 月に開催された JpGU2019 において、中間圏ジェット気流によるウインドフィルタリング効果によるものだと考えられることを発表した。

波長 630.0 nm の大気光画像に見られた MSTID においては、パワースペクトル密度に関しては冬が最も強く、主に東西方向に波が伝搬していた。このパワースペクトル密度の季節ごとの違いについて、Duly et al. [AnnGeo, 2013] の手法を参考にして、ハレアカラとその磁気共役点に対し、パーキンス不安定の最大成長率の式の中性風の項を各日・時間ごとで計算し、パワースペクトル密度分布の季節変化は中性風の季節変化だけでは説明できないことが分かった。これは MSTID の生成がパーキンス不安定だけでなくスポラディック E 層の存在に大きく影響される、というこれまでの研究結果と一致する [Yokoyama et al., JGR, 2009; Narayanan et al., JGR, 2018]。また冬に見られた東西方向の伝搬について、東西方向のケオグラムを作ることでイベントごとに詳細に解析した結果、東方向の伝搬にプラズマバブルが混在していないこと、見られた MSTID は日本で観測されるものと比較すると波長が大きく、2-3 パルスのみで波の連続性があまり見られないことが分かった。

ISS-IMAP/VISI観測による中間圏大気重力波の変動とプラズマバブル発生との関係性について

岡田 凌太 [1]; 齊藤 昭則 [2]; 池田 孝文 [2]; 品川 裕之 [3]; 津川 卓也 [3]; 坂野井 健 [4]
[1] 京大・理・地球惑星; [2] 京都大・理・地球物理; [3] 情報通信研究機構; [4] 東北大・理

Relationship between mesospherical airglow disturbance and occurrence of equatorial plasma bubbles

Ryota Okada[1]; Akinori Saito[2]; Takafumi Ikeda[2]; Hiroyuki Shinagawa[3]; Takuya Tsugawa[3]; Takeshi Sakanoi[4]
[1] Earth and Planetary, Kyoto Univ.; [2] Dept. of Geophysics, Kyoto Univ.; [3] NICT; [4] Grad. School of Science, Tohoku Univ.

762 nm airglow data observed by Ionosphere, Mesosphere, upper Atmosphere and Plasmasphere mapping mission from the ISS / Visible and near Infrared Spectral Imager (ISS-IMAP/VISI) to investigate relationship between mesospheric gravity waves and the occurrence of Equatorial Plasma Bubbles (EPBs). EPBs are depletion of electron density in the equatorial ionosphere. According to the previous study EPBs can be generated through the Rayleigh-Taylor (R-T) instability in the ionosphere. Medium-scale gravity waves with horizontal scales of a few hundred kilometers in the bottom side of the F region have been frequently suggested to play a key role in EPBs seeding. Gravity wave occurrence may depend on seasonal and longitudinal variation and may have oscillation whose period is few days. This several days oscillation of gravity wave may affect the variation of EPBs occurrence that can not be explained only by the R-T growth rate. Previous research of concentric gravity waves (CGWs) using observed by ISS-IMAP/VISI shows more mesospheric CGW events occur in the west side of the African continent than the east side of the African content. It indicate occurrence of CGWs is different between nearby areas. Objective of this study is to elucidate relationship between mesospheric gravity waves and longitudinal dependence of EPB occurrences. ISS-IMAP/VISI was operated for three years from September 2012 to August 2015. ISS-IMAP/VISI observed the airglow in the nadir direction on the nightside with two FOVs facing 45 degrees in the forward and backward of the orbital direction. We analyzed 762nm airglow data and compared with occurrence rate of EPBs and Growth rate of R-T instability. Occurrence rate of EPBs using Rate of TEC Index (ROTI) that is standard deviation of differential of GPS-TEC. Growth rate of R-T instability was calculated by using parameters from Ground-to-topside model of Atmosphere and Ionosphere for Aeronomy (GAIA). In this study, we investigated relationship between occurrence of EPBs observed by GPS-TEC data, linear growth rate of the R-T instability in the ionosphere obtained with GAIA, and mesospheric gravity wave activities observed by ISS-IMAP/VISI.

Ionosphere, Mesosphere, upper Atmosphere and Plasmasphere mapping mission from the ISS の Visible and near Infrared Spectral Imager(ISS-IMAP/VISI) の波長 762nm 大気光データを解析し、中間圏における大気重力波がプラズマバブルの発生にどのような影響を与えているのか調べた。赤道電離圏において電子密度が大きく減少した領域が観測されることがあり、プラズマバブルと呼ばれている。プラズマバブルは、電離圏底部の微小擾乱がレイリー・テイラー不安定性によって成長するという発達機構が考えられているが、先行研究からはこの微小擾乱としては中規模（~600km）の大気重力波が有力視されている。大気重力波の発生には経度や季節による変動が予想されており、また数日程度の短周期の変動があると考えられている。そのような大気重力波の変動が、プラズマバブルの発生においてレイリー・テイラー不安定性の成長率だけでは説明できない変動の原因となっていると考えられる。大気重力波の経度による変動としては、ISS-IMAP/VISI の波長 762nm 大気光データを用いて同心円上大気重力波の分布を示した先行研究によりアフリカ西部地域の方が東部地域よりも同心円上重力波が多く見られることが報告されており、近接する地域でも発生が大きく異なることが知られている。本研究では中間圏における大気重力波がプラズマバブルの経度による出現特性の違いにどのように寄与しているのかを調べた。ISS-IMAP/VISI は 2012 年 9 月から 2015 年 8 月に渡って夜間の大気光を高度約 400km を約 8km/s で移動しながら天底方向に、軌道方向に対して 45 度の前後 2 方向への視野で観測した。ISS-IMAP/VISI から得られた波長 762nm 大気光データを解析して高度 95km における大気の擾乱度を同定した。GPS-Total Electron Content（TEC）データの偏差の標準偏差値、Rate of TEC Index (ROTI) を用いて得られたプラズマバブルの発生率や大気圏・電離圏統合モデル Ground-to-topside model of Atmosphere and Ionosphere for Aeronomy(GAIA) によって得られたパラメータから算出されたレイリー・テイラー不安定性の成長率などと比較した。GPS-TEC データによるプラズマバブル発生の様子と大気圏・電離圏統合モデル GAIA の結果から算出して得られたレイリー・テイラー不安定性の線形成長率との関係性に ISS-IMAP/VISI の 762nm 大気光データから得られる高度 95km の大気重力波の様子がどのように関わるのかについて調べた結果を報告する。

静止軌道衛星ひまわり8号可視バンドによる極中間圏雲の観測

穂積 裕太 [1]; 津田 卓雄 [1]; 安藤 芳晃 [2]; 細川 敬祐 [1]; 鈴木 秀彦 [3]; 中村 卓司 [4]; 村田 健史 [5]
[1] 電通大; [2] 電通大 I 専攻; [3] 明治大; [4] 極地研; [5] 情報通信研究機構

Polar mesospheric clouds observation by the visible band of Advanced Himawari Imager on Himawari-8

Yuta Hozumi[1]; Takuo Tsuda[1]; Yoshiaki Ando[2]; Keisuke Hosokawa[1]; Hidehiko Suzuki[3]; Takuji Nakamura[4]; Ken T. Murata[5]
[1] UEC; [2] Dept. of Comp. and Network Eng., The Univ. of Electro-Comms.; [3] Meiji univ.; [4] NIPR; [5] NICT

Polar mesospheric clouds (PMCs) consist of water-ice particles, and have been observed near the summer polar mesopause region. Production and disruption of PMC are sensitive to the background mesospheric state, such as temperature and water vapor conditions. Its distribution is strongly affected by the background wind. Hence, PMC is a good proxy of the thermal structure and dynamics at the high latitude summer mesosphere. Observations of PMC have been widely performed by various methods from the ground as well as from the space. However, these past methods have some limitations, especially in local time coverage or observational continuity to monitor the long-term PMC activity.

Recently, we reported that PMC emission layers are captured in the limb of the Earth in the full disk image taken by the Advanced Himawari Imager (AHI) onboard Himawari-8 [Tsuda et al., Atmospheric Measurement Techniques, 2018]. PMC data from the geostationary orbit satellite have great advantages on the wide and stable field of views and the local time coverage. PMC observation by Himawari-8 is expected to provide new information on the PMC studies, majority of which are based on the ground-based or low-orbit-satellite observations. In the presentation, we report the PMC signals in the visible band of AHI. The blue visible band (Band No: 1, Central wave length: 470 nm) is the most suitable band for the PMC observation in the 16 bands of AHI. We analyzed the band to examine the PMC signatures in it. The spatial structures and the local variations will be presented. The detection capability, especially the limit of sensitivity, of AHI on the PMC observation will be also discussed.

ISS-IMAP/VISIで観測された中間圏擾乱構造の水平空間スケール依存性

齊藤 昭則 [1]; 穂積 裕太 [2]; 坂野井 健 [3]; 岡田 凌太 [4]
[1] 京都大・理・地球物理; [2] 電通大; [3] 東北大・理; [4] 京大・理・地球惑星

Horizontal scale dependency of the mesospheric disturbances observed by ISS-IMAP/VISI

Akinori Saito[1]; Yuta Hozumi[2]; Takeshi Sakanoi[3]; Ryota Okada[4]
[1] Dept. of Geophysics, Kyoto Univ.; [2] UEC; [3] Grad. School of Science, Tohoku Univ.; [4] Earth and Planetary, Kyoto Univ.

The horizontal structures of the mesospheric disturbances have been widely investigated with ground-based all-sky imagers (ASIs). The wave characteristics, such as wavelength and propagation velocity, are derived from sequences of two-dimensional images of the mesospheric airglow. It is reported that the horizontal wavelength of the mesospheric structures has a maximum between 10 km and 30km. The structures whose wavelength is longer than 100 km are, however, difficult to be observed by ground-based ASIs because of the limitation of ASI's field-of-view. Visible and near Infrared Spectral Imager (VISI) of Ionosphere, Mesosphere, upper Atmosphere and Plasmasphere (IMAP) mission onboard the International Space Station (ISS) observed the mesospheric airglow structures from 2012 to 2015. It covered the wave length range from 500nm to 900nm. The airglow of 730nm (OH, Alt. 85km), 762nm (O2, Alt. 95km), and 630nm (O, Alt. 250km) were mainly observed besides the other airglow, such as 589nm (Na) and 557 (O). The 762nm airglow from the molecular oxygen is used to investigate the mesospheric structures. The size of the field-of-view is 600km in the direction perpendicular to the ISS trajectory, and longer than 10,000km along the trajectory. The observed airglow disturbances are categorized in three scales. The scale dependency of the mesospheric disturbances will be discussed in the presentation.

Mesospheric temperature derivation using ISS-IMAP VISI data

Ryo Murakami[1]; Akinori Saito[2]; Takeshi Sakanoi[3]; Yuta Hozumi[4]
[1] Earth and Planetary Science, Kyoto University; [2] Dept. of Geophysics, Kyoto Univ.; [3] Grad. School of Science, Tohoku Univ.; [4] UEC

Satellite observation data of the airglow spectrum is difficult to analyze because its wavelength resolution is inferior to ground observation data. In this research, we analyze data of the airglow emission in the mesosphere observed by the visible and near-infrared spectral imaging device (VISI), which is an observational instrument mounted on the International Space Station (ISS) for the ISS-IMAP mission from 2012 to 2015 to estimate the temperature of the mesospheric OH layer around 85 km. It is known that the relative existence distribution of rotational levels follows the Boltzmann distribution determined by OH rotational temperature when OH molecules make a transition between vibrational levels. This method has been applied for the ground-base OH airglow observation. In this research, we apply this method to observational data from VISI to obtain OH temperature in the wider area than that observation from the ground-base. We use the spectral mode data. The spectral mode data was focused on 6 region of interest (ROI) to observe the emission spectrum of airglow, and the observation data was recorded along with the spatial position information. Multi wavelength data of OH airglow near 828nm are processed to suppress the influence of salt-and-pepper noise derived from cosmic-ray and white noise derived from observation equipment. Thereafter, in order to compensate for the resolution in the wavelength direction of the spectrum diagram, we fit it with a Gaussian function and estimate temperature by linear regression, and derive the temperature and evaluate it.

大気光イメージ観測による関東平野上空の山岳波動の研究:卓越波長とその伝搬特性の検証

石井 智士 [1]; 鈴木 秀彦 [2]
[1] 明大・理工・物理; [2] 明治大

Study of the mountain waves above Kanto plain by an airglow imaging observation

Satoshi Ishii[1]; Hidehiko Suzuki[2]
[1] Meiji Univ.; [2] Meiji univ.

Imaging observation of OH airglow from Meiji University, Japan (35.613^{o}N,139.549^{o}E) has been conducted to study propagation and excite mechanisms of mountain waves since Dec. 2015. Since this observation site locates in the middle of the Kanto plain surrounded by rich mountains, many mountain waves are expected to be detected. However, an observed occurrence of the wave events which has zero phase speed to the ground is only 6 events between Dec. 2015 and Jun. 2019. In addition, observed mountain waves have typical wavelengths between 10 and 30 km and rarely have longer wavelength (˜100 km) [Ishii et al., 2018]. Moreover, some of the observed wave-like structures are likely to be the ripple structures [Okuda, 2017]. The possible reasons for this rareness of mountain wave signatures in observed airglow images are (1) The occurrence of excitation of mountain waves in the lower atmosphere is rare, and/or (2) most of excited mountain waves in the lower atmosphere are difficult to propagate up to the airglow layer. To verify these hypothesis, occurrence and properties of mountain waves excited in the lower atmosphere are examined by using color images taken by Himawari-8 meteorological satellite. Cloud image taken by Himawari-8 often shows wave-like signature in a lee side of the mountain area. These are considered to be the mountain wave structures excited as a result of the interaction between lower atmospheric wind and mountains. Wind speed and direction at the time can be referred from the re-analysis meteorological data, MERRA-2. Thus, by comparing the wind at lower atmosphere and properties of wave structures (direction of wavenumber and dominant wavelength) deduced from the Himawari-8 image, the relationship between wind speed at mountain height and dominant wavelength of the excited mountain wave is obtained. This relationship is considered to be valid even under clear night and thus an initial properties of excited mountain waves at lower atmosphere during the airglow observation can be estimated. Possibility of propagation of this excited mountain waves to upper atmosphere is then verified by Ray-tracing method by using MERRA-2 data as a background atmosphere. In this study, results of the verification to check whether observed mountain-wave-like signatures in airglow images are propagated from neighboring mountains or not are presented.

本研究では、関東平野上空に伝搬する山岳波の励起伝搬特性の解明を目指し 2015 年 12 月より、神奈川県川崎市にある明治大学生田キャンパス（35.613^{o}N,139.549^{o}E）を拠点とした OH 大気光イメージング観測を継続している。これは関東平野が北方と西方に山岳地形を有することから、山岳波の励起伝搬が多く起こると期待したためである。しかし、これまでの観測結果から対地位相速度を持たない大気重力波構造は複数例検出されているものの、その頻度は 2015 年 12 月より 2019 年 6 月の期間で 6 例に留まっている。また、イメージャーの視野と同程度のスケールの波動構造を検出する解析法を用いて、長波長構造（～100km）の検出も試みたが [石井, 2018]、観測される多くの波動はそれよりも小さいスケールのもの（10-30km）が多いことが明らかになってきた。さらに [奥田,2018] によれば小スケールの構造の中には不安定構造の一種であるリップルが含まれている可能性もある。期待されたほど山岳波の大気光層への伝搬例が少ない理由としては、（１）そもそも下層大気で山岳波動が励起される頻度が低い、（２）下層大気で山岳波動は励起されるが大気光層まで伝搬してこない。の２つの理由が考えられる。そこで、本研究では 2018 年におけるひまわり 8 号の可視画像の雲画像に頻繁に現れる山岳波構造の解析を行い、下層における山岳波構造の出現頻度と波面方向の特性を調査した。さらに、この解析結果と客観解析データ MERRA-2 の下層風データを照合することで、どのような風速の時に、どのような波長、波面の山岳波が下層大気に励起されるのかを調査した。本発表では、この関係性が、大気光観測が可能な雲のない晴天時においても保たれていると仮定し、大気光画像中に検出された山岳波動と思われる構造が、当時の風速によって下層に励起された山岳波が伝搬してきたものであるかを検証した。すなわち、イベント時の下層大気の風速度の情報から、下層大気で励起される波動のパラメーター（波束の励起位置、波面方向）を定め、この波動が大気光層まで伝搬するか否かを、MERRA-2 を背景場としたレイトレーシング手法により検証した結果を報告する。

ラグランジュ型化学輸送モデルによる中間圏大気組成の短期変動機構の研究

中西 慎吾 [1]; 長濱 智生 [2]; 水野 亮 [2]; 中島 拓 [2]
[1] 名大・理・宇宙; [2] 名大・宇地研

Study on machanism of short-term variations of chemical composition in mesosphere using a Lagrangian chemical transport model

Shingo Nakanishi[1]; Tomoo Nagahama[2]; Akira Mizuno[2]; Taku Nakajima[2]
[1] Particle and Astrophysical Science, Nagoya Univ.; [2] ISEE, Nagoya Univ.

Mesospheric chemical composition largely varies caused by environmental changes from the earth inside and outside. Recent studies reported enhancement of NOx and HOx and ozone depletion in the polar mesospheric region at a large solar proton event. These suggest that precipitation of other high energy particles such as a high energy electron from the magnetosphere also has influence on the chemical composition in the mesosphere. For these reasons, we have installed millimeter-wave spectrometers in Rikubetsu-cho, Hokkaido (Japan), Syowa Station (Antarctic), Atacama (Chile), Rio Gallegos (Argentine) and Tromso (Norway), and have been observing steady atmospheric minor molecules such as Ozone, NOx, HOx and ozone-depleting substances in the stratosphere and mesosphere to understand the atmospheric composition changes caused by natural phenomena such as Energetic Particle Precipitation (EPP).

In addition to these observations, we have been developing a Lagrangian chemical transport model, which is suitable for a simulation of a sudden and a local event to evaluate the influence of the atmospheric composition mechanism in the stratosphere and mesosphere. Our developing model is an extension of the Lagrangian particle dispersion model (FLEXPART) by incorporating meteorological fields data and chemical reactions in the mesosphere. FLEXPART can analyze a trajectory from the ground to about 40 km in altitude using the reanalysis data of NCEP and ECMWF as meteorological fields input data. In this study, we incorporated a new reanalysis dataset (MERRA2) as meteorological fields input data to extend the analysis range toward the mesosphere, and as a result, trajectory an analysis ranging from the ground to about 80 km in altitude can be made. Moreover, only OH reactions are considered in FLEXPART, although it needs to calculate non-linear chemical reactions separately in this study because chemical reactions caused by EPP include not only reactions by natural molecules but also ion-molecular reaction, ionization, dissociation and ion recombination, and so on. For this reason, we incorporated chemical reactions of the stratosphere and mesosphere in FLEXPART using Kinetic Preprocessor (KPP) which is chemical reaction computation software. Now, we can simulate for 10 days in 40 hours (about 2 days) using our desktop PC.

In this presentation, we will report the details about time and distribution changes of NO and ozone at some EPP events as well as the results of comparison between our developing model and Whole Atmosphere Community Climate Model (WACCM) and so on about distribution change.

中間圏の大気微量分子組成は、そこでの大気密度が小さいことから地球内外の環境変動の影響を受け、大きく変動する。近年人工衛星等による観測から、太陽活動に起因した高エネルギー荷電粒子の地球大気への大規模な降りこみ（Energetic Particle Precipitation: EPP）による極域中間圏の NOx や HOx 増加とそれによるオゾンの減少が検出されており、同様のことが磁気圏加速電子の降りこみ等、各種の高エネルギー粒子の振りこみ現象に付随して起こることが予想される。そこで我々は、これまでに北海道陸別町、昭和基地（南極）、アタカマ高地（チリ）、リオ・ガジェゴス（アルゼンチン）、トロムソ（ノルウェー）にミリ波分光観測装置を設置し、成層圏・中間圏のオゾンや NOx・HOx、オゾン層破壊物質等の大気微量分子の定常観測を行い、高エネルギー粒子の振りこみ等の自然現象による大気組成変動機構に関する研究を進めている。

これらの観測に加えて、我々は様々な EPP 等による成層圏・中間圏の大気微量分子組成変動機構を解明し、その影響を評価するために、局所的・突発的なイベントのシミュレーションに適しているラグランジュ型化学輸送モデルの開発を行った。このモデルはラグランジュ型拡散モデル（FLEXPART）を拡張し、中間圏の気象場データと化学反応過程を取り込んだものである。FLEXPART は現在、気象場のインプットデータとして NCEP と ECMWF の再解析データが利用でき、地表から高度約 40km まで流跡線解析が可能であるが、本研究の対象である中間圏は含まれていない。そこで我々は、シミュレーション範囲を中間圏まで拡張するために、新たにインプットデータとして MERRA2 再解析データを利用できるように拡張し、地表から高度約 80km までの流跡線解析が可能となった。また、FLEXPART では化学反応過程として OH による消失のみを考慮しているが、EPP 等による化学反応過程では、中性分子の反応だけでなく、イオン分子反応、電離・解離、イオン再結合などを含むため、非線形化学反応を別途計算する必要がある。そこで我々は、化学反応計算ソフトウェアである Kinetic Preprocessor（KPP）を FLEXPART に組み込むことで、成層圏・中間圏における各種化学反応過程を取り込んだ。現在、デスクトップパソコンで 10 日間のシミュレーションを約 2 日間 (40 時間) で行うことが可能である。

本発表では、いくつかの EPP 事例の際のオゾン及び NO の時間変化と分布変化について詳細を発表する。また、全大気領域気候モデル（Whole Atmosphere Community Climate Model : WACCM）などのオイラー型 3D モデルとの分布比較を行う。

小スケール大気重力波に伴う温度・風速変動の観測的評価

鈴木 臣 [1]; 野澤 悟徳 [2]
[1] 愛知大学; [2] 名大・宇地研

Observational evaluation of temperature and wind perturbations associated with small-scale gravity waves

Shin Suzuki[1]; Satonori Nozawa[2]
[1] Aichi Univ.; [2] ISEE, Nagoya Univ.

The Tromsoe Na lidar operated by the Institute for Space-Earth Environmental Research, Nagoya University has monitored wind and temperature structures associated with auroral activity in the high latitude upper atmosphere since 2010. Although the observations are limited during the winter night, the lidar detected atmospheric wave signatures with period of a few hours and temperature change related to the wave propagation with high precision (less than 1K). Furthermore, this lidar started five-direction observation from 2012: horizontal distance between the beam positions are 58 km or 22 km at a height of 100 km and the observational setup can detect smaller-scale perturbations.

In this study, we tried to identify small-scale (less than 100 km) and short-period (less than 1 h) gravity waves by using the Tromsoe Na lidar. Gravity waves contribute significantly to the wind field and thermal balance in the mesosphere and lower thermosphere (MLT) region because they vertically transport horizontal momentum from the lower atmosphere. It is also pointed that, in particular, smaller-scale and shorter-period waves tend to transport larger momentum. Small-scale gravity waves in the MLT region are mainly studied with airglow imaging measurements. The airglow measurements, however, cannot observe temperature and wind perturbations directly, which are necessary for the estimation of wave′s momentum flux. Based on temperature and wind perturbations with the five-direction lidar, we evaluate dynamical effect of small-scale gravity waves propagating in the upper atmosphere quantitatively.

In this presentation, we will report some initial results derived from simultaneous measurements of the lidar and airglow imaging in 2013-2016.

中間圏・下部熱圏における季節内振動と成層圏準２年周期振動及び成層圏半年振動との相関

秋山 瑞樹 [1]; 三好 勉信 [2]
[1] 九大・理・地惑; [2] 九大・理・地球惑星

The relation between the intraseasonal oscillation in the MLT and the stratospheric QBO/SAO

Mizuki Akiyama[1]; Yasunobu Miyoshi[2]
[1] Earth and Planetary Sciences, Kyushu Univ; [2] Dept. Earth & Planetary Sci, Kyushu Univ.

Recent satellite observations, such as HRDI/UARS, have revealed intraseasonal oscillations of the zonal wind with periods from 20 to 120 days in the equatorial mesosphere and lower thermosphere (MLT). In this study, using an atmosphere-ionosphere coupled model (GAIA), we investigate the detailed characteristics of intraseasonal oscillation variation using the global data of the GAIA model and its correlation with between the stratospheric quasi-biennial oscillation (QBO) and the stratospheric semi-annual oscillation (SAO). First, our analysis indicated that the oscillation with periods from 18 days to 36 days are significant in low latitudes (30S-30N) between 80 and 120 km heights. Furthermore, the amplitude of the intraseasonal oscillation in the equatorial MLT has strong seasonal and interannual variations. For example, the amplitude of the intraseasonal oscillation has a maximum during January-February in 2011, whereas the amplitude has a minimum during September-December in 2010. Our analysis showed that the amplitude of the intraseasonal oscillation is enhanced (attenuated) during the easterly (westerly) phase of the QBO and SAO. In the next step, we study the relation between the amplitude of intraseasonal oscillation and atmospheric wave activity, such as tides and equatorial waves.

近年の衛星観測（HRDI/UARS）により赤道域の中間圏及び下部熱圏において 20 日から 120 日周期の東西風の季節内振動が存在していることが明らかになっている。本研究は大気圏電離圏結合モデル（GAIA）を用いて季節内変動のより詳細な特徴を調べ、さらに成層圏準 2 年周期振動及び成層圏半年振動との相関を考察してみた。はじめに２００７年から２０１６年について、スペクトル解析を実施し、振動周期が 18 日から３６日の変動が卓越していることが分かった。また周期成分の緯度・高度分布から季節内振動は南緯３０度から北緯３０度の低緯度域、高度８０から１２０ km の領域で起きていることが確認できた。次に成層圏準２年周期振動及び成層圏半年振動との相関について解析を行った。季節内振動の振幅は、年々変動・季節変動が顕著で、特に季節内振動の振幅が、2011 年の 1 月から 2 月に最大となり、一方、2010 年の 9 月から 12 月で最小となることが分かった。季節内振動の振幅は、成層圏準２年周期振動及び成層圏半年振動がともに東風の場合に季節内振動は強く現れ、一方でも西風である場合には表れにくいという結果が得られた。今後は下層からの大気潮汐波や赤道波などの大気波動の年々変動・季節変動との相関についても解析していく予定である。

気象再解析データERA5における南極域での大気重力波再現性

吉田 理人 [1]; 江尻 省 [2]; 冨川 喜弘 [2]
[1] 総研大・複合・極域; [2] 極地研

Reproducibility of gravity waves over the Antarctic in the ERA5 meteorological reanalysis

Lihito Yoshida[1]; Mitsumu K. Ejiri[2]; Yoshihiro Tomikawa[2]
[1] Polar Science, SOKENDAI; [2] NIPR

Gravity waves are generated by mountains, jet streams, etc., and propagate into the mesosphere, which decelerate the mesospheric jet stream. Although this effect is essential in long-term forecast and climate change prediction, it needs to be implemented in models through gravity wave drag parameterization because of its smaller spatial scales than the model grid. However, it is still incomplete because of no horizontal propagation in the gravity wave drag parameterization scheme and lack of observations in the Antarctic region. Even the latest climate models cannot sufficiently reproduce the timing of polar vortex breakdown. Therefore, it is planned to perform meteorological observations of the Antarctic lower stratosphere with superpressure balloons, which can estimate the momentum transport by gravity waves. Since superpressure balloons move along with an air parcel on a constant density surface, this observation is the only way to obtain information of momentum flux and kinetic / potential energy for the entire period range (approximately 5 minutes to more than 10 hours) of gravity waves.

On the other hand, increasing resolution of the latest objective and reanalysis data encourages us to estimate the momentum flux and energy of gravity waves from them. It is reported that the European Centre for Medium-Range Weather Forecasts (ECMWF) operational analysis reproduced the horizontal distribution of momentum flux due to gravity waves, which was similar to but smaller than the observations by a factor of 3-5. It is probably because small-scale gravity waves cannot be represented in the ECMWF model. In addition, it is pointed out that the gravity wave drag due to small-scale gravity waves cannot be sufficiently reproduced in the WACCM model because the horizontal and vertical wind speeds do not follow the power law near the limit of the horizontal resolution of the model.

In this research, spectral features and gravity waves in the latest meteorological reanalysis data ERA5 are compared with various observations, and evaluated in their reproducibility (i.e., altitude and period dependence, and orographic and non-orographic difference). The primary purpose of this study is to carry out a preliminary survey of gravity wave features in ERA5 for comparison with the planned superpressure balloon observations in Antarctica around 2021. Since the previous research compared superpressure balloon observations from September to December 2010 with the ECMWF operational analysis, we will investigate differences in gravity wave reproducibility using ERA5 during the same period. We also compare them with the data of brightness temperature disturbances obtained by AIRS onboard NASA's satellite Aqua. In addition, we plan to compare them with gravity wave spectrum of the whole frequency range obtained by the PANSY radar at Syowa Station in Antarctica.

重力波は山岳やジェット気流を波源とする波で、中間圏まで伝播し中間圏ジェット気流を減速させる。この働きは長期予報や気候変動予測において重要だが、重力波の空間スケールがモデルのグリッド間隔に対して小さいため、パラメタリゼーションによってその効果を取り入れる必要がある。しかし、重力波の効果をパラメタリゼーションする際に水平伝播を考慮できないことや南極域における観測の不足から最新の気候モデルにおいても極渦の崩壊時期等が十分に再現できていない。そこで、重力波による運動量輸送を推定することができ、なおかつ南極域を面的に観測することができるスーパープレッシャー気球による下部成層圏の気象観測が計画されている。スーパープレッシャー気球は等密度面を空気塊とともに動くため、同観測は重力波の全周期帯（約5分～十数時間）の運動量フラックスや運動・ポテンシャルエネルギーの情報を得ることができる唯一の手段といえる。

一方、高解像度化が進む気象客観・再解析データで重力波の運動量フラックスやエネルギーを推定する試みも近年増えてきている。欧州中期予報センター（ECMWF）モデルでは、重力波による運動量フラックスの水平分布は現実と近いものが再現されるものの、小規模重力波が表現できないため、その大きさは現実の数分の一になることが報告されている。また気候モデルWACCMでは、モデルの分解能の限界に近くなると水平・鉛直風速がべき乗則に従わなくなるため、小規模重力波による重力波ドラッグを十分に再現できていないことが示唆されている。

本研究では、最新の気象再解析データERA5を様々な観測と比較し、各高度、各周期、地形性・非地形性毎での再解析データにおける重力波の再現性を調べ、2021年頃に実施予定の南極での重力波のスーパープレッシャー気球観測との比較に向けた予備調査を実施することを目的とする。先行研究では2010年の9月から12月のスーパープレッシャー気球観測とECMWF現業解析を比較しているため、同時期のERA5を用いて重力波の再現性の差異を調べる。また、NASAのAqua衛星搭載AIRSにより得られる輝度温度擾乱のデータとも比較する。さらに、南極昭和基地大型大気レーダーPANSYで得られる全周波数帯の重力波スペクトルとの比較も行う予定である。

Geomagnetic activity-related Na layer and CNA variations observed over Syowa, Antarctic

Takuo Tsuda[1]; Takuya Kawahara[2]; Yoshimasa Tanaka[3]; Mitsumu K. Ejiri[4]; Takanori Nishiyama[4]; Takuji Nakamura[4]
[1] UEC; [2] Faculty of Engineering, Shinshu University; [3] NIPR/SOKENDAI; [4] NIPR

Metallic layers, such as Na, Fe, Mg, K, and Ca layers, exist in the mesosphere and lower thermosphere (MLT). The height range of the MLT region corresponds to the ionospheric D and E regions, and in the polar region energetic particles precipitating from the magnetosphere can often penetrate into the E region and even into the D region. Therefore, the influence of energetic particles on the metallic layers is of interest regarding changes in atmospheric composition accompanied by auroral activity or geomagnetic activity.

In the present study, we have performed a statistical analysis on geomagnetic activity-related Na layer responses using Na density data, together with cosmic noise absorption (CNA) data. Those data were obtained from simultaneous observations at Syowa, Antarctic (69.0S, 39.6E) in 2000-2002. Utilizing the ground-based observational data, we can investigate local-time characteristics in the geomagnetic-related Na layer response, while it was difficult to see local-time variations in such Na layer responses from the statistical investigation by our previous work because of its dataset obtained from the polar orbit satellite.

As the results, it is found that the Na densities around the topside of Na layers tended to decrease but the CNA tended to increase during geomagnetic active days. The amounts of Na density responses, i.e., Na density decrease or Na loss, were increasing with magnetic local time (MLT) from dusk hours to dawn hours, and those of CNA responses, i.e., CNA increase, were also increasing with MLT. Thus, there were clear negative correlations between the Na density and the CNA variations. These MLT characteristics would be observational evidences for the the Na loss induced by the energetic particle precipitation during geomagnetic active days.

Naライダーで観測される鉛直風オフセットに関するライダーシステムからの考察

川原 琢也 [1]; 野澤 悟徳 [2]; 斎藤 徳人 [3]; 津田 卓雄 [4]; 和田 智之 [3]; 川端 哲也 [2]
[1] 信州大・工; [2] 名大・宇地研; [3] 理化学研究所基幹研; [4] 電通大

Na lidar at Tromso and discussion about the observed vertical wind velocity offset

Takuya Kawahara[1]; Satonori Nozawa[2]; Norihito Saito[3]; Takuo Tsuda[4]; Satoshi Wada[3]; Tetsuya Kawabata[2]
[1] Faculty of Engineering, Shinshu University; [2] ISEE, Nagoya Univ.; [3] ASI, RIKEN; [4] UEC

An Nd:YAG laser-based sodium temperature/wind lidar was developed for the measurement of the northern polar mesosphere and lower thermosphere at Tromsø (69.6N, 19.2E), Norway. The Na lidar is able to measure vertical wind velocity (generally thought to be 0 m/s) but our data in the past show the wind offset of 5-10 m/s at any altitudes. The wind velocity is largely dependent on the laser frequency locking accuracy and its locking stability during the observation. So we examined the past wind data, extract the wind offset in each observation day and discussed about the laser locking accuracy or stability. In this presentation, we show the results.

ノルウェー・トロムソ（北緯69度）のナトリウム温度・風ライダーでは、視線方向（レーザ射出方向）でNa層のドップラーシフト周波数を検出し風速を導出している。ライダー観測では、射出レーザ波長を1/1000 pmの精度でNaD2線内の特定の絶対波長に合わせる。観測中はレーザがその波長にロッキングされ、ロッキング精度が維持されていることが絶対風速を求める前提となる。現在の手法では、1時間に1回、ドップラーフリー法により高精度に波長を合わせ、波長計での値でフィードバックをかけて安定化させている。仮に観測時の波長ロッキング精度が甘い場合、鉛直風の中心値は風速0 m/sとならず一定の風速オフセットが乗る。また観測最中に時間とともにロッキング波長が外れていく場合、見かけ上、時間とともに鉛直風速が変化していく結果が得られることになる。トロムソのNaライダーでは鉛直方向観測からは高度80-115kmの範囲の鉛直風が計測されるが、これまでの観測結果には+5m/sから+10m/sの鉛直風オフセットが計測されていた。この結果に対してライダー観測に問題があると考えており、風速計測に影響を与えるレーザのスペクトル特性や周波数ロッキング精度、解析手法に原因があることを前提に検証を行っている。解析結果はレーザの安定性を反映するため、逆に鉛直風のデータからレーザ波長のロッキングの安定性を知ることができる。そこからその原因となるレーザ制御の原因を突き止め、観測に反映することができると考えている。本講演では、これまでの鉛直風データを抽出し、ライダーシステムから生じる風速オフセットに関して、射出レーザ波長のロッキング精度、鉛直風速オフセットの観測日ごとの違い、解析手法から検証を行った結果を発表する。レーザ波長のロッキング精度は年々改善を試みており、現在では極めて精度が高い。レーザ制御と解析結果とを比較し、その原因を究明する。